AWARD NUMBER: W81XWH-07-1-0248

TITLE: Novel Methods for Imaging PET Biomarkers and Gene Therapy of Cancer

PRINCIPAL INVESTIGATOR: Gabor Tigyi, M.D., Ph.D.

CONTRACTING ORGANIZATION: University of Tennessee Health Science Center
Memphis, TN 38163

REPORT DATE: May 2009

TYPE OF REPORT: Final

PREPARED FOR: U.S. Army Medical Research and Materiel Command
Fort Detrick, Maryland 21702-5012

REPORT DOCUMENTATION PAGE

Form Approved
OMB No. 0704-0188

1. REPORT DATE	2. REPORT TYPE	3. DATES COVERED
1 May 2009	Final	1 May 2007 – 30 Apr 2009

4. TITLE AND SUBTITLE

Novel Methods for Imaging PET Biomarkers and Gene Therapy of Cancer

5a. CONTRACT NUMBER

5b. GRANT NUMBER
W81XWH-07-1-0248

5c. PROGRAM ELEMENT NUMBER

6. AUTHOR(S)
Gabor Tigyi, M.D., Ph.D., David Townsend Ph.D., Lorraine Albritton, Ph.D., Lawrence Pfeffer, Ph.D., Jonathan Wall, Ph.D., Stephen Kennel, Ph.D., Yuko Fujiwara, Ph.D.

E-Mail: gtigyi@physio1.utmem.edu

5d. PROJECT NUMBER

5e. TASK NUMBER

5f. WORK UNIT NUMBER

7. PERFORMING ORGANIZATION NAME(S) AND ADDRESS(ES)

University of Tennessee Health Science Center
Memphis, TN 38163

8. PERFORMING ORGANIZATION REPORT NUMBER

9. SPONSORING / MONITORING AGENCY NAME(S) AND ADDRESS(ES)
U.S. Army Medical Research and Materiel Command
Fort Detrick, Maryland 21702-5012

10. SPONSOR/MONITOR'S ACRONYM(S)

11. SPONSOR/MONITOR'S REPORT NUMBER(S)

12. DISTRIBUTION / AVAILABILITY STATEMENT
Approved for Public Release; Distribution Unlimited

13. SUPPLEMENTARY NOTES

14. ABSTRACT
Cancer mortality in the USA ranks Tennessee number 43 in incidence and 5th in the nation in mortality—both numbers suggesting much work to be done. Altogether, there are over 660,000 citizens with active military or veteran status in our state constituting over 15% of the general population. Therefore, the poor cancer mortality statistics negatively affects not only the state's general population but also military and veteran families living in the state. A self-evaluation of the strengths and weaknesses of our state-wide University of Tennessee Cancer Institute programs revealed two major weaknesses impairing progress toward advancing translational research into the detection and treatment of cancer patients in Tennessee. Both are deficiencies in infrastructure: the first, is the lack of a core diagnostic and prognostic imaging facility and the second, is the lack of a core facility for investigational and therapeutic viral vector production and development. In this award we set forth the objectives to set up two core facilities at the University of Tennessee Cancer Institute: One for the generation of PET biomarkers using microfluidic chemistry and validate their effectiveness for PET/CT-based monitoring of conventional and novel anticancer therapy in animal models; The other a viral vector core for the generation of investigational tools for anticancer therapies at UT Health Science Center Memphis. These cores laboratories have been set and we successfully completed a pilot project that involved the generation of B16/F10 melanoma cells modified by lentivirus-mediated gene therapy and the in vivo PET imaging of the tumor-bearing mice.

15. SUBJECT TERMS
cancer, gene therapy, positron-emission tomography (PET)

16. SECURITY CLASSIFICATION OF:			17. LIMITATION OF ABSTRACT	18. NUMBER OF PAGES	19a. NAME OF RESPONSIBLE PERSON
a. REPORT	b. ABSTRACT	c. THIS PAGE			USAMRMC
U	U	U	UU	62	19b. TELEPHONE NUMBER *(include area code)*

Table of Contents

Final Report: W81XWH-07-1-0248
Years 1 & 2

INTRODUCTION

This project set forth the goal to create the infrastructure for delivering and evaluating gene therapy based interventions against cancer.

The work was subdivided into tow segments. The first part was to develop a core for the synthesis of a new positron emitting (PET) tracer, 3'-Deoxy-3'-[^{18}F]fluorothymidine: ([^{18}F]FLT), to image cancer using PET tracer ^{18}FDG. The second part was for the development of a viral vector core (VVC) for the generation of recombinant viruses targeting cancer cells.

OBJECTIVE 1

Final report on preparing ^{18}F-FLT using micro-fluidic chemistry and the visualization of subcutaneous melanoma xenografts in mice at UTGSM

SOW 1. Microfluidic chemistry biomarker core (MCBC)

1. Design and fabricate microfluidic components
2 Design and fabricate micro HPLC components
3. Micro-PET/CT monitoring anti-cancer therapy using the B16 murine melanoma model – months

With the support of the DOD grant, we have developed and tested chemistry routes for the synthesis of 3'-Deoxy-3'-[^{18}F]fluorothymidine: ([^{18}F]FLT) using an automated microfluidic platform. In addition, we have evaluated the growth of the murine melanoma B16/F10 tumors in mice and examined methods to quantify in situ the tumor burden using micro positron emission tomography (PET) using [^{18}F]-2-fluoro-2-deoxy-D-glucose (FDG).

1. Infrastructure and Personnel

The PET biomarker core (PBC) facility is located in a dedicated PET imaging area which also houses organic chemistry laboratories, the Preclinical and Diagnostic Molecular Imaging Laboratory (PDMIL) and is adjacent to the recently completed PetNet production facility which supplies F-18 to the PBC generated on an RDS 111 (Eclipse HP) negative ion cyclotron with an 11-MeV proton energy. The laboratories within the PBC have recently been remodeled to provide areas dedicated to purification and analysis of biomarkers contiguous with the wet-lab that contains the hot-cell. To perform the synthesis of ^{18}FLT we purchased a Minuteman Liquid Flow Microchemistry platform (Advion Biosystems, Ithaca, NY). .

2. Microfluidic synthesis of ^{18}FLT

3'-Deoxy-3'-[^{18}F]fluorothymidine: ([^{18}F]FLT) is a structural analog of the DNA constituent, thymidine. [^{18}F]FLT is a radiolabeled imaging agent that has been proposed for investigating cellular proliferation with positron emission tomography (PET). Although [^{18}F]FLT is not

incorporated into DNA it is trapped in the cell, due to phosphorylation by thymidine kinase, a part of the proliferation pathway. As such it has the potential to image proliferating tumor due to the increase in DNA synthesis rate.

We have investigated two synthetic pathways using the NanoTek LF microfluidic synthesizer. The first involved the displacement of a nitrophenylsulfonyl group at the 3'-hydroxy position (Scheme 1). This labeling occurred in high yield in the microfluidic reactor; however the second phase of the synthesis, hydrolysis, was not nearly as efficient. A modified hydrolysis vessel was constructed and tested to provide [^{18}F]FLT for purification and QC. The overall yield of this process has been on the order of 55% from the start of synthesis.

Scheme 1: Synthesis of [^{18}F]FLT from 3-*N*-Boc-5'-*O*-dimethoxytrityl-3'-*O*-nosyl-thymidine.

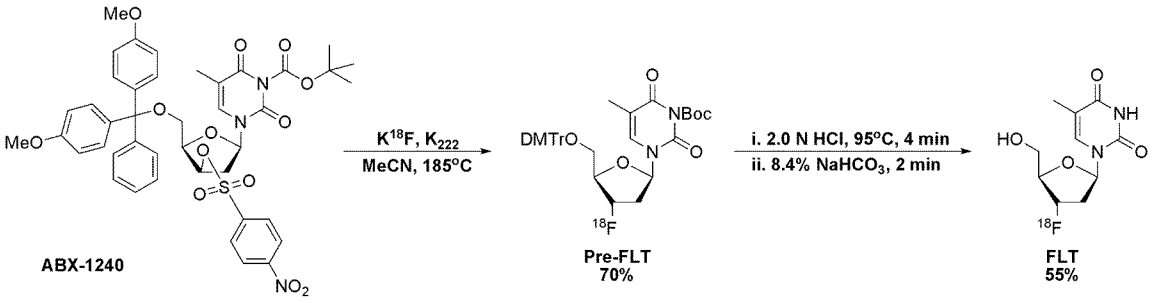

Our second approach began with the more common 5'-*O*-Benzoyl-2,3'-anhydrothymidine precursor (Scheme 2). The labeling step was problematic from the beginning. We used an array of solvents and found the best was DMSO, generating a modest 25% yield in the labeling step. This reaction, however, was not reproducible in the microfluidic reactor. The benzoyl deprotection, on the other hand, was a very efficient process using 2.0 N sodium hydroxide.

Scheme 2: Synthesis of [^{18}F]FLT from 5'-*O*-Benzoyl-2,3'-anhydrothymidine.

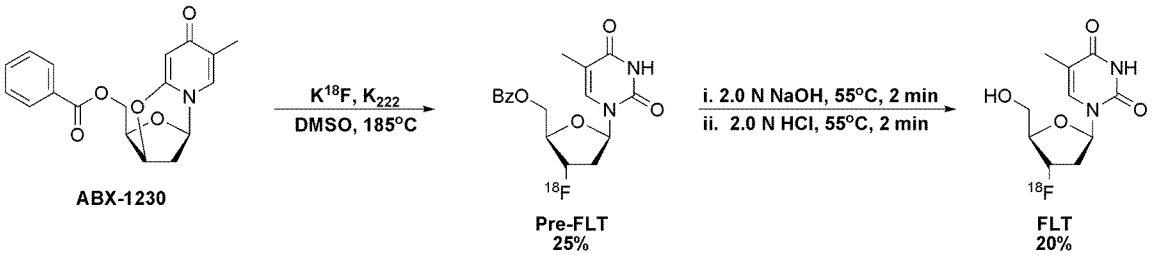

To aid purification of [^{18}F]FLT we directly connected an HPLC to the NanoTek LF unit (Figure 1). The [^{18}F]FLT final product solution was collected using a Waters® XTerra® column (150 x 3.4 mm) and a 5% ethanol (aq) mobile phase at 2.0 mL/min. The retention time was ~ 8-10 minutes.

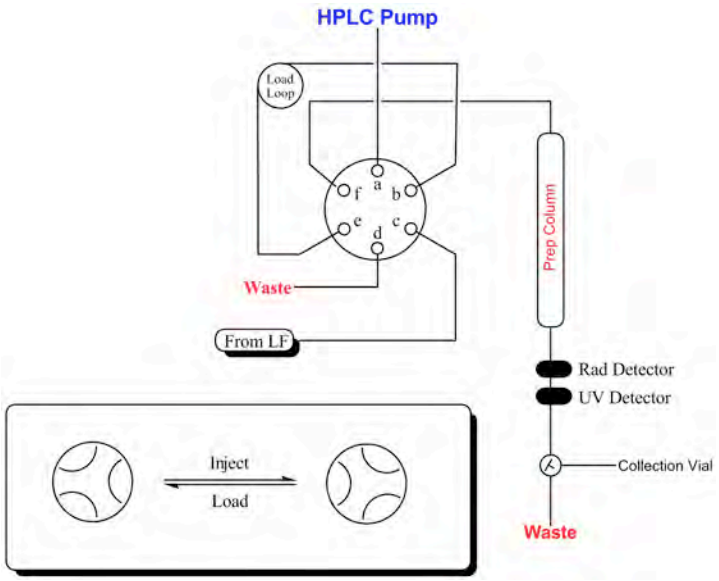

Figure 1: NanoTek LF to HPLC injector loop.

In collaboration with Dr. Giamis and his colleagues at Advion (formerly Nanotek Inc.) we also tested two different sets of automation that control the synthesis of [^{18}F]FLT:- Sequence Discovery (Figure 2) and Batch (Figure 3). The Sequence Discovery mode allows the operator the ability to quickly optimize labeling or hydrolysis reaction conditions. Unique to the Discovery modes is the joining of reagent flows at a “mixing T” prior to the reactor. As the reagents meet, in a laminar flow environment, the residence time and temperature in the reactor generate the products in high yield. The Batch mode involves the pre-mixing of the precursor and the dried [^{18}F]fluoride. The solution is then pumped through the reactor at the determined rate and temperature for optimal yield. This mode of operation will be used primarily for high radioactivity production runs.

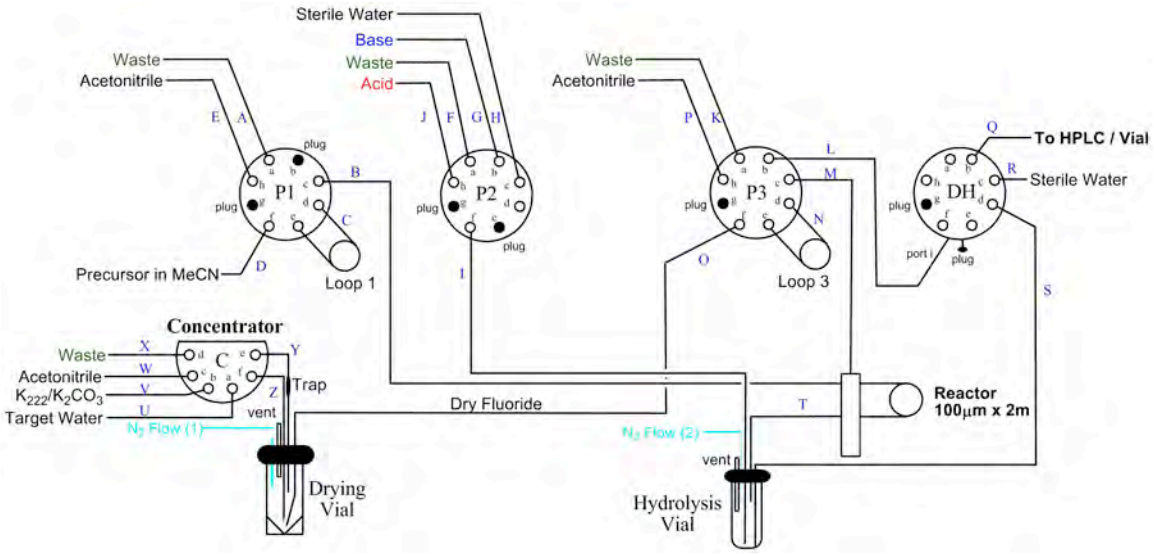

Figure 2: Sequence Discovery plumbing diagram.

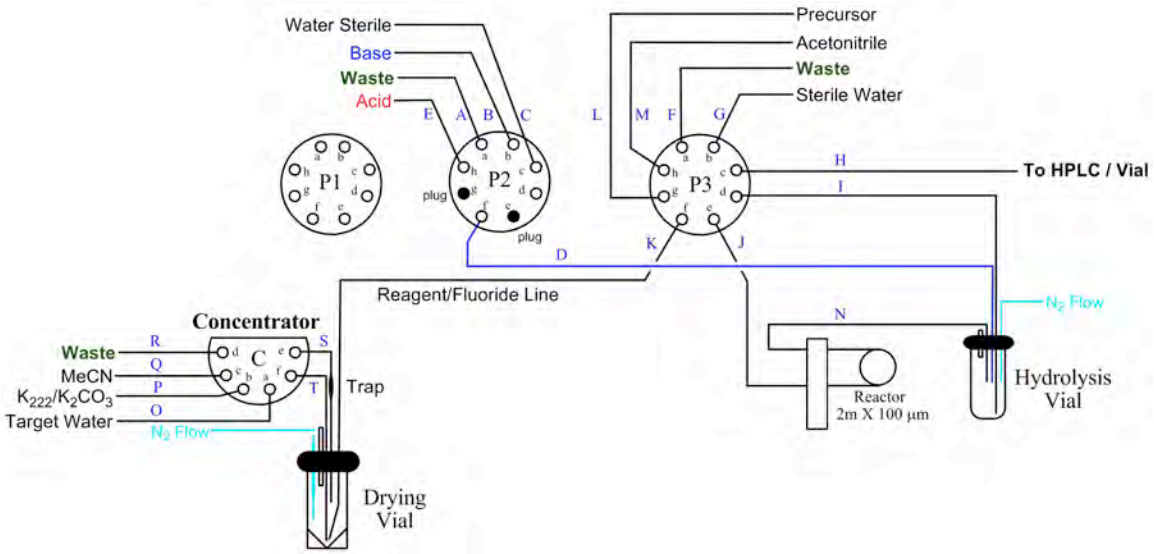

Figure 3: Batch plumbing diagram.

Before Advion/Nanotek left the labs at UTMCK, they were unable to produce a single dose of FLT for use in this project. For this reason, all of the work reported on imaging has been completed with the standard tracer [^{18}F]FDG supplied to the small animal imaging center by PET/NET, Inc (Knoxville, TN) for research purposes.

3. Preliminary Studies: Live PET imaging of B16/F10 xenografts in mice

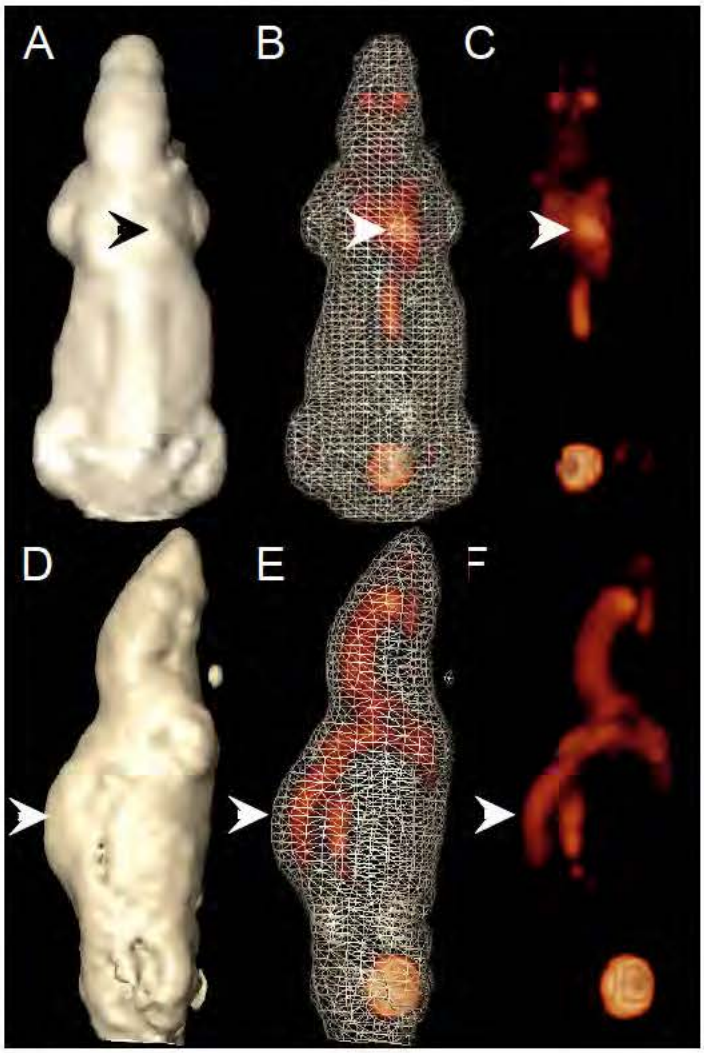

Figure 4. PET imaging of FDG in mice with B16/F10 tumors. ^{18}FDG injected iv was evidenced in the sc B16/F10 xenograft (arrowheads) in live mice using micro PET imaging. A & D) Volumetric representation of the mouse, B & E) Subcutaneous appearance of ^{18}FDG in the tumor, and C & F) ^{18}FDG PET activity image alone.

A major preliminary goal was to assess the ability of ^{18}FLT to image melanoma xenografts implanted in C57BL/6 mice and to further compare this with the commonly used biomarker ^{18}FDG. Unfortunately, ^{18}FLT was never produced by our Advion collaborators and thus we have focused our attention on the use of commercially available ^{18}FDG. C57Bl/6 mice were injected with 10^6 B16/F10 murine melanoma cell sc and left for 10 days. After this time, mice received ~300 µCi of ^{18}FDG (purchased from PetNet) and 30 min thereafter the mice were anesthetized using 1-3% isoflurane administered from a vaporizer in 2 L of oxygen and delivered through a nose-cone. The PET data were acquired using a microPET P4 apparatus (Siemens Preclinical Solutions, Knoxville, TN). The data were reconstructed using a 2D

ordered subset expectation maximization (OSEM) algorithm and are visualized using the image analysis software Amira.

The PET images revealed the presence of a subcutaneous lesion indicating uptake of [^{18}F]FDG in the lesions; however there was considerable accumulation within the interscapular brown fat, heart, and abdominal spine. Notably, the lungs were devoid of activity. We continued these experiments by introducing the B16/F10 cells iv to induce pulmonary lesions. These mice were imaged using ^{18}FDG in order to test the efficacy of this biomarker at imaging the small lesions that develop in the lungs over a 21 day period post-injection. In addition, a procedure was adopted that limited uptake of FDG in the brown fat of the test animals. ^{18}FDG was injected iv and the mice were immediately anesthetized with 3% isoflurane gas in a warmed chamber. After a 15 min uptake period, mice were sacrificed by isoflurane overdose. All subsequent images were acquired postmortem.

A standard procedure for cell growth, harvest and injection was established. Cell lines were received from Dr. Tigyi in the mail as viable cultures with the exception of B16F10 EV which was sent frozen. Cells were grown to ~80% confluency and samples were frozen in storage medium containing DMSO. For experiments, cells were recovered from frozen stocks, grown to 80% confluency and then released from the culture dish by trypsin treatment. Briefly, media was aspirated from the cells and they were washed once with sterile PBS. One mL of trypsin solution was added, the excess aspirated and the 100 mm dish put at 37° C for 5 min. The cells were then resuspended in 10 mL of growth medium containing FBS and a sample was taken for counting using a hemocytometer. The remainder of the cells were centrifuged at 1000× g for 5 min and then were suspended in PBS at a concentration of 6-7 × 10^5 cells per mL and the tube placed on ice. The usual cell yield was a little less than 10^7 cells per plate. The cells were then counted again and adjusted to the correct concentration by addition of appropriate amounts of PBS.

Female 8-12 week-old C57Bl6 mice were then warmed under a heat lamp and were administered 100 µL of the cell suspension iv from a 1 mL syringe with a 27g needle in a smooth infusion. The injections were completed within 30 min of cells being suspended in PBS. The cells remaining in the tube after injection were again counted on a hemocytometer to verify concentration and viability.

An initial experiment was performed to determine whether B16F10 tumor colonies in the lung could be detected at day 10 or day 14 post-injection. Groups of 4 or 5 mice were injected with either 1 × 10^4 or 5 × 10^4 parent B16F10 cells iv, as described above. At either 10 days or 14 days post-injection, animals were imaged using ^{18}FDG and then density of tumor colonies in the lung analyzed from histologic sections prepared using lung tissue obtained at necropsy. The PET images were all dominated by the significant uptake of the ^{18}FDG in the myocardium, associated with normal glucose utilization of the heart Analysis of the microPET images indicated that there was no obvious increase in lung ^{18}FDG content in animals injected with B16 F10 cells at either dose or at either time point, as compared to normal C57Bl6 mice. Subsequent analyses of histologic sections showed that lung colonies could be detected at day 10 in the mice that had received 5 × 10^4 cells, but that the colonies were very small (<0.5 mm). Even by day 14, the colonies were very small. At day 10 and day 14, lung colonies were observed in histologic lung sections in only 1 of 4 mice injected with 1 × 10^4 cells. These data indicated that PET imaging of lung tumors could only be achieved at time points later than 14 days post injections (e.g. 21 days) and furthermore that the sign ificant uptake of FDG in the heart would undoubtedly compromise our ability to quantify tumor burden in the lungs using this technique.

To determine the contribution of ^{18}FDG uptake in the lung, normal C57Bl/6 mice were injected with ^{18}FDG and PET images acquired 15 min post injection. The animals were then

sacrificed, the lungs inflated with 0.6 mL of Bouin's solution instilled through a 20G tracheal catheter, the heart lung block excised, the heart dissected away and PET images of the fixed lungs acquired ex vivo. A comparison of the ^{18}FDG content of lungs imaged in situ and ex vivo was made by quantifying the radioactivity in a region of interest encompadssing the lung tissue in both images. After decay correction, there was appeared to be 10-fold more ^{18}FDG in the lungs imaged in vivo as compared to lungs imaged in isolation. This indicated that the activity observed in lung region of interest was influenced dramatically by "shine" from ^{18}FDG uptake in other organs-particularly, but not limited to the heart. This complication persisted even when conservative segmentation of the lung distal from the heart was done. We concluded that detection of B16F10 tumor burden in lungs by in vivo PET scanning with ^{18}FDG would be significantly compromised by the high background associated with normal ^{18}FDG distribution in the heart and other organs spilling into the lung volume.

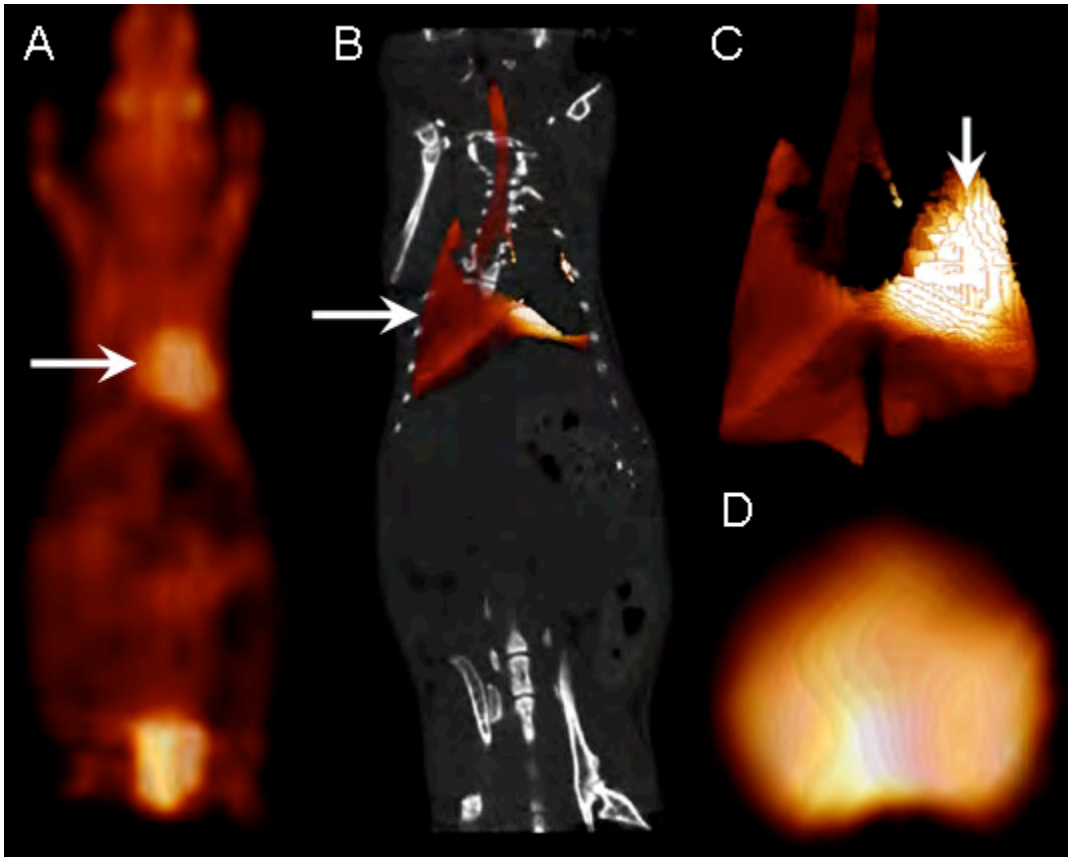

Figure 5. Quantification of pulmonary ^{18}FDG uptake in mice is complicated by "shine" from the heart and other organs. A) PET image of mouse indicating the myocardial uptake of tracer (arrow). B) 3D segmentation of the lung tissue was performed using the microCT images (arrow) and used to generate a pulmonary region of interest [ROI]. C) Image of PET activity associated with the pulmonary ROI – the shine from the heart is evidenced by the "hot spot" in one lobe (arrow). D) PET image of inflated lungs from the same mouse excised at necropsy - image were data acquired ex vivo and the ^{18}FDG activity appeared to be uniform and significantly different as compared to the images of the lung acquired in situ.

4. **Gene therapy of Cancers using PET-CT Monitoring**

SOW Gene therapy of Cancers using PET-CT Monitoring

1. Gene therapy of B16 melanoma using ATX shRNA and DN-STAT3 containing lentivirus in C57-BL6 mice monitored by micro-PET/CT.
2. Gene therapy of B16 melanoma using coinjection of ATX shRNA and DN-STAT3 containing lentiviruses in C57-BL6 mice monitored by micro-PET/CT.
3. Gene therapy of B16 melanoma using lentivirus containing tandem ATX shRNA and DN-STAT3 insert in C57-BL6 mice monitored by micro-PET/CT

4.1 Gene therapy of B16 melanoma using ATX shRNA and DN-STAT3-containing lentivirus in C57Bl/6 mice monitored by microPET/CT

Either normal C57Bl/6 mice or mice injected with 5 x 10^4 cells iv with 5 different cell lines (B16F10 parent; B16F10 B1; B16F10 SC; B16F10 STAT3 or B16F10 EV) were analyzed for lung colonies and scanned with FDG PET/CT. For scanning day 21 post cell injection, mice were injected iv with 600-1500 µCi of ^{18}FDG in 200 µL of PBS and then placed in 3% isoflurane in a warmed container for 15 min to allow for uptake. Six mice were injected with each cell line and 7 normal mice were analyzed in parallel. The animals were then sacrificed by exposure for 3 min to a lethal dose of isoflurane and the lungs were inflated with 0.6 mL of Bouins solution delivered through a 20G tracheal catheter and the trachea was then tied off with suture and the heart/lung block carefully excised and suspended, submerged, in Boiuns solution. After 30 min, the heart, thymus and any other extraneous material was removed and the ^{18}FDG radioactivity associated with the fixed lung counted (time noted) in a CAPINTEC dose calibrator before microPET images were acquired using a P4 microPET scanner. After images were acquired, the radioactivity in the whole samples was measured in a gamma scintillation counter, and digital pictures of the fixed lungs were taken to document the surface tumor density and gross pathological features. Individual lobes of the fixed lung were inspected for colonies and then prepared for paraffin sectioning. Single 6-µm thick sections of all lung lobes, stained with hematoxylin and eosin were examined microscopically and tumor colonies counted. Lung radioactivity determined either in the CAPINTEC or the gamma scintillation counter was corrected for F-18 decay to the time of injection of the original dose.

PET/CT scanning:
It was determined in pilot experiments reported earlier that the high activity of the heart and accessory tissue in the heart-lung block dominated the activity in the lungs even when animals had relatively high tumor burden. For this reason, the protocol described above was adopted to assess whether individual pulmonary tumor colonies could be imaged and further, to test our hypothesis that the total lung burden of ^{18}FDG correlated positively and linearly with tumor burden as assessed by manual colony counting. In certain groups of animals there was a weak correlation between residual pulmonary radioactivity at 30 min post-injection and the number of colonies observed manually; however, this did not hold true for all cell groups and was not considered a suitable way to measure tumor burden (Fig. 6). Selected PET images of high tumor burden lung (Fig 7) showed slightly enhanced lung images when compared with normal control animals; however, the individual tumors could not be resolved. This is not surprising since the tumors range in size from pinpoint to about 2 mm in diameter. The resolution of the P4 microPET instrument is about 2 mm under optimal conditions of boundaries and high radioactivity.

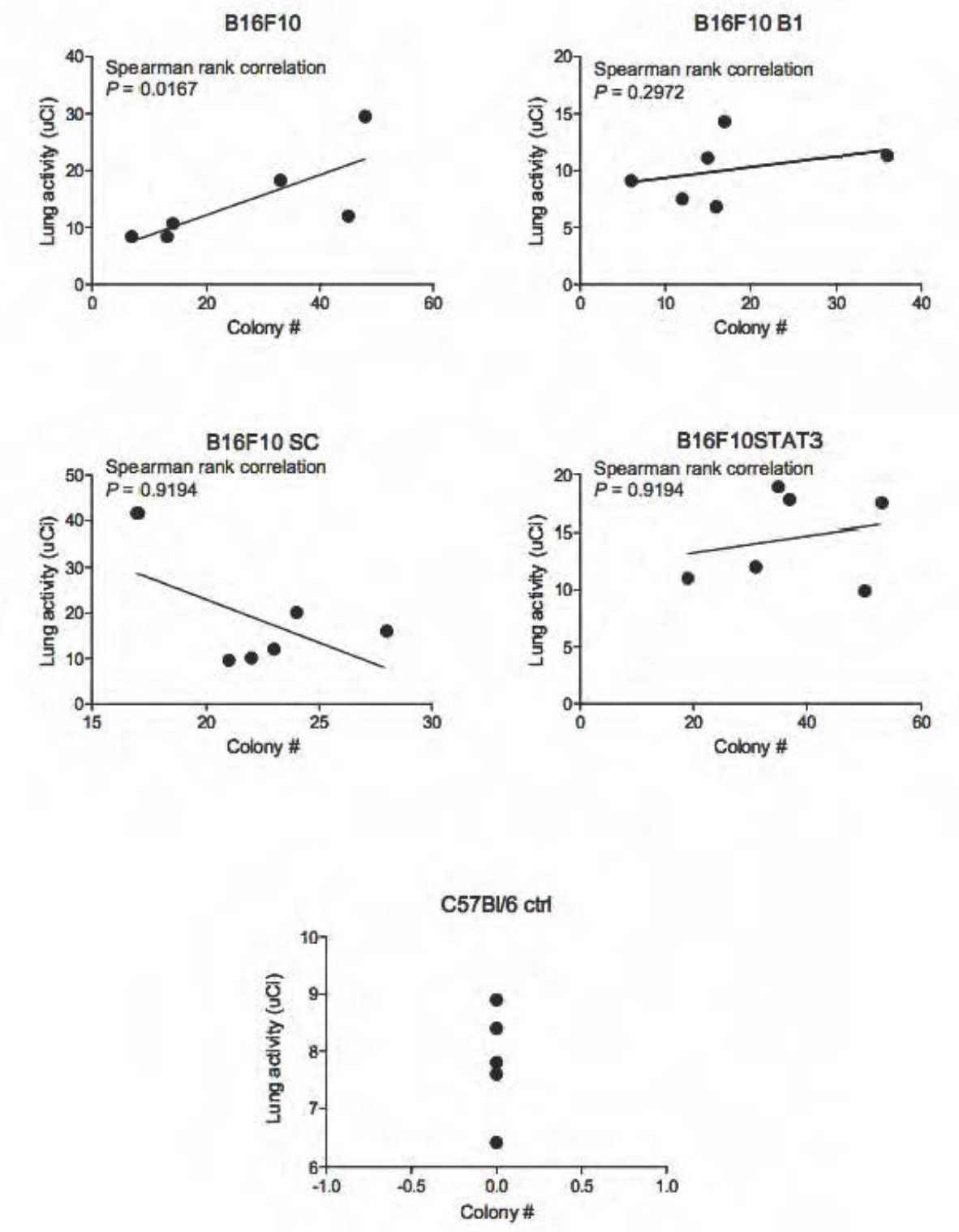

Figure 6. Correlation analysis of pulmonary tumor colony number with the ^{18}FDG-associated radioactivity in excised mouse lungs. A positive and significant correlation ($P < 0.025$) was observed only for the mice injected with parental B16F10 cells

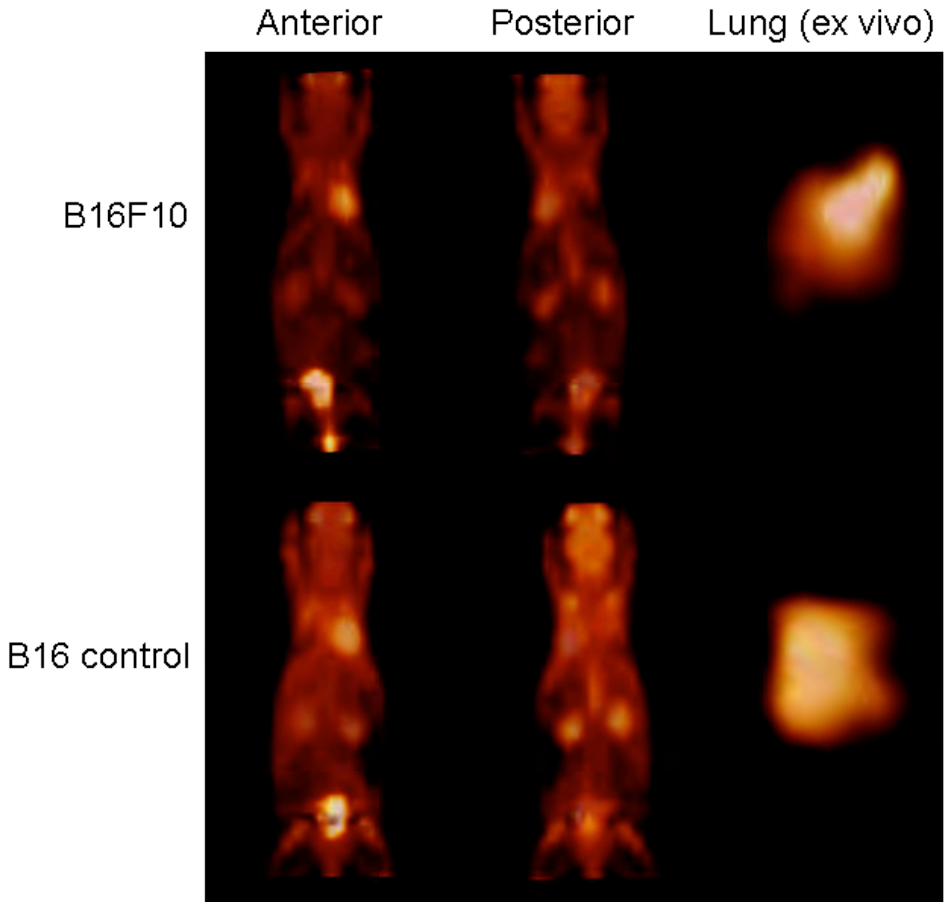

Figure 7. Example of microPET images of lungs in sittu and ex vivo from mice with high (B16F10) and no (B16 control) lung-tumor burden. The B16F10 mouse had 14 colonies counted grossly, 4 colonies found histologically. It retained 10.7 µCi from a total of 991 µCi injected (~ 1% of the decay-corrected injected dose). No colonies were observed either grossly or histologically in the control mouse, which retained approximately the same % injected dose in the lungs.

5. Tumor colony counting

Tumors were counted from gross examination of fixed lung (see Fig. 8) separated lobes or from single slice histology slides crossing the major cross sections of embedded lung lobes for several different experiments (Fig. 9). The gross colony counts varied significantly from animal to animal within a group. The colony range was nearly as great as the range for all experimental groups of animals resulting in very large standard deviations from the average. Furthermore, colony size varied dramatically as mentioned above. In some instances, particularly with the STAT3 cells, both white and black colonies were observed indicating that some tumors had lost melanin expression for unknown reasons (Fig. 10). Colony counts from histology slides also varied widely with a poor correlation of these numbers with numbers collected from gross colony counting. These variations resulted in average colony counts per experimental animal group that were not statistically different from each other. Neither the colony count nor the residual FDG in the lungs gave a reliable method of quantitation of lung tumor burden.

		COLONIES		
B16F10 (3/9/09)	Injected Dose (µCi)	Gross	Histology	Recovered lung activity (µCi; γ counter)
1	991	13	4	8.4
2	1290	33	13	18.3
3	1072	7	3	8.4
4	1080	45	15	12
5	1000	48	20	29.5
6	1188	14	4	10.7
B16F10 B1 (3/9/09)				
1	1040	17	10	14.3
2	1090	16	3	6.8
3	1280	6	4	9.1
4	1281	15	9	11.1
5	1296	12	8	7.5
6	1439	36	7	11.3
B16F10 SC (3/9/09)				
1	1170	23	4	12
2	1220	17	14	41.6
3	1570	24	11	20.1
4	1270	21	5	9.6
5	1120	22	6	10.1
6	1170	28	9	16
B16F10 STAT3 (3/10/09)				
1	990	19	7	11
2	1110	50	14	9.9
3	960	53	26	17.5
4	1060	31	11	12
5	1200	37	16	17.8
6	1350	35	13	18.9
C57Bl/6 normal 3/10/09				
1	1360	0	0	8.9
2	1470	0	0	7.6
3	1200	0	0	7.8
4	1200	0	0	8.4
5	1140	0	0	6.4
C57Bl/6 EV 3/25/09				(from dose calibrator)
1	720	9	1	4
2	750	27	9	6

3	600	9	12	4
4	620	7	2	4
5	850	9	12	6
6	870	33	7	6
C57Bl/6 normal 3/25/09				
1	870	0	0	3
2	850	0	0	4

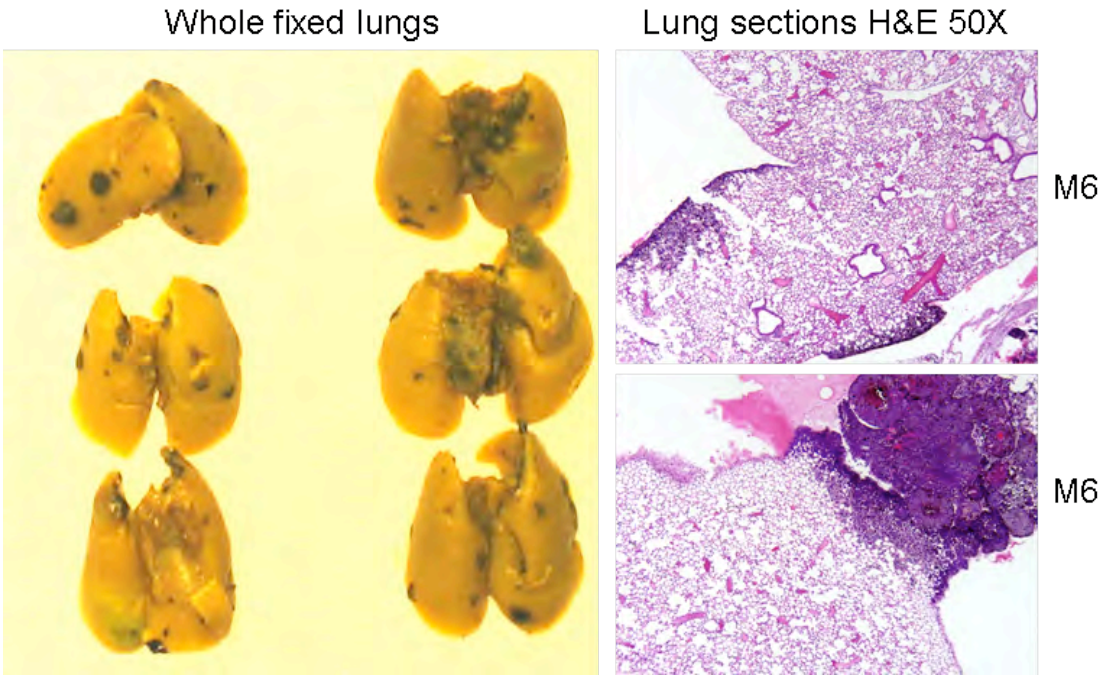

Figure (8).

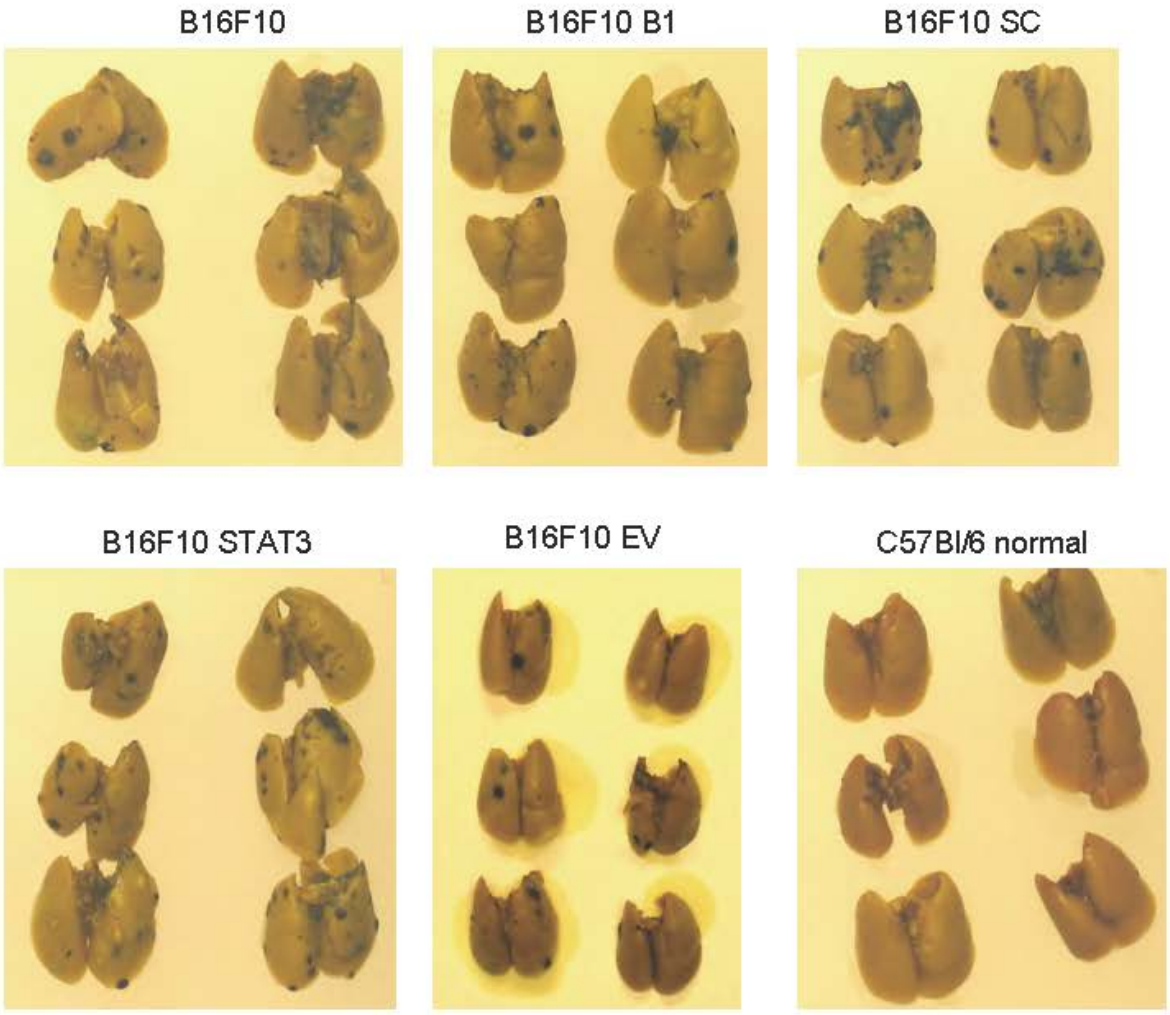
B16F10
B16F10 B1
B16F10 SC
B16F10 STAT3
B16F10 EV
C57Bl/6 normal

Figure 9.

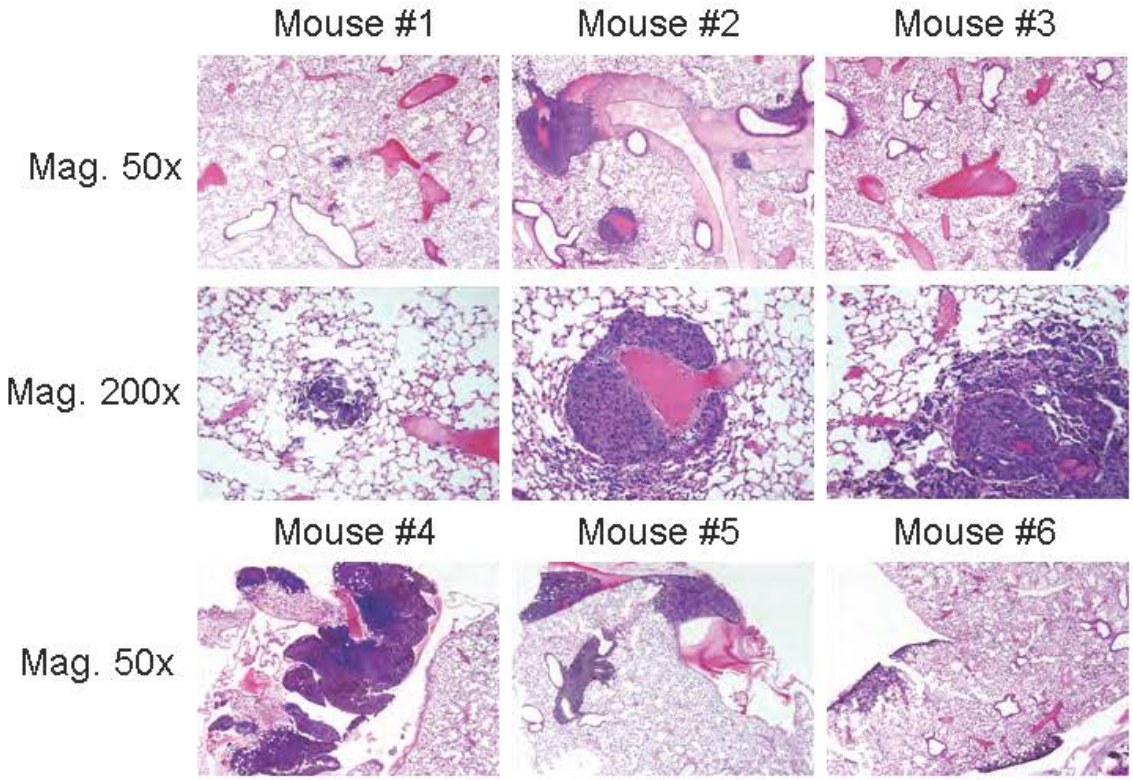
Mouse #1
Mouse #2
Mouse #3
Mag. 50x
Mag. 200x
Mouse #4
Mouse #5
Mouse #6
Mag. 50x

Figure 10.

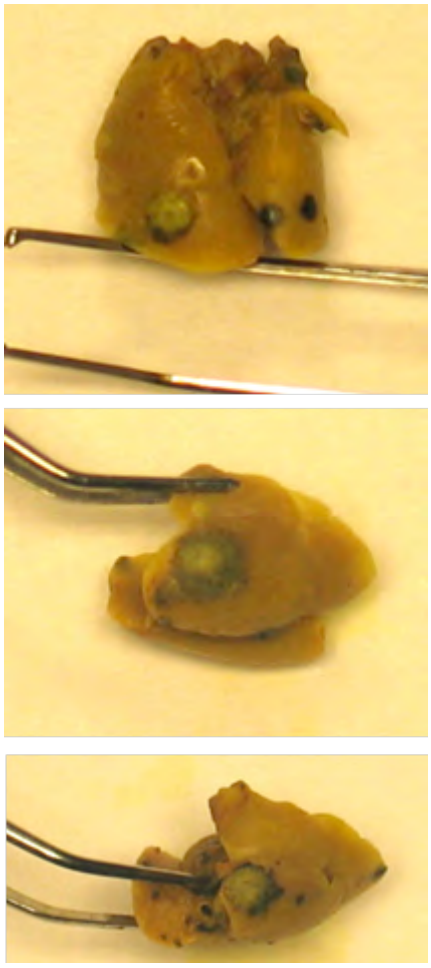

Figure 11.

OBJECTIVE 2. SET UP OF THE VIRAL VECTOR CORE FACILITY (VVC) FOR THE GENERATION OF INVESTIGATIONAL TOOLS FOR ANTICANCER THERAPIES AT UT HEALTH SCIENCE CENTER MEMPHIS (UTHSC).

SOW <u>Viral Vector Core (VVC)</u>

1. Set up core and obtain regulatory approvals
2. Construction of vectors with ATX shRNA and DN-STAT3 inserts
3. Construction of replication defective Adenovirus with fiber modifications
4. Production of lentiviral vectors with ATX shRNA and DN-STAT3
5. Production of fiber modified replication defective Adenovirus
6. Construction of a tandem vector with both ATX shRNA and DN-STAT3 inserts
7. Production of tandem ATX shRNA and DN-STAT3 vectors
9. Production of conditionally replicating oncolytic adenovirus vectors

2.1. Set up core and obtain regulatory approvals.

The VVC was conceived as a critical partnership between UTCI investigators and experienced virologists and viral vector production staff for the purpose of producing quality-controlled stocks of viral vectors as investigational tools for cancer research and as novel anti-cancer therapeutics. In addition to production of viral vectors, the VVC would provide critical services to UTCI cancer researchers that would enable them to use the viral vectors. These enabling services included assisting in selecting the appropriate viral vector system, planning the plasmid constructions for vector production, providing methods for transduction of cells *in vitro* and *in vivo*, performing quality control of vector productions (titration of vectors and testing for replication competent recombinants in the case of lentiviral vectors and replication defective adenoviral vectors) and training personnel in investigator's laboratories in the safe use of viral vectors.

Infrastructure of VVC completed. The UTHSC administration assigned the VVC core laboratory three rooms (276, 278 and 279) in the new Cancer Research Building (formerly the Basic Science Building) at 19 Manasses Street on campus. Room 279 is a 500 sq ft wet bench laboratory and Rooms 276 and 278 are adjacent BSL2 cell culture rooms across the hall from the wet bench laboratory. In addition, an 80 sq ft office nearby was also assigned to the VVC. Dr. Albritton participated in the final stages of architectural planning for the Cancer Research Building and designed this suite of rooms specifically to accommodate a viral vector core facility. We set up the BSL1 wet bench lab in room 279 for construction of lentiviral and adenoviral vectors using standard molecular biology techniques. This wet bench lab has been fully functional since September, 2007. We furnished it with a thermal cycling machine for PCR, three gel electrophoresis units, two electrophoresis power supplies, two table-top microcentrifuges, a microwave oven, two heat blocks, a pH meter, a water bath, a -20 °C freezer, a refrigerator, vortex, two sets of pipetman, a shaking water bath, and a 37 °C incubator.

In rooms 276 and 278, we established the BSL2 level tissue culture facilities for production of viral vectors. Both rooms have been fully functional since September 2007. Room 278 does not have direct access to the common hallway; access is through room 276. Taking advantage of this physical arrangement we set up two biosafety cabinets in the inner room 278, one for use in lentiviral vector production and the other for adenoviral vector production. This room also contains a refrigerated low speed table-top centrifuge with seal rotor buckets, an inverted phase light microscope and two stacked CO_2 incubators (one for lentivirus producing cultures and one for adenovirus producing cultures). The outer room 276 was set up for maintaining cell lines and adeno-associated viral vector production. It contains a biosafety cabinet and an ultracentrifuge. In the common equipment room 204, we have a -80 °C freezer and one cell storage unit.

Personnel hired. We hired three people to staff the vector core facility. The first individual hired was Junming Yue, Ph.D. as Director of the core facility in charge of the daily operation of this core laboratory. Dr. Albritton is Scientific Director of the core. Dr. Yue was previously a managing director of a viral vector core at the University of Pittsburgh specializing in lentiviral vector production. The second individual hired was a senior research assistant Axia Ren, Ph.D., and the third a research assistant Sravya Penmatsa, B.S. Dr. Ren's expertise is in adenoviral vector construction and production. Ms. Penmatsa is experienced in molecular biology and cell culture techniques.Dr. Yue supervised Dr. Ren and Ms. Penmatsa on a daily basis and Dr. Albritton met with the staff once weekly to review progress and plans.

Regulatory approvals obtained. The VVC laboratory applied for registrations of lentiviral and adenoviral vector construction and production. Dr. Albritton worked with Ms. Francine Rogers, the university Biosafety Officer (BSO), to develop a plan that gives flexibility to vector core for large numbers of productions and at the same time provides scrutiny of the individual viral genome constructs and their intended use. The Institutional Biosafety Committee (IBC) of the UTHSC approved a three year registration to construct and produce lentiviral vectors and a separate three year registration to construct and produce adenoviral vectors. The order form for requesting viral vectors from the VVC contains a section that requests the faculty investigator provide the approval date and registration number for registration to possess and use the viral vector, and if vectors will be used in animals then the date of approval and protocol number from the Institutional Animal Care and Use Committee (IACUC). Immediately after a completed order form is received, it is forwarded to the BSO for her signature verifying that the IBC and IACUC approvals are current and cover the use of that viral vector. The BSO returned the signed vector request form to Dr. Yue at the VVC and then he schedules the construction and production of the vector order. In cases where the faculty investigator leaves this section blank or states that no current registration is available, Dr. Yue contacts the faculty to offer assistance in the

preparation of regulatory approvals and works with the BSO to help the faculty in their preparation.

Advertising the VVC services to the UTHSC research community. The new core facility was introduced to faculty and research staff in three phases. In the initial phase Dr. Yue discussed the core and its services with individual faculty identified by Drs. Tigyi, Pfeffer and Albritton as potential clients for the core facility. The second phase broadened our outreach to include all faculty and researchers at UTHSC. Drs. Yue and Albritton gave departmental seminars describing the vector core, its location, and the services it provides as well as a giving a brief introduction to each of the vector types and presenting data obtained using viral vectors constructed and produced at the new UTHSC core facility. Dr. Yue posted on bulletin boards throughout the campus a one page flyer announcing the vector core services and Dr. Albritton wrote an article for the monthly university research newsletter *Research Notes*. In the third phase Drs. Albritton and Yue designed webpages for the vector core and these were posted with links to the webpages on the university Clinical & Translational Science Institute (CTSI) webpages at https://ctsi.utmem.edu/viralvector/index.php and the Research Administration webpages at http://www.utmem.edu/research/research_resources/viral_vector/index.php. The order request form is available as a download from these vector core webpages. In addition to services provided the webpages include contact information and the location of the core facility.

Services provided by the VVC to faculty investigators at UTHSC during the funding period of May 1, 2007 to April 30, 2009. The vector core exceeded its milestones in extending services to UTHSC faculty. As the core facility staff completed construction and production of the sets of viral vectors committed to the research investigations of the anti-tumor activity of anti-autotaxin silencing RNA and the dominant negative STAT3, the core facility began providing services to faculty investigators throughout the UTHSC. While we had planned to begin providing these services in the last months of the funding period, progress in setting up the vector core and producing vectors for the B16 melanoma studies was more rapid than we anticipated and we were able to open the core to services by faculty much sooner than planned. Lentiviral vectors became available beginning in April 2008 and adenoviral vectors beginning in September 2008. The core also began providing Letters of Support for faculty grant applications, biosafety training for use of viral vectors and assistance in experimental design and regulatory approval for vector use in June 2008. The services are available to faculty on the three medical campuses of UTHSC located in Memphis, Knoxville and Chatanooga, TN. Table 1 shows the UTHSC faculty clients served including those services planned in the funded application. Specific services provided to these clients are listed in Table 2. Table 3 lists services by investigator and vector type and Table 4 lists the services for preparation of grant applications.

In addition to providing core services to the faculty, Dr. Albritton designed and Dr. Yue constructed two specialized lentiviral vectors that are now available as valuable investigational tools for cancer researchers at UTHSC. Both new vectors use state-of-the-art technology in which a short sequence encodes a copy of the 2a “self-cleaving” or “ribosome skip” peptide from a picornavirus. The first vector was LV-X-2a-EGFP, a lentiviral vector into which any gene of interest can be inserted in front of enhanced green fluorescent protein (EGFP) with the 2a peptide in between so that the two proteins express as separate molecules in stoichiometric amounts. Tumor cells expressing this vector can be visualized in in vitro experiments using fluorescence. The second new vector resource LV-Luc2-2a-mKate2 expresses two reporter genes: a Luc2, the latest most powerful version of the firefly luciferase gene; and mKate2, a far-red shifted fluorescent protein separated by the 2a peptide. The resulting Luc2-2a-mKate2 fusion gene expresses both reporter genes in stoichiometric quantities. Tumor lines infected by this new lentiviral vector can be transplanted into mouse models and the implanted cells detected by live whole body imaging in the IVIS Xenogen system currently operational in the first floor of the Cancer Research Building. The imaging system detects luciferase by chemiluminescence and mKate2 by fluorescence. mKate2 is particularly powerful addition for cancer researchers since its excitation and emission wavelengths are not absorbed well by hemoglobin in the mice.

Table 1. Faculty clients served by the Viral Vector Core.		
College	Department	Number of faculty clients
College of Medicine	Department of Anatomy and Neurobiology	1
College of Medicine	Department of Medicine	2
College of Medicine	Department of Molecular Sciences	2
College of Medicine	Department of Pathology	4
College of Medicine	Department of Pharmacology	2
College of Medicine	Department of Physiology	2
	Total Clients	13 .

Table 2. Services provided to UTHSC faculty.	
Type of Service	Quantity
Production of quality-controlled stocks of viral vectors.	28
Standardized RCL assays for replication-competent lentivirus.	5
Assistance in grant application with experimental design section.	7
Letters of Support for grant applications.	9

Table 3. April 1, 2008 – April 30, 2009. Viral vector production services provided to UTHSC faculty.

DEPARTMENT	FACULTY	NUMBER of LENTIVIRAL VECTORS
Anatomy and Neurobiology	Thomas Schikorski	1
Medicine	Lisa Jennings	2
Medicine	Bo Tang	2
Molecular Sciences	Tony Marion	1
Molecular Sciences	Lorraine Albritton	2
Pathology	Yi Lu	1
Pathology	Larry Pfeffer	6
Pathology	Tiffany Seagroves	1
Pathology	Andrzej Slominski	1
Pharmacology	K. U. Malik	1
Pharmacology	Ed Parks	1
Physiology	A. P. Naren & Leonard Johnson	1
Physiology	Gabor Tigyi	7
Viral Vector Core Resource	(LV-Luc2-2a-mKate2 and LV-X-2a-EGFP)	2

Table 4. April 1, 2008 – April 30, 2009. Grant application services provided by VVC to UTHSC faculty:				
DEPARTMENT	FACULTY	TYPE OF SERVICE		STATUS
Medicine	Lisa Jennings	Experiment design & use of lentiviral vectors.	Letter of Support	Pending
Pediatrics	Russell Chesney & Xiaobin Han	Experiment design & use of lentiviral vectors.	Letter of Support	Resubmit
Pathology	Andrjez Slominski	Experiment design for lentiviral vector.	Letter of Support	Pending
Pathology	Lawrence Pfeffer	Experiment design for lentiviral vector.	Letter of Support	In Prep
Pathology	Yi Lu	Experiment design for lentiviral vector.	Letter of Support	Not Funded
Pharmacology	K. U. Malik	Experiment design for lentiviral vector for two separate grant applications.	Letters of Support (2)	1 Funded & 1 in prep
Physiology	Gabor Tigyi	Experiment design & use of lentiviral vectors.	Letter of Support	Funded
Pharmaceutical Sciences (Pharmacy)	John Buolamwini	Experiment design for lentiviral vector.	Letter of Support	Pending

Cost recovery plan for long term maintenance of the VVC. The original long term plan for maintaining operation of the VVC was to be through cost sharing by a core set of six to eight cancer investigators who would each budget 10-20% of the Director's salary, 25-50% of a Research Associate's salary and 50% of a Technician's salary on their five year grant awards. However, we discovered that there was a much larger base of faculty whose research would benefit from the core facility services and in order to serve them effectively we adapted a cost recovery schedule, that is a fee for service schedule. This was possible primarily because Dr. Yue obtained a set of lentiviral vector plasmids and genome that was not covered by a restrictive Materials Transfer Agreement and so could be propagated and cost recovered for vector construction using these plasmids.

Projected long term use of the Viral Vector Core Facility. On May 1, 2009 the core facility moved to the cost recovery system. A total of 25 clients signed a list of faculty who will order services from the core for the university's fiscal year July 1, 2009 to June 30, 2010. This almost doubles the number of faculty clients that will be served by the core facility and we expect to continue to grow our client numbers as grant applications submitted with Letters of Support from the core are funded and the work begins. The breadth of faculty using the core facility will also expand next year and importantly will bring our first faculty from the Veterans Administration Medical Center adjacent to the UTHSC campus in Memphis, TN. Table 5 lists the number of colleges and departments served that will be served.

Table 5. Projected faculty clients fiscal year July 1, 2009 – June 30, 2010.		
College	Department	Number of faculty clients
College of Medicine	Department of Anatomy and Neurobiology	1
College of Medicine	Department of Medicine	1
College of Medicine	Department of Molecular Sciences	1
College of Medicine	Department of Pathology	6
College of Medicine	Department of Pharmacology	5
College of Pharmacy	Department of Pharmaceutical Sciences	1
College of Dentistry	Dental Research Center	1
VA Medical Center		1
College of Medicine	Department of Physiology	8
	Total Projected Clients	25 .

2.2. Lentiviral Vector system (SOW 2-7)

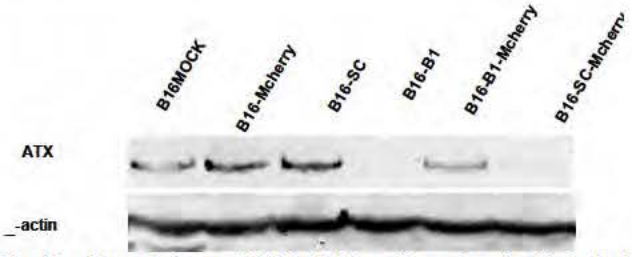

Fig.12 Knockdown ATX in B16 cells using lentiviral shRNA. (B16 SC: scramble shRNA transduced B16 cells; B16-B1: lentiviral shRNA against ATX transduced B16 cells)

The lentiviral vectors for gene overexpression and gene knockdown using shRNA or miRNA have been constructed and tested. First we produced autotaxin (ATX) shRNA and scrambled lenitviral vectors. The ATX lenti-shRNA have been transduced into B16 melanoma cells and MDA-231 cells. The endogenous ATX expression was greatly reduced in ATX lenti-shRNA transduced B16 cells compared with the cells transduced with scrambled shRNA (Fig.12). The miRNA mediated ATX knockdown vector has also been generated. In an initial test we observed dramatic knockdown of ATX expression.

In addition, we have constructed EGFP, lysophosphatic acid (LPA) and four more mutant lentiviral vectors. The stable expression cell lines have been established using these vectors. The EGFP lentiviral vector has been used to transduce several different cell lines, such as mouse fibroblasts, rat intestinal epithelial cells, rat smooth muscle cells, which resulted in transduction efficiency of more than 95% in all cell lines examined.

We also constructed a doxycline induced lentiviral vector system, which showed no background leakiness. We tested this system in MDA-231 cells using EGFP reporter gene, which a robust EGFP expression was induced with the doxycline at a concentration of 1ug/ml (Fig.13).

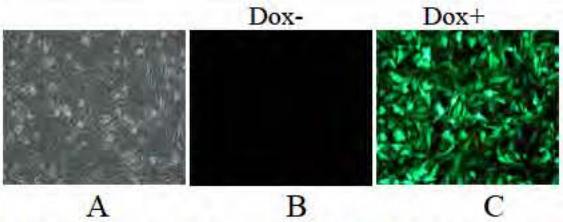

Fig.13 Doxcycline induced EGFP expression in lentivral vector transduced MDA-231 cells.
(A: MDA-231 cells under light field, B: no doxcycline, C: with doxycline)

As proposed in this grant, The VVC has constructed a STAT3, a dominant-negative STAT3 (DN-STAT3), as well as two additional mutant STAT3 lentiviral vectors. All four mutant STAT3 constructs have been transduced into mouse fibroblasts with high efficiency (~90%.) By immunoblotting we have determined that transduced cells have high and stable expression of STAT3 (Fig. 14).

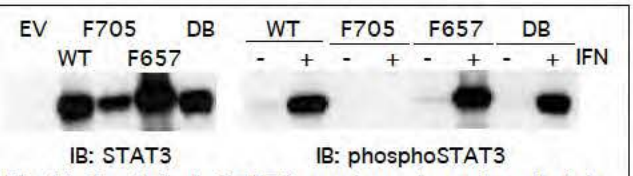

Fig.14 Lentiviral STAT3 vectors transduced into STAT3- mouse embryo fibroblasts. (EV: empty vector; WT: wild type STAT3, F705: STAT3 mutation in tyrosine phosphorylation site, F657: STAT3 mutation in putative PI3K binding site; and DB: STAT3 mutation in putative DNA binding site.). Cells were treated in the absence or presence of interferon (IFN) and immunoblotted with Abs against STAT3 or phospho-STAT3.

3. Adenoviral vector system

The VVC has constructed adenoviral vector systems for gene expression, shRNA-based gene knockdown and doxycline-inducible gene expression and miRNA-mediated gene knockdown systems.

For gene overexpression and shRNA-mediated gene knockdown, the gene of interest can be subcloned into multiple cloning sites and driven by CMV promoter in a shuttle vector with the adeno-Easy system. The polymerase III promoter H1 and U6 promoter has been inserted in a shuttle vector and are ready to express shRNA in the proposed studies to knockdown gene expression.

We have also constructed a single adeno-genome vector for doxycline-inducible expression that the reverse transactivator rtTA3, a third generation production has been inserted in E3 region, and the gene of interest is inserted in E1 region of adenogenome. We have validated the inducibility of this system with a EGFP reporter gene. The replication defective viruses produced can efficiently transduce human HeLa cells (Fig.15) rat smooth muscle cells following the doxycline treatment.

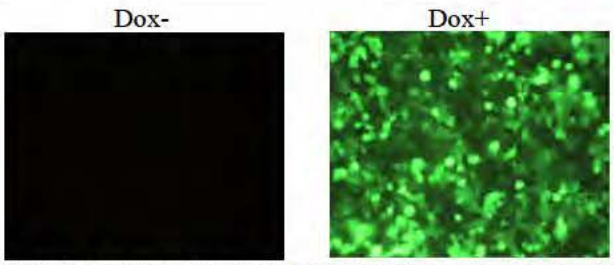

Fig.15 Doxycline induced EGFP expression in Hela cells transduced with a single adenoviral genome vector

We also established a miR-21 based doxcycline gene knockdown adenoviral vector. We found that this system can efficiently knockdown the expression of an EGFP reporter after induction with doxycline.

KEY RESEARCH ACCOMPLISHMENTS

1. Microfluidic chemistry core was set up. Two synthetic pathways for the synthesis of 3'-Deoxy-3'-[^{18}F]fluorothymidine using the NanoTek LF microfluidic synthesizer have been established.
2. Live imaging of C57Bl/6 mice injected with 10^6 B16/F10 murine melanoma cells using ^{18}FDG has been accomplished for the first time.
3. Live imaging of genetically modified B16/F10 cells expressing shRNA to ATX, dnSTAT3, or both has been accomplished.
4. The VVC has been established and obtained regulatory approval.
5. The VVC has produced lentiviruses using the sh-RNA to autotaxin and a dominant negative STAT3 constructs.
6. An adenovirus-based doxycline-inducible gene expression and miRNA-mediated gene knockdown system has been developed.
7. The kockdown of ATX expression by lentivirus-mediated sh-RNA treatments has been validated in vitro and in vivo.
8. Lentiviral delivery and stable expression of STAT3 constructs has been validated in vitro and in vivo.
9. Plans are in place for the long-term operation of the VVC.

REPORTABLE OUTCOMES

Paper:
Shuyu E, Yun-Ju Lai, Ryoko Tsukahara, Chen-Shan Chen, Yuko Fujiwara, Junming Yue, Huazhang Guo, Akio Kihara, Gábor Tigyi and Fang-Tsyr Lin. The LPA_2 Receptor-Mediated Supramolecular Complex Formation Regulates Its Antiapoptotic Signaling (2009) J. Biol. Chem. Mar 17. [Epub ahead of print] – in press

Manuscript submitted:
Aixia Ren, Sravya Penmatsa, Lorraine M. Albritton, Gabor Tigyi, Junming Yue, A tightly regulated single genome Tet-On adenoviral vector. – submitted to Biotechology Letters

Invention Disclosures:

1. Lentiviral vector mediated antagomiR-21 in cancer and cardiovascular disease gene therapy

2. MicroRNA-21 (miR-21)-based gene knockdown system

CONCLUSION

This award has enabled the creation of critical and formerly non-existing infrastructure for the synthesis of a new PET tracers and the generation of recombinant viruses. In vitro and in vivo proof of principle experiments validated the effectiveness of gene delivery using the viruses. In vivo proof of principle of tumor labeling and PET imaging using 3'-Deoxy-3'-[^{18}F]fluorodeoxyglucose has been achieved.

LIST OF PERSONNEL

UTHSC – Memphis
Gabor Tigyi, M.D., Ph.D. – PI
Lawrence Pfeffer, Ph.D. – Co-PO
Lorraine Albritton, Ph.D. –Co-PI
Junming Yue, MD, Ph.D. – Investigator
Axia Ren – Research Technician
Sravya Penmatsa – Research Technician

UTHSC – Knoxville
David Townsend, Ph.D. – Co-PO
Jonathan S. Wall, Ph.D. – Investigator
Stephen J. Kennel, Ph.D. – Investigator
Alan Stuckey, Ph.D. – Investigator
Claude Nahmias, M.D. – Investigator
Jay Wimalasena, Ph.D. – Investigator
Claude Nahmias, M.D. – Investigator
Weimin Miao, Ph.D. – Investigator

THE JOURNAL OF BIOLOGICAL CHEMISTRY VOL. 284, NO. ??, pp. 1–xxx, ???? ??, 2009

The Lysophosphatidic Acid 2 Receptor-mediated Supramolecular Complex Formation Regulates Its Antiapoptotic Effect*[S]

Received for publication, January 9, 2009, and in revised form, February 23, 2009 Published, JBC Papers in Press, March 17, 2009, DOI 10.1074/jbc.M900185200

Shuyu E[‡1], Yun-Ju Lai[§1], Ryoko Tsukahara[‡], Chen-Shan Chen[§], Yuko Fujiwara[‡], Junming Yue[‡], Jei-Hwa Yu[¶], Huazhang Guo[‡], Akio Kihara[‖], Gábor Tigyi[‡2], and Fang-Tsyr Lin[§3]

From the [‡]Department of Physiology, University of Tennessee Health Science Center, Memphis, Tennessee 38163, the Departments of [§]Cell Biology and [¶]Biochemistry and Molecular Genetics, University of Alabama, Birmingham, Alabama 35294, and the [‖]Laboratory of Biomembrane and Biofunctional Chemistry, Faculty of Pharmaceutical Sciences, Hokkaido University, Kita 12-jo, Nishi 6-choume, Kita-ku, Sapporo 060-0812, Japan

AQ: A

The G protein-coupled lysophosphatidic acid 2 (LPA_2) receptor elicits prosurvival responses to prevent and rescue cells from apoptosis. However, G protein-coupled signals are not sufficient for the full protective effect of LPA_2. LPA_2 differs from other LPA receptor subtypes in the C-terminal tail, where it contains a zinc finger-binding motif for the interactions with LIM domain-containing TRIP6 and proapoptotic Siva-1, and a PDZ-binding motif through which it complexes with the NHERF2 scaffold protein. In this report, we identify AQ: B **a unique *CXXC* motif of LPA_2 responsible for the binding to TRIP6 and Siva-1, and demonstrate that disruption of these macromolecular complexes or knockdown of TRIP6 or NHERF2 expression attenuates LPA_2-mediated protection from chemotherapeutic agent-induced apoptosis. In contrast, knockdown of Siva-1 expression enhances this effect. Furthermore, a PDZ-mediated direct interaction between TRIP6 and NHERF2 facilitates their interaction with LPA_2. Together, these results suggest that in addition to G protein-activated signals, the cooperation embedded in the LPA_2-TRIP6-NHERF2 ternary complex provides a novel ligand-dependent signal amplification mechanism that is required for** AQ: C **LPA_2-mediated full activation of antiapoptotic signaling.**

Fn4 Lysophosphatidic acid (LPA)[4] is a growth factor-like lysophospholipid abundantly present in biological fluids. It mediates diverse cellular responses important for cell survival, growth, differentiation, migration, inflammation, angiogenesis, and platelet aggregation (1, 2). At least eight G protein-coupled LPA receptors have been identified: LPA_1, LPA_2, and LPA_3 of the endothelial differentiation gene family and the structurally distinct LPA_4/P2Y9, LPA_5/GPR92, LPA_6/GPR87, LPA_7/P2Y5, and LPA_8/P2Y10 of the purinergic receptor cluster (3–5). These receptors couple to $G_{i/o}$, $G_{q/11}$, G_s, and/or $G_{12/13}$ proteins to activate various signaling pathways. However, the molecular mechanisms underlying the specificity and diversity with which different LPA receptors regulate these wide ranging cellular responses are not yet fully understood. AQ: D

Substantial evidence has demonstrated that LPA is a survival factor that protects non-transformed cells from different stress-induced apoptosis (6) and renders cancer cells resistance to apoptosis-inducing treatments (1, 2). Among the various G protein-coupled LPA receptors, LPA_2 has been shown to mediate the antiapoptotic effect of LPA *in vivo*. $LPA_2^{-/-}$ mice show significantly increased rates of radiation-induced apoptosis and less crypt survival (7). LPA protects gut epithelial cells from radiation-induced apoptosis in WT and $LPA_1^{-/-}$ mice but not in $LPA_2^{-/-}$ mice (7). The classical paradigm for G protein-coupled receptor (GPCR)-mediated prosurvival signaling involves the coupling of ligand-bound receptors to heterotrimeric G proteins that sequentially activate the downstream effectors involved in Ras/ERK, phosphatidylinositol 3-kinase (PI3K)/AKT, and NF-κB signaling pathways (6). However, recent evidence suggests that non-G protein-coupled signals mediated via the unique C-terminal binding motifs of LPA_2 may be required for its antiapoptotic function. LPA_2 is the only LPA receptor subtype known to interact with various molecules via the unique binding domains present in its C terminus (8). The last four amino acids, DSTL, of LPA_2 bind to several PDZ proteins, including NHERF2 (Na^+/H^+ exchanger regulatory factor), PDZ-RhoGEF, LARG (leukemia-associated RhoGEF), and MAGI-3 (membrane-associated guanylate kinase with an inverted domain structure-3) (9–13). These scaffold proteins modulate LPA-induced activation of ERK and/or RhoA. NHERF2 can also regulate phospholipase C-β3 signaling pathways and bridge LPA_2 to cystic fibrosis transmembrane regulator Cl^- channel (9, 10). Through the PDZ-mediated interactions, membrane-localized NHERF2 and MAGI-3 can recruit the phosphatase and tensin homolog in close proximity to the cell surface to restrict PI3K/

* This work was supported, in whole or in part, by National Institutes of Health Grants CA92160 (to G. T.), AI 080405 (to G. T.), and CA100848 (to F. L.). This work was also supported by a grant from the Marsha Rivkin Center for Ovarian Cancer Research (to F. L.). G. T. is a founder of RxBio Inc. and a member of the scientific advisory board.

[S] The on-line version of this article (available at http://www.jbc.org) contains ZSI supplemental Figs. S1–S4.

[1] Both authors contributed equally.

[2] To whom correspondence may be addressed. Tel.: 901-448-4793; Fax: 901-448-7126; E-mail: gtigyi@physio1.utmem.edu.

[3] To whom correspondence may be addressed. Tel.: 205-975-5060; Fax: 205-975-5648; E-mail: flin@uab.edu.

AQ: I [4] The abbreviations used are: LPA, lysophosphatidic acid; GPCR, G protein-coupled receptor; 2-BP, 2-bromopalmitate; ERK, extracellular signal-regulated kinase; PI3K, phosphatidylinositol 3-kinase; WT, wild type; siRNA, small interfering RNA; BSA, bovine serum albumin; DMEM, Dulbecco's modified Eagle's medium; PTX, pertussis toxin; MEF, mouse embryonic fibroblast; DKO, double knock-out; S1P, sphingosine 1-phosphate; GFP, green fluorescent protein.

AKT activity (14, 15). However, NHERF2 can also serve as a scaffold protein for PDK1 (3-phosphoinositide-dependent protein kinase 1), which plays a central role in the activation of AGC family kinases, including AKT (16). It has been reported that knockdown of NHERF2 attenuates LPA-induced AKT activation in colon cancer cells (12). Thus, the function of NHERF2 in restricting or promoting PI3K/AKT signaling may depend on the relative cellular expression levels of phosphatase and tensin homolog *versus* PDK1.

Two zinc finger proteins, including the LIM domain-containing TRIP6 and Siva-1 proapoptotic protein, have been found to bind to the C-terminal tail of LPA$_2$ (17, 18). The LIM domain is comprised of two zinc finger motifs, which are critical for protein-protein interactions (19). The association of TRIP6 with LPA$_2$ enhances LPA-induced ERK activation and cell migration in a c-Src-dependent manner (20). However, it is unknown whether TRIP6 plays any role in the LPA$_2$-mediated antiapoptotic effect. In contrast, Siva-1, a transcriptional target of p53 and E2F1, functions as a proapoptotic protein during DNA damage response (21). The binding of LPA$_2$ to Siva-1 promotes LPA-dependent ubiquitination and down-regulation of Siva-1 expression (18).

As different LPA receptors show overlapping patterns of G protein coupling, LPA$_2$-mediated protein-protein interactions may be particularly important in the signal amplification and diversification of this receptor subtype. Here we demonstrate that an LPA-induced ternary complex of TRIP6 NHERF2 and LPA$_2$ regulates antiapoptotic function. We have mapped the *CXXC* zinc finger-binding motif of LPA$_2$ and found the LPA$_2$-mediated antiapoptotic effect was abolished only when both *CXXC*- and PDZ-binding motifs were disrupted, indicating that the supramolecular complexes formed via the C-terminal tail of LPA$_2$ are required for the full antiapoptotic function of LPA$_2$, and thus play a critical role in the chemoprotective action of LPA in cancer cells.

EXPERIMENTAL PROCEDURES

Plasmid Construction and Site-directed Mutagenesis—The cDNA sequences encoding one of the deletion mutants or point mutants of FLAG-LPA$_2$ were amplified by overlapping extension PCR and inserted into pcDNA3.1 (Invitrogen). These cDNA fragments were subsequently subcloned into pcFUW-puro lentiviral vector. The cDNA sequences encoding full-length NEHRF2, NHERF-PDZ1 (residues 8–99), or NHERF2-PDZ2 (residues 149–228) were inserted in-frame into pEGFP (Clontech) or pGEX-6P3 (Amersham Biosciences). The full-length TRIP6 cDNA sequences were inserted in-frame into pEBFP-C1. The expression vectors of GST-LPA$_2$-CT mutants in which Cys-311 and/or Cys-314 were mutated to Ala were constructed by

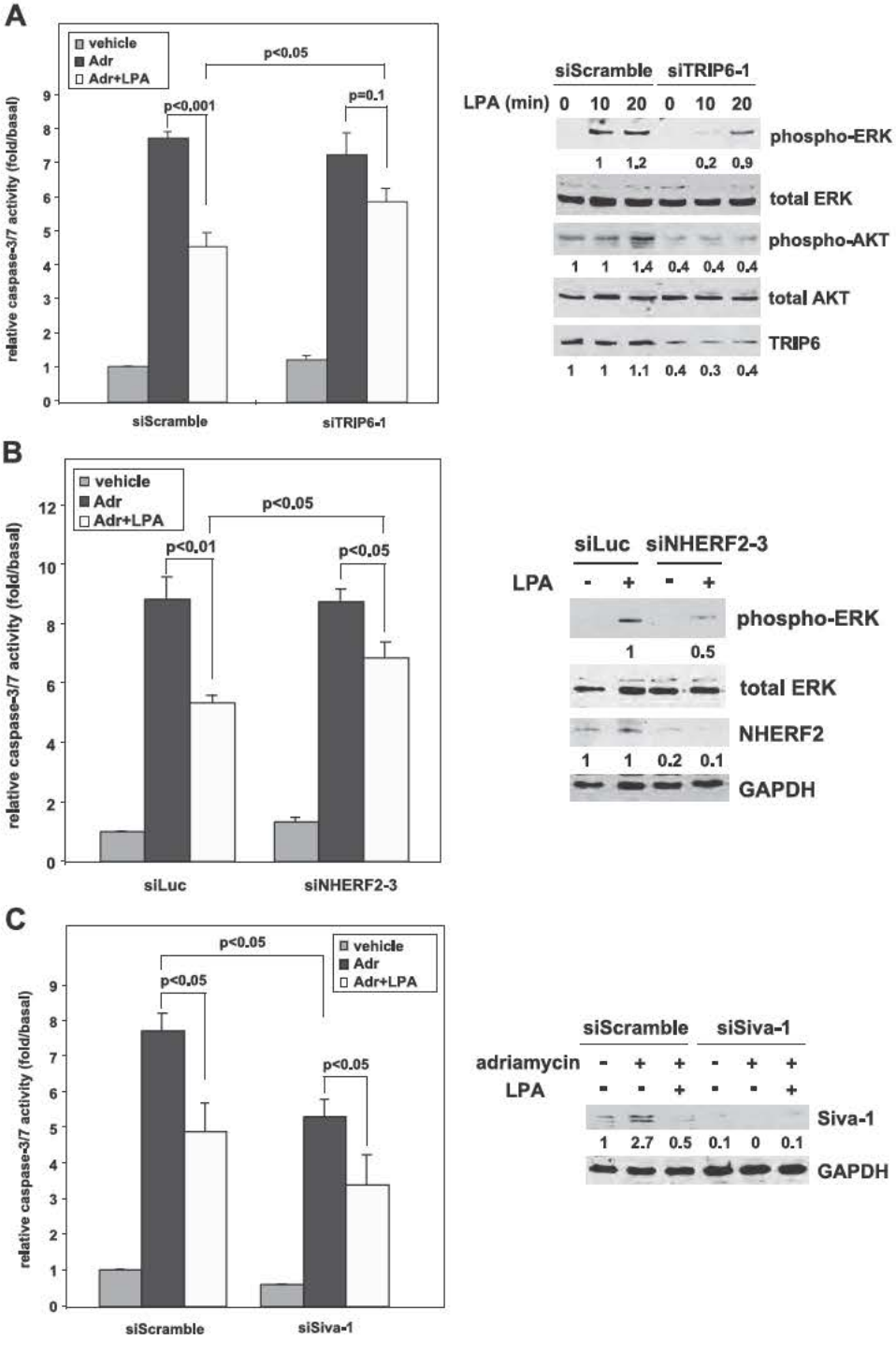

QuikChange site-directed mutagenesis (Stratagene) using pGEX-6P1-LPA_2-CT (17) as the template. The pLVTHM (Addgene) lentiviral vector was used to direct the expression of a short hairpin RNA that specifically targets the 19-nucleotide sequences of mouse TRIP6 (siTRIP6-1) (20), human TRIP6 (siTRIP6-2, siTRIP6-3) (17), mouse Siva-1 (18), or human NHERF2 cDNA (siNHERF2-4 (10) and siNHERF2-5, 5′-CCTGCATAGTGACAAGTCC-3′), respectively. The pGIPZ lentiviral expression vector (Openbiosystems) was used to direct the expression of a miR-30-based mouse NHERF2 short hairpin RNA (siNHERF2-3) or a luciferase control short hairpin RNA, which specifically targets the 22-nucleotide sequences of mouse NHERF2 cDNA (5′-ATCAGAGAAGGACAATGAGGAT-3′) and luciferase cDNA (5′-CCACTTACGCTGAGTACTTCGA-3′), respectively. pCMV-FLAG-ΔTTDC was constructed by deleting the cDNAs encoding the distal four amino acids, TTDC, of TRIP6 using QuikChange site-directed mutagenesis (Stratagene). All of these cDNA constructs have been verified by DNA sequencing.

Stable Transfection—Primary mouse embryonic fibroblasts (MEF) were isolated from E13.5 $LPA_{1/2}$ DKO embryos and continuously cultured to obtain the spontaneously immortalized MEF cell lines. These MEFs were transduced with an empty lentivirus or the lentivirus harboring WT or one of the FLAG-LPA_2 mutants and selected with puromycin to establish the stable cell lines.

Cellular Co-immunoprecipitation, In Vitro Binding, Immunoblotting, Immunostaining, and LPA-induced Calcium Activation Assay—Experiments and purification of the recombinant Siva-1 and TRIP6 were performed as described previously (7, 17, 18, 20). To detect the interactions of LPA_2, NHERF2, and TRIP6 at physiological levels, SKOV-3 cells expressing a scrambled siRNA, a TRIP6 siRNA, or a NHERF2 siRNA were starved in 0.1% fatty acid-free bovine serum albumin (BSA)-containing DMEM overnight, followed by addition of 2 μM LPA for 10 min and harvested. Endogenous LPA_2 was immunoprecipitated with an anti-LPA_2 rat antibody (a gift from Dr. Junken Aoki) or a control rat IgG. TRIP6 was immunoprecipitated with an anti-TRIP6 mouse monoclonal antibody (BD Biosciences) or a control mouse IgG. Proteins were resolved by SDS-PAGE and subjected to immunoblotting using an antibody specific to NHERF2, LPA_2 (gifts from Dr. A. P. Naren), or TRIP6 (Bethyl Laboratories), respectively.

Palmitoylation of LPA_2—HEK 293T cells expressing WT or one of the point mutants of FLAG-LPA_2 were incubated with [^{3}H]palmitic acid (60 Ci/mmol, Amersham Biosciences) at 37 °C for 2 h. FLAG-LPA_2 in the whole cell lysates was immunoprecipitated with the anti-FLAG M2 monoclonal antibody-conjugated agarose beads, resolved by SDS-PAGE, and detected by autoradiography. The blot was then probed with an anti-FLAG antibody to detect FLAG-LPA_2. The effect of 2-bromopalmitate (2-BP, Sigma) on the inhibition of LPA_2 palmitoylation was determined by pretreating the transfected HEK 293T cells with 100 μM 2-bromopalmitate for 30 min followed by labeling with [^{3}H]palmitic acid.

To determine whether inhibition of palmitoylation affects LPA_2 binding to Siva-1, TRIP6, or NHERF2, HEK 293T cells transiently expressing GFP-Siva-1, GFP-TRIP6, or GFP-NHERF2 with or without FLAG-LPA_2 were pretreated with 100 μM 2-BP in 0.1% fatty acid-free BSA-containing DMEM for 4 h, followed by addition of 2 μM LPA for 10 min. After immunoprecipitation of FLAG-LPA_2, half the precipitates were resolved by SDS-PAGE. Immunoblotting was performed to detect the co-immunoprecipitated GFP-Siva-1, GFP-TRIP6, or GFP-NHERF2. The rest of the samples were subjected to the acyl-biotinyl exchange procedure (22) to determine the levels of palmitoylated LPA_2. Precipitated LPA_2 was pretreated with 50 mM *N*-ethylmaleimide (Pierce) for 1 h, followed by the acyl-biotinyl exchange with 1 M hydroxylamine and 0.2 mM EZ-link biotin-*N*-[6-(biotinamido)hexyl]-3′-(2′-pyridyldithio)propionamide (HPDP) (Pierce) for another hour at room temperature. Biotinylated FLAG-LPA_2 was eluted from the anti-FLAG beads using 100 μg/ml FLAG peptides (Sigma) for competition and subsequently pulled down with avidin beads (Amersham Biosciences). After SDS-PAGE, immunoblotting was performed using an anti-FLAG rabbit polyclonal antibody (Sigma).

Apoptosis Assays—Stable MEFs were starved in 0.1% fatty acid-free BSA-containing DMEM with or without 10 μM LPA for 1 h followed by the addition of 1.5 to 2 μM adriamycin for 7–9 h. Caspase-3/7 activity was determined by cleavage of the luminogenic substrate containing the DEVD sequence (Promega) and was normalized by protein concentrations. To determine the effect of pertussis toxin (PTX) on apoptosis, DKO-LPA_2 MEFs were pretreated with 100 ng/ml PTX overnight before the apoptosis assay. Alternatively,

FIGURE 1. **LPA_2-mediated protection from adriamycin-induced apoptosis is regulated by proteins interacting with its C-terminal tail.** *A*, knockdown of TRIP6 expression reduces LPA_2-mediated ERK and AKT activation and protection from adriamycin-induced caspase-3/7 activation. $LPA_{1/2}$ DKO MEFs stably expressing FLAG-LPA_2 (*DKO-LPA_2*) were transduced with the lentivirus harboring a mouse TRIP6 siRNA (*siTRIP6-1*) or a scrambled control siRNA (*siScramble*). After starvation for 4 h, cells were treated with 2 μM LPA for 10 or 20 min, and immunoblotting was performed to determine the levels of activated phospho-ERK or phospho-AKT, respectively (*right panel*). The same blot was reprobed with an antibody specific to ERK, AKT, or TRIP6, respectively. The intensity of each protein was quantified by NIH IMAGE J software and the relative expression of phospho-ERK or phospho-AKT was normalized by the levels of total ERK or AKT. The same cells were starved in 0.1% fatty acid-free BSA-containing DMEM with or without 10 μM LPA for 1 h followed by the addition of 1.7 μM adriamcyin for 9 h, and caspase-3/7 activity was determined by cleavage of the luminogenic substrate containing the DEVD sequence and was normalized by protein concentrations (*left panel*). Data shown are the mean ± S.E. of five independent experiments. Statistic significance ($p < 0.05$) was determined by Student's *t* test. *B*, knockdown of NHERF2 expression attenuates LPA_2-mediated ERK activation and protection from adriamycin-induced apoptosis. DKO-LPA_2 MEFs were transduced with the lentivirus harboring a mouse NHERF2 siRNA (*siNHERF2-3*) or a luciferase control siRNA (*siLuc*). The starved cells were treated with LPA for 10 min and the levels of activated ERK, total ERK, NHERF2, and glyceraldehyde-3-phosphate dehydrogenase (*GAPDH*) in the whole cell lysates were determined by immunoblotting. Adriamycin-induced caspase-3/7 activation were assayed as described in *A*. Data shown are the mean ± S.E. of three independent experiments. *C*, inhibition of Siva-1 expression enhances LPA_2-mediated protection from adriamycin-induced apoptosis. DKO-LPA_2 MEFs were transduced with the lentivirus harboring a Siva-1 siRNA or a scrambled siRNA. The effect of LPA on adriamycin-induced caspase-3/7 activation was determined as described in *A*. Data shown are the mean ± S.E. of three independent experiments. Immunoblotting was performed to detect the expression of Siva-1 and control GAPDH in the whole cell lysates.

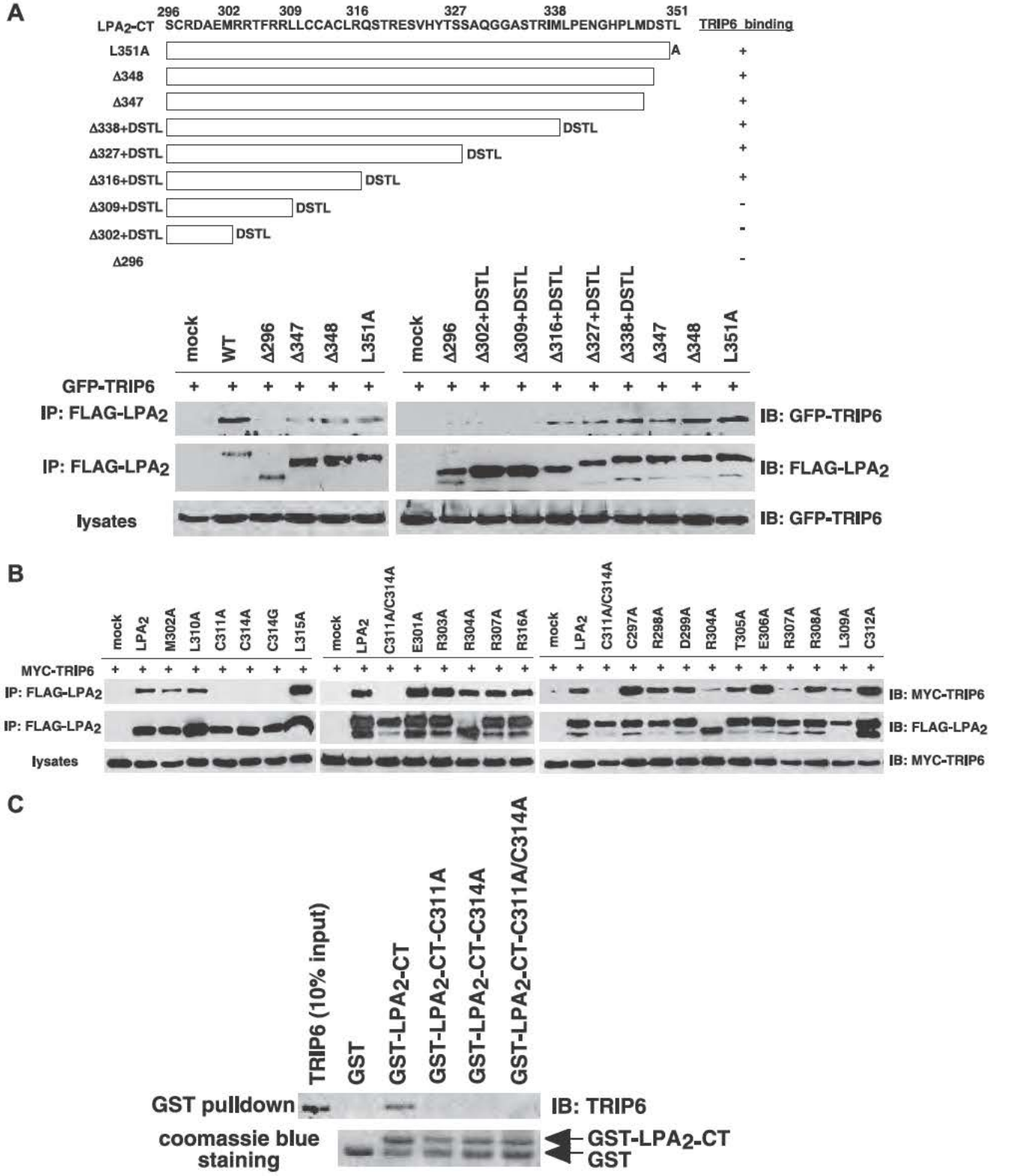

FIGURE 2. **The ^{311}CXXC^{314} motif of LPA$_2$ is required for the interaction with TRIP6.** *A*, the TRIP6-binding motif of LPA$_2$ is located in the region proximal to Arg-316 of the C-terminal tail. GFP-TRIP6 was expressed in HEK 293T cells with FLAG-LPA$_2$ or one of the LPA$_2$ deletion mutants with or without the DSTL sequences as indicated in the *top panel*. After stimulation of the cells with 2 μM LPA for 10 min, LPA$_2$ was immunoprecipitated (*IP*) with anti-FLAG M2 antibody-conjugated agarose beads and resolved by SDS-PAGE. GFP-TRIP6 co-immunoprecipitated with LPA$_2$ was detected by immunoblotting (*IB*) using an anti-GFP antibody. *B*, the ability of LPA$_2$ to bind to TRIP6 is eliminated by mutation of Cys-311 and/or Cys-314 to Ala. MYC-TRIP6 was co-expressed with WT or one of the point mutants of LPA$_2$ in HEK 293T cells. Co-immunoprecipitation was performed as described above. MYC-TRIP6 co-immunoprecipitated with LPA$_2$ was detected with an anti-MYC polyclonal antibody. *C*, Cys-311 or Cys-314 of LPA$_2$ mediates the binding to TRIP6 *in vitro*. Purified recombinant TRIP6 was incubated with glutathione *S*-transferase (*GST*), GST-LPA$_2$-CT, or one of the GST-LPA$_2$-CT mutants at 4 °C for 3 h. TRIP6 pulled down by GST-LPA$_2$-CT was resolved by SDS-PAGE and detected by immunoblotting using an anti-TRIP6 antibody. The *bottom panel* shows Coomassie Blue staining of GST and GST-LPA$_2$-CT proteins. Data shown in each figure are representative of three independent experiments.

apoptosis was determined by annexin V-fluorescein isothiocyanate staining (BD Biosciences) and analyzed by flow cytometry following a 14-h treatment. SKOV-3 cells transduced with the lentivirus harboring a scrambled siRNA, TRIP6 siRNA, or a NHERF2 siRNA were starved and pretreated with LPA followed by the addition of 50 μM cisplatin for 20 h. Apoptosis was determined by caspase-3/7 activity assay and immunoblotting using an antibody specific to PARP-1 (BD Biosciences).

To determine apoptosis by DNA fragmentation assay, stable MEFs were seeded on plates coated with 0.1 mg/ml poly-L-lysine overnight followed by the addition of 3 μM adriamycin in 0.5% fetal bovine serum-containing DMEM. Two μM LPA were added 1 h later. After a 6-h treatment, DNA fragmentation was measured by enzyme-linked immunosorbent assay following the procedure of the Cell Death Detection Kit (Roche).

Statistic Analysis—Statistic significance ($p < 0.05$) was determined using Student's *t* test.

RESULTS

LPA$_2$-mediated Protection from Chemotherapeutic Agent-induced Apoptosis Is Regulated by Proteins Interacting with the C terminus of LPA$_2$—To elucidate the unique properties of LPA$_2$ leading to the attenuation of DNA damage-induced apoptosis, we tested the hypothesis that LPA$_2$-elicited antiapoptotic signaling could be regulated through the interactions with its C terminus-binding partners. We knocked down the expression of TRIP6, NHERF2, or Siva-1 in LPA$_{1/2}$ double knock-out (DKO) MEFs stably transduced with a human LPA$_2$ (designated DKO-LPA$_2$ MEFs). These LPA$_{1/2}$ DKO MEFs were chosen because LPA fails to induce ERK/AKT activation in these MEFs required for the antiapoptotic effect (Fig. 5*C*), and cannot protect them from

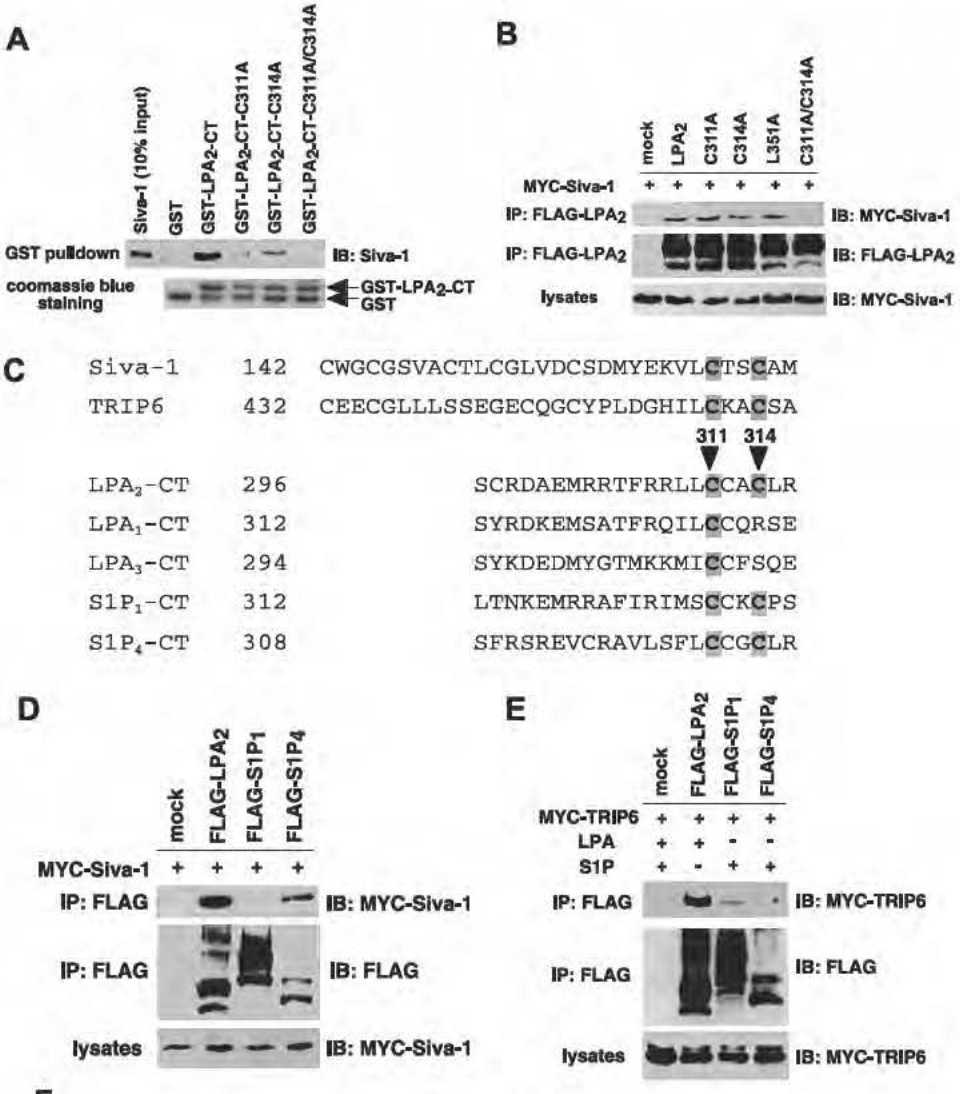

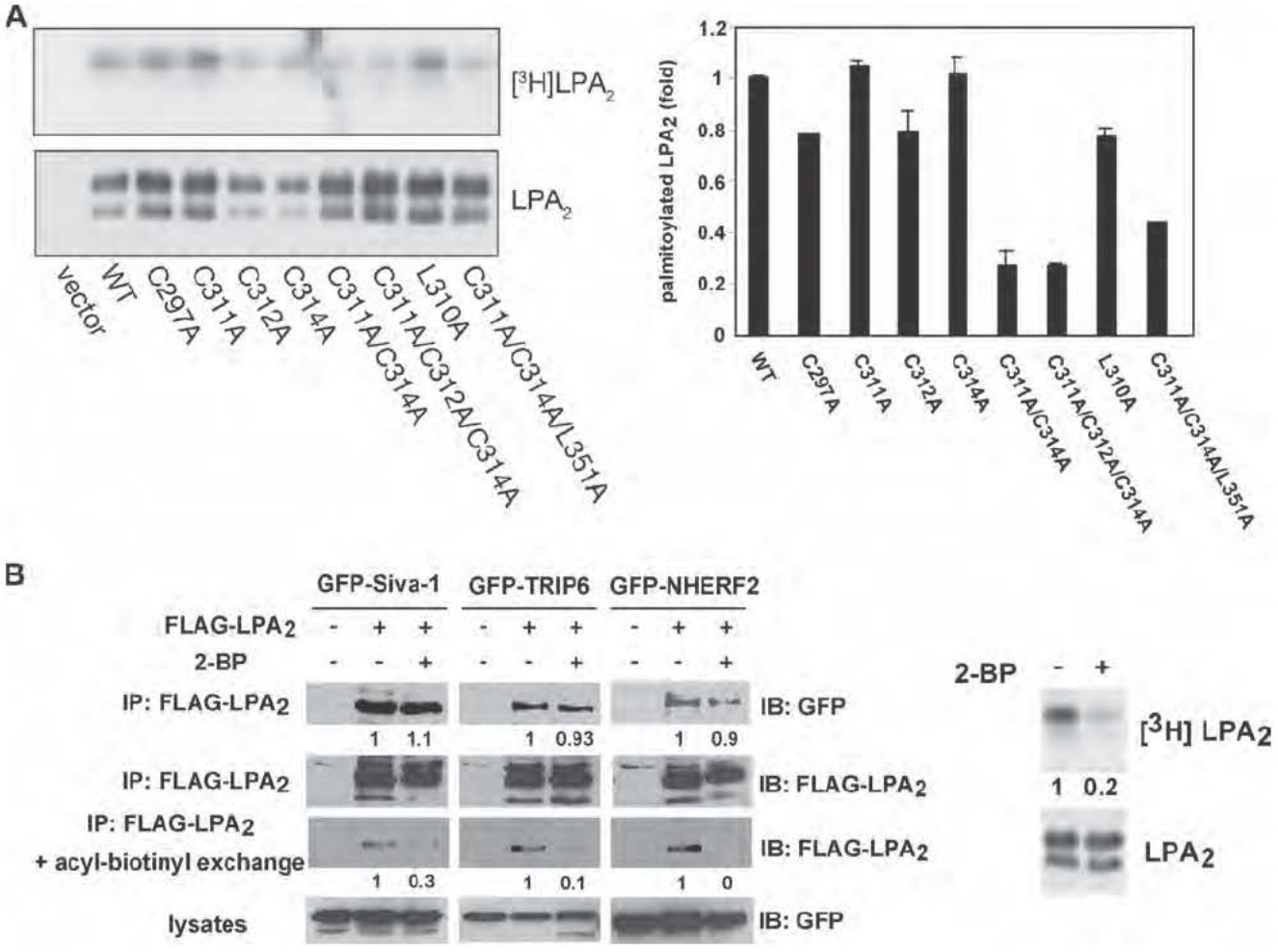

FIGURE 4. **Palmitoylation modification does not affect LPA_2 binding to TRIP6, Siva-1, or NHERF2.** *A*, palmitoylation of LPA_2 is partially impaired by mutation of the cysteine residues in the proximal end of its C-terminal tail. WT or one of the point mutants of FLAG-LPA_2 were transiently expressed in HEK 293T cells and labeled with [^{3}H]palmitic acid at 37 °C for 2 h. FLAG-LPA_2 was immunoprecipitated with anti-FLAG M2 monoclonal antibody-conjugated agarose beads, resolved by SDS-PAGE, and detected by autoradiography (*left top panel*), followed by immunoblotting (*IB*) with an anti-FLAG antibody (*left bottom panel*). The *right panel* shows the relative levels of palmitoylation of each mutant compared with WT LPA_2 after normalization by total receptor expression. Data shown are the mean of two to three independent experiments. *B*, association of LPA_2 with Siva-1, TRIP6, or NHERF2 is not affected by blocking palmitoylation of LPA_2. GFP-Siva-1, GFP-TRIP6, or GFP-NHERF2 was co-expressed with FLAG-LPA_2 in HEK 293T cells. After treatment with 100 μM 2-BP in 0.1% fatty acid-free BSA-containing DMEM for 4 h, cells were stimulated with LPA for 10 min and FLAG-LPA_2 was immunoprecipitated with anti-FLAG M2 monoclonal antibody-conjugated agarose beads. Half the precipitates were resolved by SDS-PAGE and the immunoblot (*IB*) was probed with an anti-GFP polyclonal antibody to detect co-immunoprecipitated GFP-Siva-1, GFP-TRIP6, or GFP-NHERF2. The rest of the samples were subjected to the acyl-biotinyl exchange procedure to determine levels of palmitoylated LPA_2 as described under "Experimental Procedures." A separate experiment was performed to determine the effect of 2-BP on blocking palmitoylation of LPA_2 by pretreating the FLAG-LPA_2-expressing HEK 293T cells with 100 μM 2-BP for 30 min followed by labeling with [^{3}H]palmitic acid for 2 h (*right panel*). The relative levels of Siva-1, TRIP6, or NHERF2 co-immunoprecipitated (*IP*) with FLAG-LPA_2 were quantified and normalized to the levels of FLAG-LPA_2 immunoprecipitates. Data shown are representative of three separate experiments.

adriamycin-induced apoptosis (Fig. 5*D*), although they endogenously express LPA_4 and LPA_7 receptor transcripts (data not shown). We found that 60% knockdown of TRIP6 expression did not further enhance adriamycin-induced caspase-3/7 activation but significantly attenuated LPA-mediated protection and the activation of ERK and AKT (Fig.

AQ: G

FIGURE 3. **Both Cys-311 and Cys-314 residues are required for LPA_2 binding to Siva-1.** *A*, *in vitro* binding of LPA_2 to Siva-1 is partially impaired by mutation of Cys-311 or Cys-314 to Ala and is completely abolished when both cysteine residues are mutated. Purified recombinant Siva-1 was incubated with glutathione *S*-transferase (*GST*), GST-LPA_2-CT, or one of the GST-LPA_2-CT mutants. Siva-1 pulled down by GST-LPA_2-CT was detected by immunoblotting using an anti-Siva-1 antibody. *B*, association of LPA_2 with Siva-1 is eliminated only when both Cys-311 and Cys-314 residues are mutated to Ala. MYC-Siva-1 was co-expressed with WT or one of the point mutants of FLAG-LPA_2 in HEK 293T cells. Cells were starved overnight and then harvested for co-immunoprecipitation (*IP*) and immunoblotting (*IB*) as described above. MYC-Siva-1 was detected with an anti-MYC polyclonal antibody. *C*, amino acid sequence alignment of the C-terminal zinc finger of Siva-1 (residues 142–172) and TRIP6-LIM3 (residues 432–462), and the proximal region of the C-terminal tail of LPA_2 (residues 296–316), LPA_1 (residues 312–332), LPA_3 (residues 294–314), $S1P_1$ (residues 312–322), and $S1P_4$ (residues 308–318). *D*, Siva-1 interacts with $S1P_4$ but not $S1P_1$. HEK 293T cells expressing MYC-Siva-1 with FLAG-tagged LPA_2, $S1P_1$, or $S1P_4$ were subjected to a co-immunoprecipitation experiment as described in *B*. *E*, TRIP6 binds weakly to $S1P_1$ and barely associates with $S1P_4$. HEK 293T cells expressing MYC-TRIP6 with FLAG-tagged LPA_2, $S1P_1$, or $S1P_4$ were starved for 8 h followed by the addition of 2 μM LPA or S1P for 10 min. Co-immunoprecipitation was performed as described above. Data shown in *A*, *B*, *D*, and *E* are representative of three independent experiments. *F*, Siva-1 colocalizes with LPA_2 and $S1P_4$ but not $S1P_1$ or the C311A/C314A mutant of LPA_2 in the cytosol. GFP-Siva-1 was transiently co-expressed with FLAG-tagged LPA_2, C311A/C314A of LPA_2, $S1P_1$, or $S1P_4$ in $LPA_{1/2}$ DKO MEFs. Cells were fixed, permeabilized, and then incubated with the anti-FLAG M2 monoclonal antibody followed by the Texas Red X-conjugated mouse secondary antibody to detect the FLAG-tagged receptors. GFP-Siva-1 was directly visualized by fluorescence microscopy.

F1

1*A*). Knockdown of NHERF2 expression by 80% also reduced LPA-induced chemoprotection and ERK activation (Fig. 1*B*). In contrast, knockdown of Siva-1 expression by more than 90% reduced adriamycin-induced caspase-3/7 activation and enhanced the LPA-mediated protective effect (Fig. 1*C*). These results suggest that in mouse embryonic fibroblasts, the antiapoptotic effect of LPA_2 involves NHERF2, TRIP6, and Siva-1.

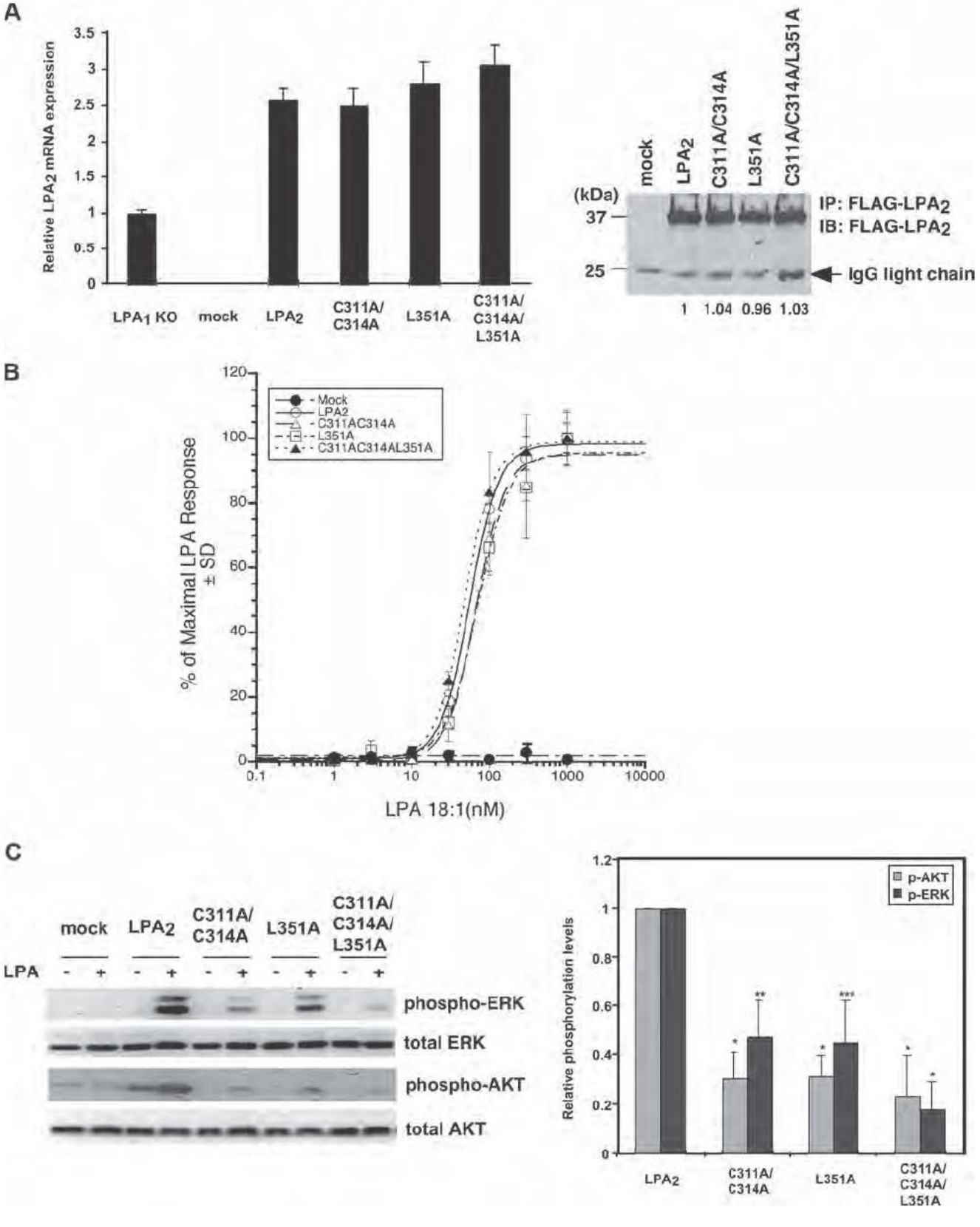

LPA_2-formed Complexes Regulate Antiapoptosis

A CXXC Motif Unique to the C-terminal Tail of LPA_2 Mediates the Interactions with TRIP6 and Siva-1—To investigate if the effects of these LPA_2-interacting partners on LPA-elicited chemoprotection are regulated through direct interactions with LPA_2, next we delineated the position of the TRIP6-interacting motif in the C terminus of LPA_2. We applied deletion mutagenesis while keeping the DSTL motif intact in the mutants to permit interactions with the PDZ partners. Cellular co-immunoprecipitation demonstrated that except for Δ309+DSTL, Δ302+DSTL, and Δ296 mutants, other deletion mutants of LPA_2, including Δ316+DSTL, Δ327+DSTL, Δ338+DSTL, Δ347, and Δ348, and the L351A point mutant that lacks PDZ binding were able to bind to TRIP6, although to a lesser degree than the WT LPA_2 (Fig. 2*A*). This result indicates that the minimal sequences required for TRIP6 binding contain residues 297–316. Alanine scanning mutational analysis of the 297–316 region identified Cys-311 and Cys-314 as the residues required for the interaction with TRIP6 (Fig. 2*B*). *In vitro* binding assays confirmed that mutation of Cys-311 and/or Cys-314 to Ala abolished the direct binding of LPA_2-CT to TRIP6 (Fig. 2*C*).

Next we examined the interaction of Siva-1 with WT or cysteine mutants of LPA_2. We found that only when both Cys-311 and Cys-314 were mutated was the interaction with Siva-1 completely abolished *in vitro* (Fig. 3*A*) and in cells (Fig. 3*B*). However, this binding was not affected by L351A mutation (Fig. 3*B*).

Among the endothelial differentiation gene family lysophospholipid receptors, the *CXXC* motif is unique only to the LPA-specific LPA_2 and sphingosine 1-phosphate (S1P)-specific $S1P_1$ and $S1P_4$ receptors (Fig. 3*C*). In contrast to LPA_2, LPA_1 and LPA_3 lack the *CXXC* motif in the C terminus (Fig. 3*C*) and fail to interact with TRIP6 and Siva-1 (17, 18). $S1P_4$ formed a complex with Siva-1 but barely bound to TRIP6; and $S1P_1$, albeit weakly, associated with TRIP6 but not Siva-1 (Fig. 3, *D* and *E*). Thus, the *CXXC* motifs of distinct endothelial differentiation gene family lysophospholipid receptors are capable of mediating interactions with the C-terminal zinc finger of Siva-1 or TRIP6-LIM3 (Fig. 3*C*), which have been shown as the LPA_2-interacting domains (17, 18); however, additional residues are required for strengthening the interactions.

Previously we have demonstrated in NIH3T3 fibroblasts that Siva-1 colocalizes with LPA_2 in the cytosol and the plasma membrane, and this association prevents nuclear translocation of Siva-1 (18). Likewise, Siva-1 colocalized with LPA_2 and $S1P_4$ but not $S1P_1$ in the cytosol in $LPA_{1/2}$ DKO MEFs (Fig. 3*F*). When both Cys-311 and Cys-314 of LPA_2 were mutated to Ala, colocalization was completely abolished and Siva-1 was found in the nucleus.

Palmitoylation of LPA_2 Does Not Affect Its Ability to Interact with TRIP6, Siva-1, or NHERF2—Many GPCRs undergo cysteine palmitoylation that may affect their coupling to G proteins, cell surface receptor expression, receptor desensitization, or trafficking (23). However, the role of palmitoylation varies among different GPCRs. Among the several cysteine residues located in the C-terminal tail of LPA_2, including Cys-297, Cys-311, Cys-312, and Cys-314, mutation of a single cysteine residue either did not or slightly reduced palmitoylation of LPA_2 (Fig. 4*A*). Mutation of two or three cysteine residues partially reduced receptor palmitoylation but did not completely abolish this modification (Fig. 4*A*).

To evaluate whether palmitoylation affects LPA_2 binding to TRIP6, Siva-1, or NHERF2, we used 2-bromopalmitate to block palmitoylation and examined these interactions. Although 2-bromopalmitate inhibits palmitoylation of LPA_2 as assayed by determining the levels of palmitoylated LPA_2 with the acyl-biotinyl exchange procedure (22) and metabolic labeling of the receptor with [^{3}H]palmitic acid, it did not significantly affect interactions of LPA_2 with TRIP6, Siva-1, or NHERF2 (Fig. 4*B*).

G Protein-mediated LPA_2 Signaling to Calcium Mobilization Is Not Affected by Mutation of the CXXC- and/or PDZ-binding

FIGURE 5. **Protein-protein interactions via the *CXXC*- and/or PDZ-binding motifs do not affect LPA_2-mediated Ca^{2+} response but regulate its chemoprotective effect.** *A*, stable expression of LPA_2 or one of the point mutants deficient in binding to the zinc finger proteins and/or PDZ proteins in $LPA_{1/2}$ DKO MEFs. Total mRNAs were isolated from LPA_1 KO MEFs or one of the $LPA_{1/2}$ DKO MEF cell lines (mock, WT LPA_2, C311A/C314A, L351A, or C3131A/C314A/L351A). Quantitative real-time reverse transcriptase-PCR was performed to determine the relative expression levels of LPA_2 mRNA compared with that expressed in LPA_1 KO MEFs and was normalized by the expression of β-actin mRNA. Results show the mean ± S.E. done in triplicates and are representative of two separate experiments. To determine total protein levels of each receptor, FLAG-LPA_2 in the whole cell lysates was immunoprecipitated using anti-FLAG M2 monoclonal antibody-conjugated agarose beads and detected with an anti-FLAG rabbit polyclonal antibody. The result shown is representative of five independent experiments. *B*, mutation of the *CXXC* motif and/or PDZ-binding motif does not affect LPA_2-mediated Ca^{2+} response. Stable $LPA_{1/2}$ DKO MEFs were stimulated with different concentrations of LPA as indicated for 5 min. LPA-induced calcium response was determined as described previously (7). The curves for WT LPA_2 and mutants were generated by normalizing the Ca^{2+} peak at various dilutions to the response elicited by the highest concentration of LPA (1 μM) applied. The values of the mock-transduced MEFs were normalized to that of WT LPA_2-transduced MEFs. Data shown are the mean ± S.D. done in triplicates and are representative of two separate experiments. *C*, mutation of the *CXXC* motif and/or PDZ-binding motif attenuates LPA_2-mediated activation of ERK and AKT. Stable $LPA_{1/2}$ DKO MEFs were stimulated with LPA for 10 min. Immunoblotting was performed to detect the levels of phosphorylated and total ERK and AKT (*left panel*). The intensity of each protein was quantified to determine the relative activation fold of phospho-ERK and AKT by LPA stimulation (*right panel*). Data shown are the mean ± S.E. of five independent experiments. *, $p < 0.001$; **, $p < 0.01$; ***, $p < 0.05$ *versus* LPA-stimulated DKO-LPA_2 MEFs (Student's *t test*). *D*, LPA-mediated protection from adriamycin-induced caspase-3/7 activation is inhibited by mutation of both *CXXC*- and PDZ-binding motifs. Different $LPA_{1/2}$ DKO MEFs transfectants were pretreated with 10 μM LPA in 0.1% fatty acid-free BSA-containing medium for 1 h, followed by addition of 1.7 μM adriamycin for 8 h. Apoptosis was determined by caspase-3/7 activity assay. Data show the mean ± S.E. of four independent experiments. *E*, mutation of the *CXXC* motif abrogates LPA_2-mediated protection from adriamycin-induced Siva-1 induction. Different $LPA_{1/2}$ DKO MEFs were pretreated with 10 μM LPA for 2 h, followed by the addition of 1.5 μM adriamycin for 14 h. Immunoblotting (*IB*) was performed to detect the expression of Siva-1 and glyceraldehyde-3-phosphate dehydrogenase (*GAPDH*) in the whole cell lysates. The relative expression of Siva-1 was compared with that expressed in the mock cells without any treatment and was normalized by the levels of GAPDH. The result shown is representative of three independent experiments. *F*, inhibition of the *CXXC* motif-mediated interaction with TRIP6-LIM3 attenuates LPA-mediated protection from adriamycin-induced apoptosis. pEGFP or pEGFP-TRIP6-LIM3 was transiently transfected by electroporation into $LPA_{1/2}$ DKO MEFs that expressed WT LPA_2 or L351A. Cells were treated with 10 μM LPA for 1 h followed by addition of 1.5 μM adriamycin for 9 h. Caspase-3/7 activity was determined and normalized by protein concentrations in each sample. Data show the mean ± S.E. of three independent experiments. The immunoblot shows the expression of GFP-TRIP6-LIM3, GFP, and β-actin in the whole cell lysates.

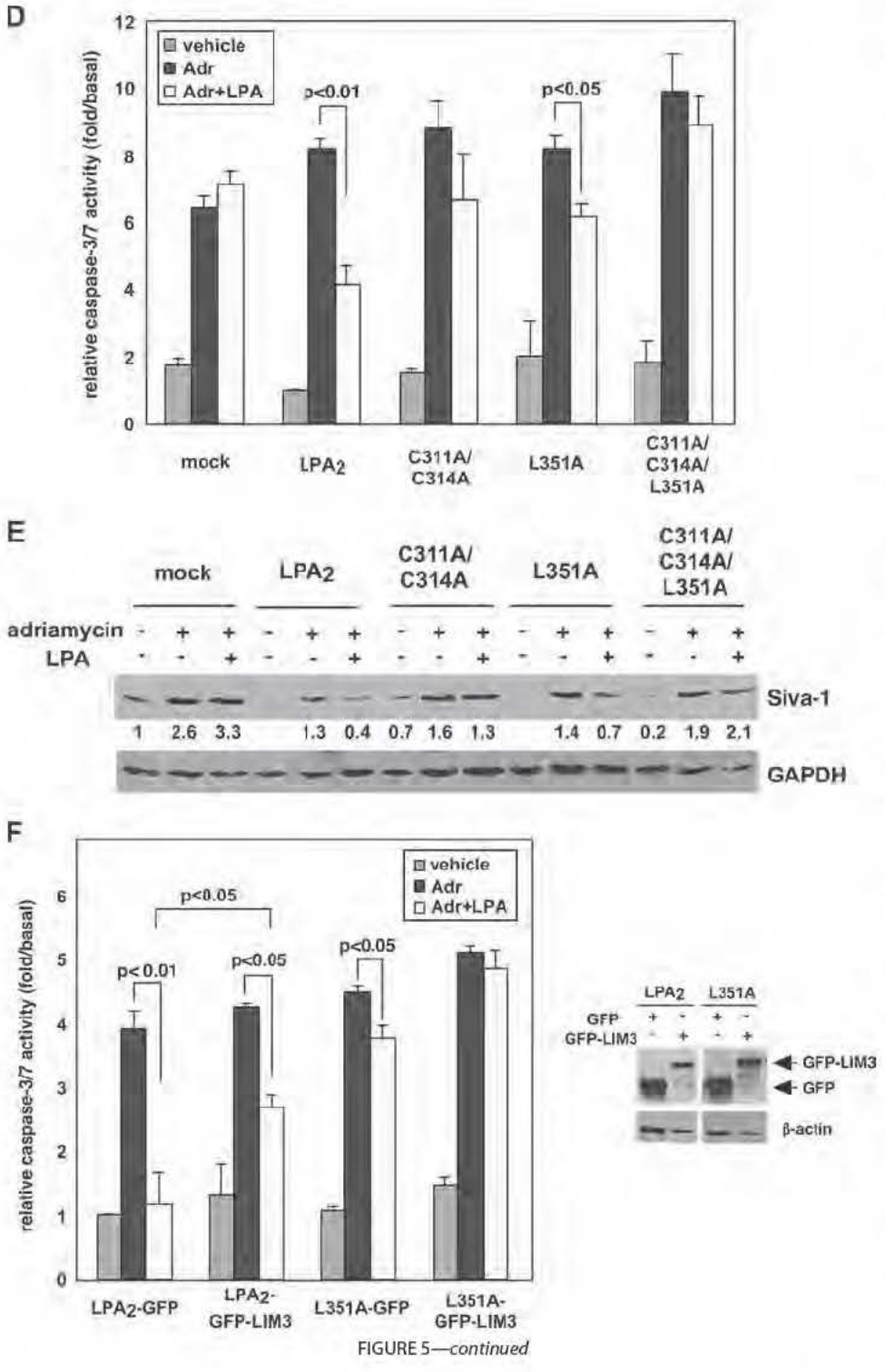

FIGURE 5—*continued*

Motifs—To investigate the impact of mutations of the C-terminal binding motifs on LPA_2 functions, lentiviral constructs harboring WT LPA_2, the C311A/C314A mutant that is unable to interact with TRIP6 and Siva-1, the L351A mutant defective in binding to PDZ proteins, or the C311A/C314A/L351A mutant that cannot bind any of the interacting partners were stably transduced into the $LPA_{1/2}$ DKO MEFs. Compared with the endogenous LPA_2 mRNA expressed in the $LPA_1^{-/-}$ MEFs, the WT and point mutants of LPA_2 mRNA were expressed at 2.5- to 3-fold higher but comparable levels in the stable $LPA_{1/2}$ DKO MEF cell lines (Fig. 5*A*). They were also expressed at similar protein levels in the whole cell lysates (Fig. 5*A*) and on the cell surface demonstrated by flow cytometry analysis (data not shown). LPA-induced Ca^{2+} mobilization showed indistinguishable dose-response curves in the MEFs expressing WT or in any of the LPA_2 mutants (Fig. 5*B*), indicating that these binding motifs do not affect the $G_{q/11}$ signaling branch. These findings also imply that $G_{q/11}$-mediated signaling events are not altered by disruption of the palmitoylation modification of Cys-311 and Cys-314.

LPA_2-mediated Chemoprotection Is Attenuated by Mutation of the CXXC- and PDZ-binding Motifs—We reasoned that if LPA_2-mediated chemoprotection is regulated by these interacting partners, disruption of the interactions in itself would eliminate the function of TRIP6 and NHERF2 in promoting LPA_2-mediated prosurvival signaling and allow the stabilization of Siva-1, which can enhance chemotherapeutic agent-induced apoptosis. Indeed, the efficacy of LPA_2 in mediating LPA-induced ERK and AKT activation was significantly attenuated by C311A/C314A or L351A mutation and was completely abolished by the C311A/C314A/L351A mutation (Fig. 5*C*). These results suggest that the CXXC- and PDZ-binding motifs cooperatively regulate LPA_2-mediated prosurvival signaling.

Next we examined the effect of LPA on protecting adriamycin-induced apoptosis in these MEFs. The DNA fragmentation assay showed that following a 6-h adriamycin treatment, LPA protected cells from apoptosis in the $LPA_{1/2}$ DKO MEFs that expressed WT LPA_2, C311A/C314A, or L351A but not in the mock-transfected $LPA_{1/2}$ DKO MEFs or those expressing the C311A/C314A/L351A mutant (supplemental Fig. S1*A*). After an 8-h treatment, the antiapoptotic efficacy of LPA_2 measured by the caspase-3/7 activity assay (Fig. 5*D*) was reduced by the C311A/C314A or L351A mutations and was completely abolished by the C311A/C314A/L351A muta-

tion. A similar effect was also observed using annexin V staining after a 14-h treatment (supplemental Fig. S1*B*).

Previously we have shown that LPA inhibits adriamycin-induced Siva-1 expression and its proapoptotic functions. Analysis of these LPA_2 mutants showed that the inhibitory effect of LPA on adriamycin-induced Siva-1 expression was eliminated by mutation of the *CXXC* motif but not the PDZ-binding motif, confirming that this regulation is mediated through the direct interaction of LPA_2 with Siva-1 (Fig. 5*E*). Together, these results suggest that the *CXXC*- and PDZ-binding motifs differentially and cooperatively regulate LPA_2 function in protecting cells from adriamycin-induced apoptosis.

The role of Siva-1 in apoptosis is well established (18); however, TRIP6 has not yet been implicated in antiapoptotic signaling and for this reason we focused our investigation on this adapter protein. The LIM3 domain of TRIP6 binds to LPA_2, and has been shown to serve as a dominant-negative probe to attenuate LPA_2-mediated cell migration previously (17). Overexpression of the GFP-TRIP6-LIM3 mutant reduced the chemoprotective effect of LPA in the DKO-LPA_2 MEFs, and this inhibitory effect was augmented in the DKO-L351A MEFs (Fig. 5*F*), supporting the notion that cooperative protein-protein interactions via both *CXXC*- and PDZ-binding motifs are required for the maximal protective effect of LPA_2. NHERF2 binds to LPA_2 through its PDZ2 domain (10). However, we did not succeed in overexpressing NHERF2-PDZ2 to attenuate the protective effect of LPA (data not shown).

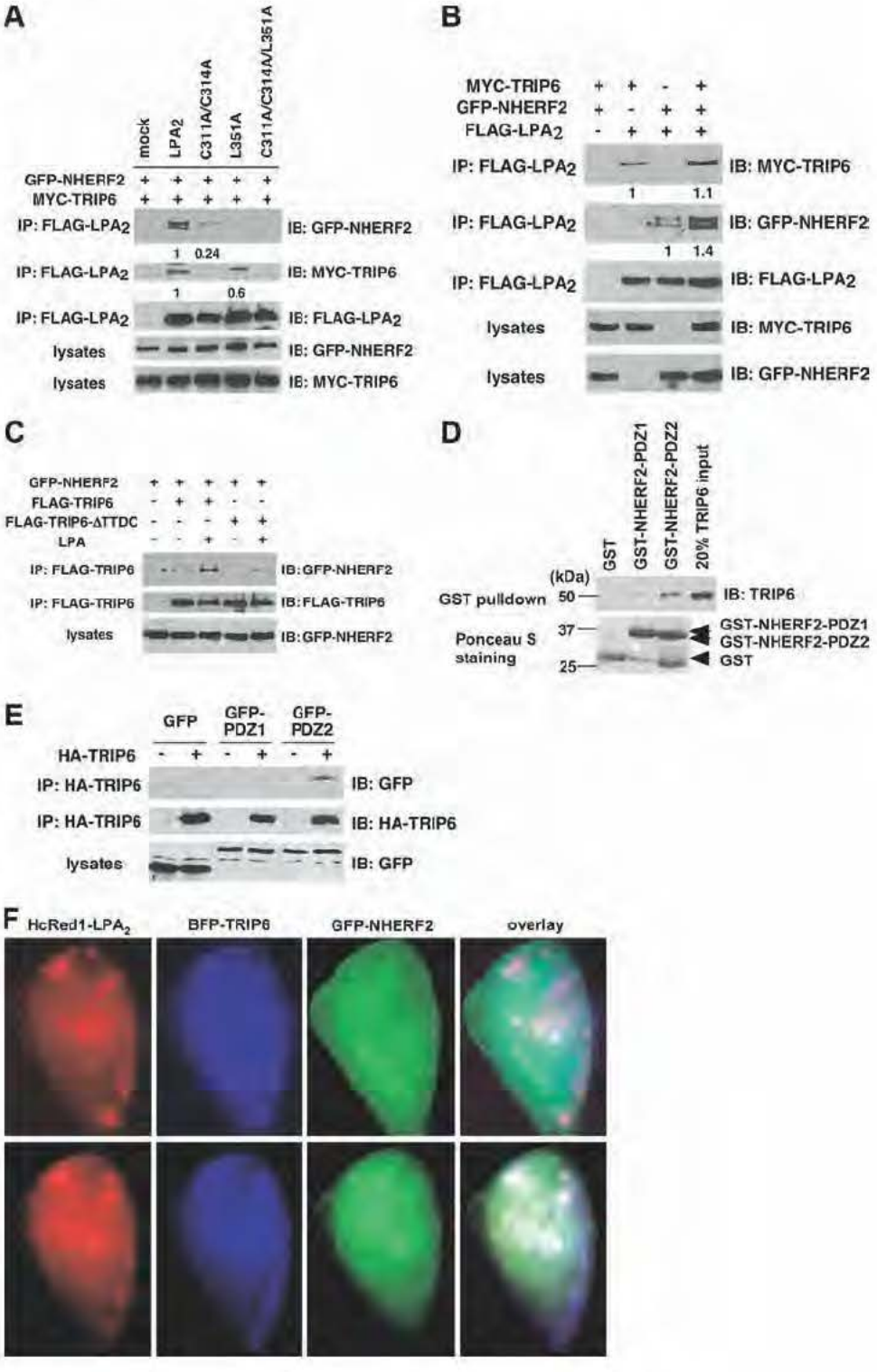

The results also showed that when $G_{i/o}$ signaling was inhibited with PTX, LPA-mediated ERK activation and protection from adriamycin-induced apoptosis were partially attenuated in DKO-LPA_2 MEFs (supplemental Fig. S2), suggesting that $G_{i/o}$ signaling to some extent is involved in the LPA_2-mediated antiapoptotic signaling. Nonetheless, LPA-induced recruitment of Siva-1, TRIP6, or NHERF2 was not significantly altered by treatment with PTX or the U73122 phospholipase C inhibitor (supplemental Fig. S3, *A* and *B*), suggesting that the macromolecular complex formation via the C terminus of LPA_2 is independent on $G_{i/o}$ or $G_{q/11}$ signaling.

The PDZ-mediated Association of TRIP6 with NHERF2 Facilitates Their Interaction with LPA$_2$—When we examined the interaction of different LPA_2 mutants with TRIP6 or NHERF2, we noticed that the C311A/C314A mutant, which does not bind to TRIP6, also showed reduced association

with NHERF2 compared with WT LPA_2 (Fig. 6*A*). Likewise, the L351A mutant defective in binding to NHERF2 showed reduced association with TRIP6 (Fig. 6*A*) but not Siva-1 (Fig. 3*B*). Conversely, the interaction of NHERF2 or TRIP6 with LPA_2 was further enhanced when all three proteins were overexpressed (Fig. 6*B*). TRIP6 contains a C-terminal TTDC PDZ-binding motif, potentially allowing it to interact with PDZ proteins, raising the possibility that cooperativity might exist between TRIP6 and NHERF2 in interacting with LPA_2. Indeed, we found LPA induced the association of NHERF2 with TRIP6 but not the TRIP6-ΔTTDC mutant in HEK 293T cells (Fig. 6*C*). Domain mapping confirmed that TRIP6 preferentially binds to PDZ2 but not PDZ1 of NHERF2 *in vitro* (Fig. 6*D*) and also in HEK 293T cells (Fig. 6*E*). Because both LPA_2 and TRIP6 bind to the PDZ2 domain of NHERF2, NHERF2 must be present in dimer form to bridge LPA_2 and TRIP6. In support of this notion, it is known that NHERF2 forms oligomers through PDZ1- and/or PDZ2-mediated self-association (24).

To address whether LPA_2, TRIP6, and NHERF2 are present in the same macromolecular complex, fluorescence microscopy was performed to examine subcellular distribution of these molecules. We found that HcRed1-LPA_2, BFP-TRIP6, and GFP-NHERF2 formed clusters and colocalized in close proximity to the plasma membrane or inside the cytosol after LPA treatment for 10 min (Fig. 6*F*). Together, these results suggest that LPA_2 forms a ternary macromolecular complex with TRIP6 and NHERF2 by LPA stimulation.

TRIP6 and NHERF2 Regulate LPA-mediated Chemoprotection in Ovarian Cancer Cells—To understand the physiological relevance of NHERF2-TRIP6-LPA_2 ternary complex formation, co-immunoprecipitation was performed in SKOV-3 cells that express high levels of these three proteins. LPA induced the association of LPA_2 with both TRIP6 and NHERF2 at physiological levels (Fig. 7*A*). When TRIP6 expression was knocked down, the interaction of NHERF2 with LPA_2 was significantly attenuated, suggesting that TRIP6 facilitates this association. However, the association of TRIP6 with LPA_2 was not significantly altered by knockdown of NHERF2 expression (supplemental Fig. S4), perhaps because either TRIP6 binds to LPA_2 with a higher affinity or other LPA_2-interacting PDZ proteins can also facilitate the association of TRIP6 with LPA_2. In SKOV-3 cells, TRIP6 associated with NHERF2 constitutively. Nonetheless, formation of the ternary complex required LPA stimulation (Fig. 7*B*).

LPA also protected cells from cisplatin-induced caspase-3/7 activation and PARP-1 cleavage in SKOV-3 ovarian cancer cells (Fig. 7*C*). We found 60% knockdown of TRIP6 expression attenuated LPA-mediated chemoprotection in SKOV-3 cells (Fig. 7*C*) as that shown in DKO-LPA_2 MEFs (Fig. 1*A*). When TRIP6 expression was knocked down by 80–90%, the protective effect of LPA on cisplatin-induced caspase-3/7 activation and PARP-1 cleavage was almost completely eliminated (Fig. 7*C*). A similar effect was found by 90% knockdown of NHERF2 expression (Fig. 7*D*). Together, these results suggest that both TRIP6 and NHERF2 play a significant role in the LPA-mediated antiapoptotic effect in SKOV-3 cells. Lacking functional p53, cisplatin only induced modest Siva-1 expression in SKOV-3 cells (Fig. 7*C*). Although both TRIP6 and Siva-1 bind to the C*XX*C motif of LPA_2, knockdown of TRIP6 expression did not alter the effect of LPA on reducing Siva-1 expression.

In summary, these data suggest that LPA induces the formation of a ternary complex containing LPA_2, TRIP6, and NHERF2. Our results favor the model that in addition to binding to Siva-1 and down-regulating its activity, LPA_2 forms a supramolecular complex with TRIP6 and NHERF2. Together, they coordinately regulate the antiapoptotic signaling of LPA_2 (Fig. 7*E*).

DISCUSSION

GPCRs are increasingly viewed as a nidus for generating ligand-activated intracellular signals via interactions with G proteins and non-G protein signaling molecules (25, 26). We hypothesized that the macromolecular complex formed via the unique C-terminal binding motifs of LPA_2 could be responsible for its antiapoptotic function. This hypothesis was based in part on the high degree of sequence diversity in the C termini of the endothelial differentiation gene family LPA receptors, which show only seven of 55 residues are conserved in the C terminus, in contrast to the 85% homology in their transmembrane

FIGURE 6. **A PDZ-mediated association of TRIP6 and NHERF2 facilitates their interactions with LPA_2.** *A*, mutation of the C*XX*C (PDZ-binding) motif of LPA_2 abolishes the binding to TRIP6 (*NHERF2*) and also reduces the association with NHERF2 (*TRIP6*). GFP-NHERF2 and MYC-TRIP6 were coexpressed with WT or one of the mutants of FLAG-LPA_2 in HEK 293T cells. Co-immunoprecipitation (*IP*) was performed as described above. The relative levels of co-immunoprecipitated TRIP6 or NHERF2 were quantified and normalized to the immunoprecipitated WT or mutant of LPA_2. *B*, overexpression of TRIP6 enhances association of NHERF2 with LPA_2, and vice versa. FLAG-LPA_2 was co-expressed with MYC-TRIP6 and/or GFP-NHERF2 in HEK 293T cells as indicated. After stimulation of the cells with 2 μM LPA for 10 min, co-immunoprecipitation was performed. GFP-NHERF2 and MYC-TRIP6 co-immunoprecipitated with FLAG-LPA_2 were detected with an anti-GFP antibody and an anti-MYC antibody, respectively. The blot was reprobed with an anti-FLAG antibody to detect the immunoprecipitated LPA_2. The relative levels of co-immunoprecipitated TRIP6 or NHERF2 were quantified and normalized to the immunoprecipitated FLAG-LPA_2. *C*, C-terminal TTDC sequences of TRIP6 mediate the binding to NEHRF2. FLAG-TRIP6 or FLAG-TRIP6-ΔTTDC mutant lacking the C-terminal PDZ-binding motif was co-expressed with GFP-NHERF2 in HEK 293T cells. After stimulation of the cells with LPA for 10 min, WT or the ΔTTDC mutant of TRIP6 was immunoprecipitated with anti-FLAG M2 mouse monoclonal antibody-conjugated agarose beads and resolved by SDS-PAGE. Immunoblotting (*IB*) was performed using the antibodies specific to GFP and the FLAG epitope to detect GFP-NHERF2 and FLAG-TRIP6, respectively. *D*, TRIP6 binds to the PDZ domain of NHERF2 directly *in vitro*. Purified recombinant TRIP6 was incubated with GST, GST-NEHRF2-PDZ1, or GST-NHERF2-PDZ2 at 4 °C for 3 h. TRIP6 pulled down by glutathione *S*-transferase (*GST*) fusion proteins was detected by immunoblotting using an anti-TRIP6 antibody. The *bottom panel* shows expression of GST fusion proteins by Ponceau S staining. *E*, TRIP6 interacts with the PDZ2 but not PDZ1 domain of NHERF2 in cells. HA-TRIP6 was co-expressed with GFP, GFP-NHERF2-PDZ1, or GFP-NHERF2-PDZ2 in HEK 293T cells. TRIP6 in the whole cell lysates was immunoprecipitated with anti-HA mouse monoclonal antibody-conjugated agarose beads and resolved by SDS-PAGE. The immunoblot was probed with an anti-GFP antibody to detect GFP-NHERF2-PDZ2. The blot was reprobed with an anti-HA rabbit antibody to detect the immunoprecipitated HA-TRIP6. Data shown in each figure are representative of two to four independent experiments. *HA*, hemagglutinin. *F*, LPA_2, TRIP6, and NHERF2 colocalize in cells. Hc-Red1-LPA_2 was transiently co-expressed with BFP-TRIP6 and GFP-NHERF2 in $LPA_{1/2}$ DKO MEFs. Cells were starved for 1 h, followed by addition of 2 μM LPA for 10 min. Subcellular distribution of these molecules was visualized by fluorescence microscopy.

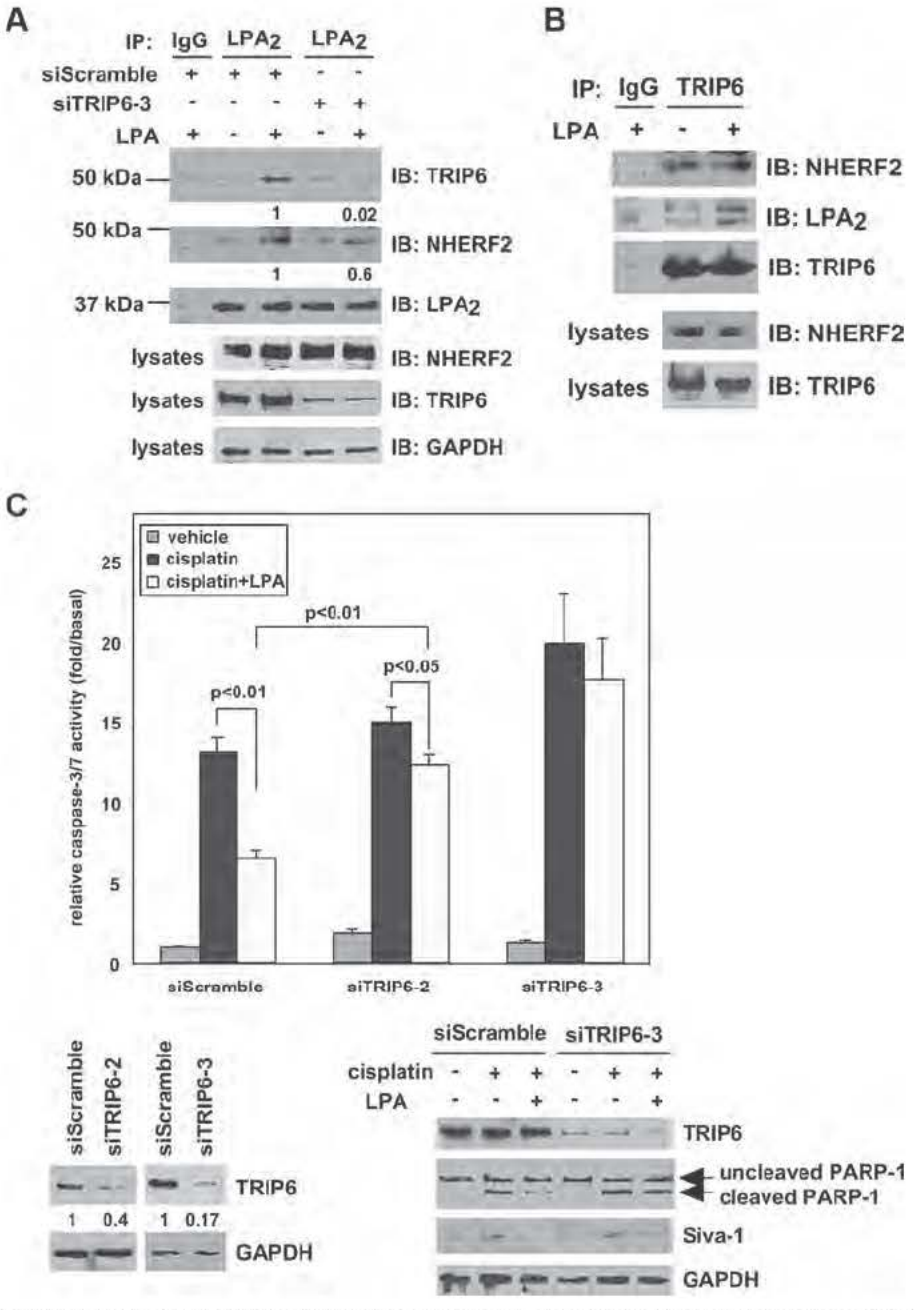

FIGURE 7. **Endogenous TRIP6 and NHERF2 form a ternary complex with LPA_2 by LPA stimulation, and regulate LPA-mediated chemoprotection in SKOV-3 cells.** *A*, inhibition of TRIP6 expression reduces LPA-induced association of NHERF2 with LPA_2. SKOV-3 cells expressing a scrambled siRNA or a TRIP6 siRNA (*siTRIP6-3*) were starved overnight followed by treatment with 2 μM LPA for 10 min. LPA_2 in the whole cell lysates was immunoprecipitated (*IP*) with an anti-LPA_2 rat antibody or a control IgG and resolved by SDS-PAGE. Immunoblotting (*IB*) was performed using the antibodies specific to NHERF2, TRIP6, and LPA_2, respectively. The *bottom three panels* show expression of NHERF2, TRIP6, and control glyceraldehyde-3-phosphate dehydrogenase (*GAPDH*) in the whole cell lysates. The relative levels of co-immunoprecipitated TRIP6 or NHERF2 were quantified and normalized to the immunoprecipitated FLAG-LPA_2. *B*, TRIP6 interacts with NHERF2 constitutively in SKOV-3 cells. SKOV-3 cells were treated with LPA as described in *A*. TRIP6 in the whole cell lysates was immunoprecipitated with an anti-TRIP6 mouse monoclonal antibody or a control IgG. After SDS-PAGE, the immunoblot was probed with an anti-NHERF2 antibody, an anti-LPA_2 antibody followed by an anti-TRIP6 antibody. Results shown in *A* and *B* are representative of three independent experiments. *C* and *D*, LPA-mediated protection of SKOV-3 cells from cisplatin-induced apoptosis is eliminated by knockdown of TRIP6 or NHERF2 expression. SKOV-3 cells expressing a scrambled siRNA or one of the siRNAs that specifically target human TRIP6 (*siTRIP6-2* and *siTRIP6-3*) (*C*) or NHERF2 (siNHERF2–4, siNHERF2–5) (*D*) as indicated were pretreated with 10 μM LPA for 1 h followed by the addition of 50 μM cisplatin for 20 h. Caspase-3/7 activity was determined. Data shown are the mean ± S.E. of three independent experiments. The knockdown effect of each TRIP6 siRNA or NHERF2 siRNA was determined by immunoblotting using an antibody specific to TRIP6 or NHERF2, respectively. Half of the lysates as indicated were subjected to immunoblotting using the antibodies specific to PARP-1, Siva-1, NHERF2, and GAPDH, respectively. *E*, a model for the regulation of LPA_2-mediated anti-apoptotic signaling through the *CXXC*-mediated interaction with Siva-1, and the *CXXC*- and PDZ-mediated LPA_2-TRIP6-NHERF2 ternary complex formation.

domains. In support of this hypothesis, it has been shown that PDZ proteins, including NHERF2, interact with the C-terminal DSTL motif of LPA_2 but not with other LPA receptor subtypes (10, 12, 13). Moreover, LPA_2 is the only LPA receptor subtype that interacts with Siva-1 and TRIP6 (17, 18).

Using the $LPA_{1/2}$ DKO MEFs that stably express a human LPA_2 as the model system, we present evidence that siRNA-mediated knockdown of TRIP6 or NHERF2 expression attenuates LPA_2-mediated chemoprotection; in contrast, knockdown of Siva-1 enhances this effect. We have mapped the $^{311}CXXC^{314}$ motif of LPA_2 required for interactions with TRIP6 and Siva-1, and demonstrated that disruption of either the *CXXC* motif or PDZ-binding motif attenuated LPA_2-mediated chemoprotection, and only when both binding motifs were disrupted, it completely abolished this effect. Together, these data indicate that LPA_2-mediated chemoprotection is regulated through these supramolecular complexes.

Palmitoylation of the four C-terminal cysteine residues of LPA_2 showed that those in the *CXXC* motif can be lipid-modified, however, inhibition of this modification did not disrupt interaction with TRIP6 or Siva-1, indicating that palmitoylation of LPA_2 is neither required nor preclusive for the interaction with TRIP6 or Siva-1. We also found that blocking $G_{i/o}$ protein activation with PTX or inhibiting $G_{q/11}$ signaling with the U73122 phospholipase C inhibitor did not affect the interaction of LPA_2 with Siva-1, TRIP6, or NHERF2, suggesting that G protein signaling is also not required for these protein interactions. On the other hand, mutation of the *CXXC*- or PDZ-binding motif of LPA_2 did not affect $G_{q/11}$-mediated Ca^{2+} transients upon LPA stimulation, indicating that these binding motifs do not affect the $G_{q/11}$ signaling branch.

Unexpectedly, we found that truncation or point mutations that

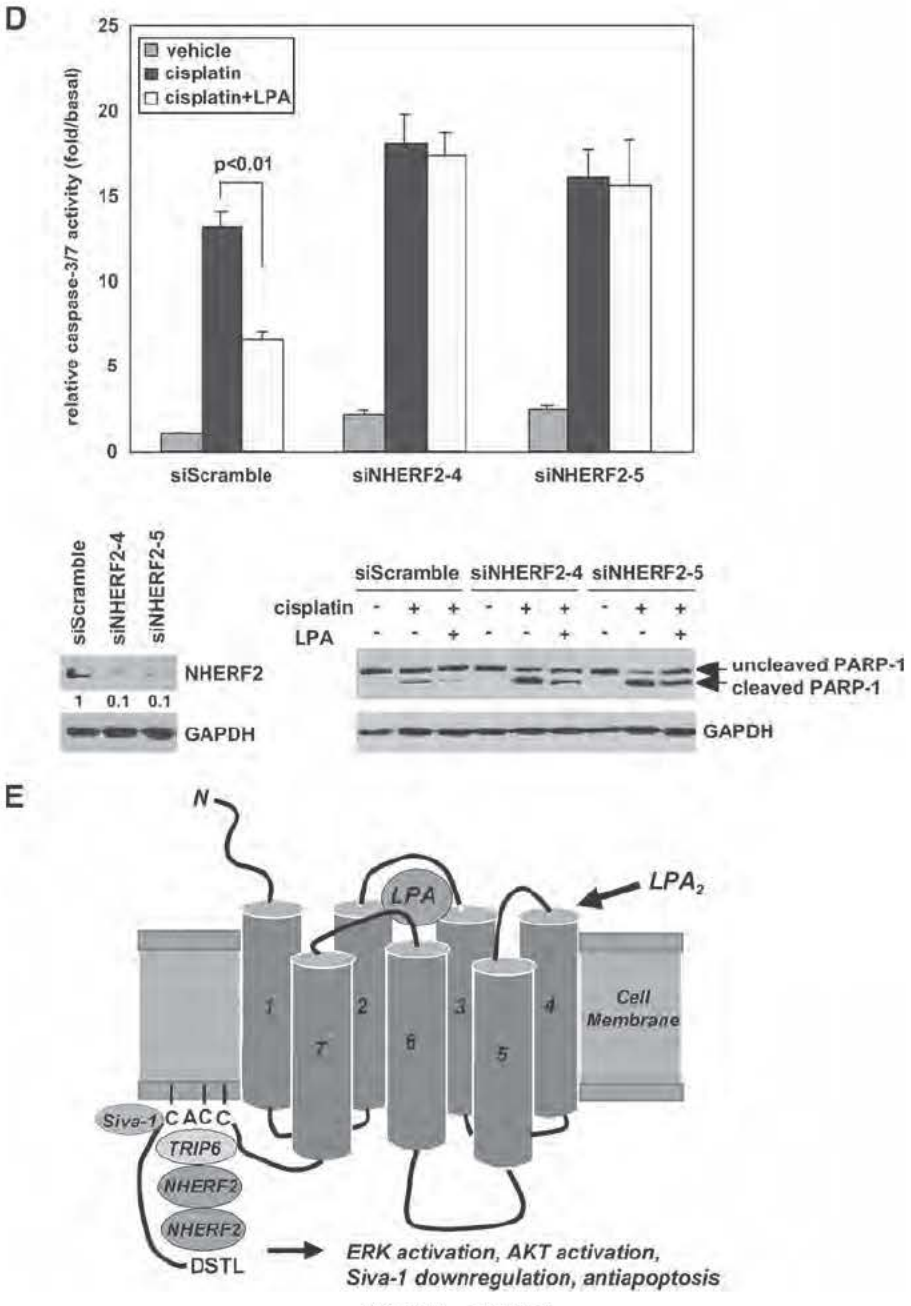

FIGURE 7—*continued*

abolish the interactions of LPA_2 with PDZ proteins also attenuated the binding of TRIP6 to LPA_2. These observations led us to hypothesize that cooperativity might exist between TRIP6 and NHERF2 in interacting with LPA_2. Indeed, we found evidence that TRIP6 interacts with the PDZ2 domain of NHERF2 via its C-terminal TTDC PDZ-binding motif. Overexpression of TRIP6 augments the complex formation between LPA_2 and NHERF2, whereas knockdown of TRIP6 diminishes it. Moreover, upon ligand activation LPA_2 colocalizes with both TRIP6 and NHERF2. Thus, it is likely that LPA_2, TRIP6, and NHERF2 form a ternary complex in the microdomain of the plasma membrane to coordinately regulate LPA_2-elicited chemoprotective effect. This complex appears to be assembled upon LPA stimulation in SKOV-3 cells at endogenous levels of the participating proteins. Our new data and previous reports (10, 12, 20, 27) show that both TRIP6 and NHERF2 are involved in LPA-induced ERK and AKT activation. SKOV-3 ovarian cancer cells show very low levels of phosphatase and tensin homolog but high activity of AKT (28, 29). When TRIP6 or NHERF2 was knocked down to a great extent, it almost completely eliminated LPA-mediated chemoprotection in SKOV-3 cells. Similarly, it has been reported that knockdown of NHERF2 expression abrogates the chemoprotective effect of LPA in colon cancer cells (27).

We also note that the *CXXC* motif is required for the antiapoptotic effect through the inhibition of Siva-1 signaling. However, Siva-1 interaction with LPA_2 does not appear to be affected by disruption of the LPA_2 interaction with PDZ proteins. Our data showed that PTX slightly attenuated LPA-induced chemoprotection, suggesting that $G_{i/o}$-mediated signals contribute to but are not sufficient for the full antiapoptotic effect of LPA_2. Assembly of the LPA_2-TRIP6-$NHERF_2$ ternary complex appears to play a fundamental role in the ability of LPA to render cancer cells resistant to chemotherapeutic agents as we have demonstrated for the case of adriamycin and cisplatin.

Taken together, these data point to a novel signal amplification/diversification mechanism originating from the GPCR signal transduction hub. We favor the hypothesis that signals from protein-protein interactions via the C-terminal *CXXC*- and PDZ-binding motifs are integrated with G protein-activated signals to cooperatively regulate the antiapoptotic function of LPA_2.

Acknowledgments—We thank Dr. Junken Aoki for providing the anti-LPA$_2$ antibody, Dr. A. P. Naren for the anti-NHERF2 antibody and pGEX-NHERF2, and Dr. Tim Towne for sharing the flow cytometry equipment.

REFERENCES

1. Mills, G. B., and Moolenaar, W. H. (2003) *Nat. Rev. Cancer* **3,** 582–591
2. Moolenaar, W. H., van Meeteren, L. A., and Giepmans, B. N. (2004) *Bioes-*

says **26,** 870–881
3. Parrill, A. L. (2008) *Biochim. Biophys. Acta* **1781,** 540–546
4. Pasternack, S. M., von Kugelgen, I., Aboud, K. A., Lee, Y. A., Ruschendorf, F., Voss, K., Hillmer, A. M., Molderings, G. J., Franz, T., Ramirez, A., Nurnberg, P., Nothen, M. M., and Betz, R. C. (2008) *Nat. Genet.* **40,** 329–334
5. Tabata, K., Baba, K., Shiraishi, A., Ito, M., and Fujita, N. (2007) *Biochem. Biophys. Res. Commun.* **363,** 861–866
6. Radeff-Huang, J., Seasholtz, T. M., Matteo, R. G., and Brown, J. H. (2004) *J. Cell Biochem.* **92,** 949–966
7. Deng, W., Shuyu, E., Tsukahara, R., Valentine, W. J., Durgam, G., Gududuru, V., Balazs, L., Manickam, V., Arsura, M., VanMiddlesworth, L., Johnson, L. R., Parrill, A. L., Miller, D. D., and Tigyi, G. (2007) *Gastroenterology* **132,** 1834–1851
8. Lin, F. T., and Lai, Y. J. (2008) *Biochim. Biophys. Acta* **1781,** 558–562
9. Li, C., Dandridge, K. S., Di, A., Marrs, K. L., Harris, E. L., Roy, K., Jackson, J. S., Makarova, N. V., Fujiwara, Y., Farrar, P. L., Nelson, D. J., Tigyi, G. J., and Naren, A. P. (2005) *J. Exp. Med.* **202,** 975–986
10. Oh, Y. S., Jo, N. W., Choi, J. W., Kim, H. S., Seo, S. W., Kang, K. O., Hwang, J. I., Heo, K., Kim, S. H., Kim, Y. H., Kim, I. H., Kim, J. H., Banno, Y., Ryu, S. H., and Suh, P. G. (2004) *Mol. Cell Biol.* **24,** 5069–5079
11. Yamada, T., Ohoka, Y., Kogo, M., and Inagaki, S. (2005) *J. Biol. Chem.* **280,** 19358–19363
12. Yun, C. C., Sun, H., Wang, D., Rusovici, R., Castleberry, A., Hall, R. A., and Shim, H. (2005) *Am. J. Physiol.* **289,** C2–C11
13. Zhang, H., Wang, D., Sun, H., Hall, R. A., and Yun, C. C. (2007) *Cell. Signal.* **19,** 261–268
14. Takahashi, Y., Morales, F. C., Kreimann, E. L., and Georgescu, M. M. (2006) *EMBO J.* **25,** 910–920
15. Wu, Y., Dowbenko, D., Spencer, S., Laura, R., Lee, J., Gu, Q., and Lasky, L. A. (2000) *J. Biol. Chem.* **275,** 21477–21485
16. Chun, J., Kwon, T., Lee, E., Suh, P. G., Choi, E. J., and Sun Kang, S. (2002) *Biochem. Biophys. Res. Commun.* **298,** 207–215
17. Xu, J., Lai, Y. J., Lin, W. C., and Lin, F. T. (2004) *J. Biol. Chem.* **279,** 10459–10468
18. Lin, F. T., Lai, Y. J., Makarova, N., Tigyi, G., and Lin, W. C. (2007) *J. Biol. Chem.* **282,** 37759–37769
19. Bach, I. (2000) *Mech. Dev.* **91,** 5–17
20. Lai, Y. J., Chen, C. S., Lin, W. C., and Lin, F. T. (2005) *Mol. Cell. Biol.* **25,** 5859–5868
21. Fortin, A., MacLaurin, J. G., Arbour, N., Cregan, S. P., Kushwaha, N., Callaghan, S. M., Park, D. S., Albert, P. R., and Slack, R. S. (2004) *J. Biol. Chem.* **279,** 28706–28714
22. Wan, J., Roth, A. F., Bailey, A. O., and Davis, N. G. (2007) *Nat. Protoc.* **2,** 1573–1584
23. Qanbar, R., and Bouvier, M. (2003) *Pharmacol. Ther.* **97,** 1–33
24. Lau, A. G., and Hall, R. A. (2001) *Biochemistry* **40,** 8572–8580
25. Hur, E. M., and Kim, K. T. (2002) *Cell. Signal.* **14,** 397–405
26. Maudsley, S., Martin, B., and Luttrell, L. M. (2005) *J. Pharmacol. Exp. Ther.* **314,** 485–494
27. Rusovici, R., Ghaleb, A., Shim, H., Yang, V. W., and Yun, C. C. (2007) *Biochim. Biophys. Acta* **1770,** 1194–1203
28. Longva, K. E., Pedersen, N. M., Haslekas, C., Stang, E., and Madshus, I. H. (2005) *Int. J. Cancer* **116,** 359–367
29. Wang, H. Q., Altomare, D. A., Skele, K. L., Poulikakos, P. I., Kuhajda, F. P., Di Cristofano, A., and Testa, J. R. (2005) *Oncogene* **24,** 3574–3582

AQ: F

A tightly regulated single genome Tet-On adenoviral vector

Aixia Ren[1,2], Sravya Penmatsa[1,2], Lorraine M. Albritton[3], Gabor Tigyi[1], Junming Yue[1,2]*

[1]Department of Physiology, [2]Viral Vector Core Laboratory, [3]Department of Molecular Sciences, The University of Tennessee Health Science Center, Memphis, TN

*Corresponding Author:

Junming Yue

Viral Vector Core Laboratory, Cancer Research Building, 19 S. Manassas St., University of Tennessee Health Science Center, Memphis, TN 38163

Phone: 901-448-2091

Fax: 901-448-3910

Email: jyue@utmem.edu

Key Words: Tet-On, adenoviral vector, single genome

Abstract: 200 words

Manuscript: 1, 634 words

Abstract

We constructed a tightly regulated single genome Tet-On adenoviral vector containing a DOX-regulated transcriptional unit for expression of the gene of interest and a constitutive transcriptional unit for expression of the Tet reverse transactivator. The first transcriptional unit consisting of the second-generation tetracycline (Tet) regulated promoter pTRE-tight was inserted into the E1 deletion region. The second unit consisting of the second-generation reverse transactivator rtTA-M2 driven by a minimal EF1α promoter was inserted into the E3 deletion region. To test this system, recombinant adenovirus expressing the reporter gene EGFP was produced in AD293 cells and used to transduce HeLa cells. Following doxycycline (DOX) treatment, EGFP expression was tightly regulated in a spatiotemporal manner with almost undetectable basal leakiness. This single genome viral vector provides a convenient and powerful tool for gene function or gene therapy studies by eliminating the inefficiency of co-infection with two separate viruses. It represents an advance from previous single vector Tet-regulated adenoviruses by virtue of the more tightly regulated pTRE-tight promoter, the higher transactivating activity of rtTA-M2 and the smaller mini-EF1α promoter.

Introduction

The tetracycline-controlled Tet-On or Tet-Off vectors are the most widely used regulated gene expression systems that allow for the dose-dependent transgene expression (1). Whereas, transcription is turned off in the presence of tetracycline in

the Tet-Off system (2), in the Tet-On system, the reverse tetracycline-responsive transcriptional activator rtTA activates transcription by binding to Tet operator sequences embedded in a promoter (3). Recent innovations in both systems resulted in tightly negative or positive control of transgene expression. Adenoviral vectors are one of the most efficient viral vector systems for delivering foreign genes into cells (4-6). The most frequently used inducible adenoviral vector systems rely on a double-infection strategy that is time-consuming and requires construction of two separate viruses each with E1 gene-substitutions (7). Moreover, the efficiency is relatively low for two viruses transducing the same cells simultaneously, even when a very high multiplicity of infection (MOI) is applied, resulting in highly variable transgene expression. Previous reports have described doxycycline (DOX) inducible single adeno-genome vector systems (8-10), but these systems use the first generation Tet-regulated promoters and first generation rtTA which are relatively leaky (high basal level of gene expression). In addition, neither of these systems has been placed in a public access reagent depository and they are not commercially available. We constructed a more tightly regulated single genome, doxcycline inducible adenoviral vector, which is very convenient to be used for gene functional studies by solely inserting the gene of interest into one of shuttle vectors, pE1.2-Tet. The recombinant adenoviral genome can be efficiently generated through phage based cosmid, which usually yields 100% correct recombination(11,12). The adenovirus can be quickly rescued by transfection of AD293 cells.

Materials and Methods

Cells and Reagents

AD293 and HeLa cell lines were maintained in DMEM culture medium supplemented with 10% fetal bovine serum (Mediatech Inc., Manassas, VA), 20 unit/mL penicillin, and 0.02% mg/mL streptomycin under 5% CO_2 at 37 °C. Restriction and modification enzymes were purchased from the New England Biolabs (Beverly, MA), and T4 DNA ligase was purchased from Takara (Pittsburgh, PA). DOX was purchased form Clontech (Mountain View, CA)

Construction of the shuttle vectors

This single genome, DOX inducible adenoviral vector system has two shuttle vectors, pE1.2-Tet and pE3.1-mini-EF1α-rtTA-M2. The pE1.2-Tet contained a DOX-regulated promoter and multiple cloning sites (MCS) as well as a polyA sequence. This shuttle vector was constructed as follows. First a DOX-regulated promoter was amplified from pTRE-Tight vector (Clontech, Mountain View, CA) using PCR with the 5' ATATCGCGACGAGTTTACTCCCTATCAGTG 3' (forward) and 5' ATAGCTAGCGGCGATCTGACGGTTCACTAA 3'(reverse) primers. The forward primer contains an NruI site (underlined) and the reverse primer contains a NheI site. The resulting PCR product was digested with NruI and NheI. This promoter was used to replace the CMV promoter from pcDNA3.1-Zeo (Invitrogen, Carlsbad, CA). The resulting plasmid pcDNA3.1-Tet-Zeo was cleaved with PuvII, the ends blunted with Klenow polymerase, and finally recleaved with BglII. The fragment containing the Tet promoter, multiple cloning sites (MCS) and bovine growth hormone polyA

sequences was purified and introduced into the BglII and Klenow-modified KpnI sites of the pE1.2 plasmid (O.D. 260 Inc., Boise, IA).

The pE3.1-mini-EF1α shuttle vector was constructed by inserting a EF1α mini-promoter, MCS and polyA sequences into pE3.1 (O.D. 260 Inc., Boise, IA). The mini-EF1α promoter was amplified by PCR from the pEF6/myc-his plasmid (Invitrogen, Carlsbad, CA) using the following primers: 5' TCGGCGCTCGCGATCTAGACGTGAGGCTCCGGTGCCCGTC 3'(forward) and 5' ACGCGCTAGCCTGTGTTCTGGCGGCAAAC 3'(reverse). The primers contain NruI and NheI sites (underlined) with an additional Xba I site (double underlined) in the forward primer. The PCR-amplified EF1α mini-promoter was digested with NruI and NheI and ligated into the NruI and XbaI sites of pcDNA3.1 in place of the CMV promoter to generate plasmid pcDNA3.1-mini-EF1α. The fragment encompassing the mini-EF1α promoter, MCS and the polyA sequences was isolated after digestion with XbaI and PvuII, then inserted into XbaI and Klenow-blunted KpnI sites of the pE3.1 plasmid. Finally, the reverse transactivator rtTA-M2 cDNA was inserted into the BamHI and EcoRI sites of pE1.3-mini-EF1α to generate the shuttle vector pE1.3-mini-EF1α -rtTA-M2.

Construction of the recombinant adenoviral genome

The reporter gene EGFP was cloned into BamHI and EcoRI sites of pE1.2-Tet to generate the shuttle vector pE1.2-Tet-EGFP. To make an EGFP recombinant adenovirus, pE1.2-Tet-EGFP and pE3.1-mini-EF1α-rtTA-M2 were digested with DraIII. The fragments containing the EGFP and rtTA-M2 expression cassettes from these two shuttle vectors were purified and ligated with Sfi-digested

AdenoQuick^{TM}13.1 adeno-genome DNA (O.D. 260, Inc., Boise, IA) in a 10 µl volume, at 16 ^{o}C overnight. A 2 µl aliquot from the ligation reaction was mixed with 6 µl λ packaging extract (Stratagene, La Jolla, CA), incubated for 90 min at room temperature, the reaction was stopped by adding 200 µl SM buffer (0.1 M NaCl, 8 mM $MgSO_4$, 50 mM Tris-HCl pH 7.5, 0.01% (w/v) gelatin) and 10 µl chloroform. After brief vortexing and centrifugation, the supernatant was used to infect *E. coli* Top 10F' (Invitrogen, Carlsbad, CA). After DNA packaging into phage and *E. coli* infection, cosmid DNA was purified from several colonies and the desired recombinants were identified by restriction enzyme analysis separately with BamHI and EcoRI.

Virus generation, purification and infection

DNA from a correct recombinant was linearized with PacI and transfected into AD293 cells using SuperFect Transfection reagent (Qiagen, Valencia, CA). Recombinant Ad-EGFP virus particles were harvested 7-10 days following the transfection, then amplified and purified with a Vivapure Adenopack (Sartorium Stedim, Inc. Concord, CA) according to the manufacturer's protocol.

Virus stocks were titrated using Adeno-X Rapid Titer Kit (Clontech, Mountain View, CA). Typically titers of the purified virus stocks were greater than 10^{10} infectious units/ml using this method. HeLa cells were infected at an M.O.I. of 10 for 2 h, followed by a single wash with DMEM and then cultured in 2 ml DMEM supplemented with 10% FBS and different concentration of doxycycline for the indicated periods of time.

Results and Discussion

As the basis of the new DOX-inducible single genome adenoviral vector system we constructed two shuttle vectors, pE3.1-mini-EF1α–rtTA-M2 and pE1.2-Tet. The first shuttle vector pE3.1-mini-EF1α-rtTA-M2 contains a cassette for expression of the second generation reverse transactivator rtTA-M2 (13) flanked by restriction enzyme sites useful for insertion into the adeno-genome (Fig.1). To drive expression we constructed a 235 bp human EF1α mini-promoter that contains the CAAT and TATA box promoter sequences but lacks the upstream enhancer and downstream intronic sequences. These segments were removed to avoid the possibility that any regulatory sequences present in them would interfere with regulation of viral gene expression after recombination into the adenoviral genome. Deleting the sequences also reduced the size of the expression cassette.

The original pE1.2 shuttle vector required the gene of interest be inserted as an entire expression cassette. For convenience, shuttle vector pE1.2-Tet was constructed. It consists of the pTRE-tight promoter containing seven copies of the Tet operator sequences embedded within a minimal CMV promoter (Fig. 1). Insertion of a gene of interest into the MCS places it under the DOX-regulated promoter flanked by recognition sites for DraIII, AlwNI, BstAPI and PflMI that enable subsequent insertion into the adeno-genome.

To test this system, we inserted an EGFP reporter gene into the pE1.2-Tet shuttle and constructed a single recombinant adenoviral genome by ligating the resulting Tet-regulated EGFP cassette into the E1 deletion region and the mini-EF1α-rtTA-M2

cassette into E3 of AdenoQuickTM13.1, an adeno-genome vector. We recovered and purified recombinant EGFP adenovirus from human AD293 then used it to transduce HeLa cells at an M.O.I. of 10. Increasing amounts of DOX were fed to the transduced cells and the expression of the EGFP transgene was observed 24hr later by fluorescent microscopy and western blot analysis. EGFP expression was tightly regulated and highly induced by DOX treatment (Fig.2).

These results indicate that the new single genome adenoviral vector is a tightly regulated DOX-inducible system. This system provides the following advantages over other single genome adenoviral vectors: 1) the new EF1α mini-promoter is smaller than previous promoters yet gave strong activity in driving second generation rtTA-M2 expression; 2) the new optimized DOX-responsive promoter $pTRE_{-tight}$ displays extremely low background; 3) the bovine growth factor polyA sequences used in both shuttle vectors provides strong polyA tail sequences to maintain transgene mRNA stability.

Although rtTA-M2 was used in this study, we recently replaced it with a third generation reverse transactivator rtTA-M3. The resulting single genome adenovector showed an approximate two-fold increase in inducibility when compared to rtTA-M2 (data not shown). These two tightly controlled, DOX-inducible single genome Tet-On adenoviral vector systems should be particularly useful for gene therapy studies and as investigational tools.

Acknowledgement: This study was supported by a grant **W81XWH-07-1-0248** from DOD to G.T and L.M.A..

Competing interests Statement: The authors declare no competing interests.

References

1. **Kitamura, M.** 1998. Transgene regulation by the tetracycline-controlled transactivation system. Exp Nephrol *6*:576-580.
2. **Gossen, M. and H. Bujard.** 1992. Tight control of gene expression in mammalian cells by tetracycline-responsive promoters. Proc Natl Acad Sci U S A *89*:5547-5551.
3. **Gossen, M., S. Freundlieb, G. Bender, G. Muller, W. Hillen and H. Bujard.** 1995. Transcriptional activation by tetracyclines in mammalian cells. Science *268*:1766-1769.
4. **Benihoud, K., P. Yeh and M. Perricaudet.** 1999. Adenovirus vectors for gene delivery. Curr Opin Biotechnol *10*:440-447.
5. **Bett, A.J., W. Haddara, L. Prevec and F.L. Graham.** 1994. An efficient and flexible system for construction of adenovirus vectors with insertions or deletions in early regions 1 and 3. Proc Natl Acad Sci U S A *91*:8802-8806.
6. **Nemerow, G.R.** 2000. Cell receptors involved in adenovirus entry. Virology *274*:1-4.
7. **Luo, J., Z.L. Deng, X. Luo, N. Tang, W.X. Song, J. Chen, K.A. Sharff, H.H. Luu, et al.** 2007. A protocol for rapid generation of recombinant adenoviruses using the AdEasy system. Nat Protoc *2*:1236-1247.

8. **Mizuguchi, H. and T. Hayakawa.** 2002. The tet-off system is more effective than the tet-on system for regulating transgene expression in a single adenovirus vector. J Gene Med *4*:240-247.

9. **Mizuguchi, H. and M.A. Kay.** 1999. A simple method for constructing E1- and E1/E4-deleted recombinant adenoviral vectors. Hum Gene Ther *10*:2013-2017.

10. **Mizuguchi, H., Z.L. Xu, F. Sakurai, T. Mayumi and T. Hayakawa.** 2003. Tight positive regulation of transgene expression by a single adenovirus vector containing the rtTA and tTS expression cassettes in separate genome regions. Hum Gene Ther *14*:1265-1277.

11. **Danthinne, X.** 2001. Simultaneous insertion of two expression cassettes into adenovirus vectors. Biotechniques *30*:612-616, 618-619.

12. **Danthinne, X. and E. Werth.** 2000. New tools for the generation of E1- and/or E3-substituted adenoviral vectors. Gene Ther 7:80-87.

13 Urlinger, S. and Thellmann, M. 2000. Exploring the sequence space for tetracycline-dependent transcriptional activators: novel mutations yield expanded range and sensitivity. Proc. Natl. Acad. Sci. 97:7963–7968

Figure Legends

Fig. 1. Construction of a single genome, DOX inducible adenoviral vector.

Two shuttle vectors, pE1.2-Tet-EGFP and pE3.1-EF1a–rtTA-M2, were constructed and inserted into the E1 and E3 deletion regions of adeno-genome through homologous recombination, respectively, as described in Materials and Methods.

Fig. 2. Induction of EGFP gene expression in HeLa cells infected by a single genome DOX-inducible adenovirus.

(A) Adherent HeLa cells were infected at an M.O.I. of approximately 10 using Ad-EGFP virus and then grown in culture medium containing different concentrations of doxycyline. Micrographs of infected cells were captured after 24h by fluorescent microscopy (magnification 100X). (B) EGFP expression at 24 h post-infection was also determined by Western blot.

Fig.1:

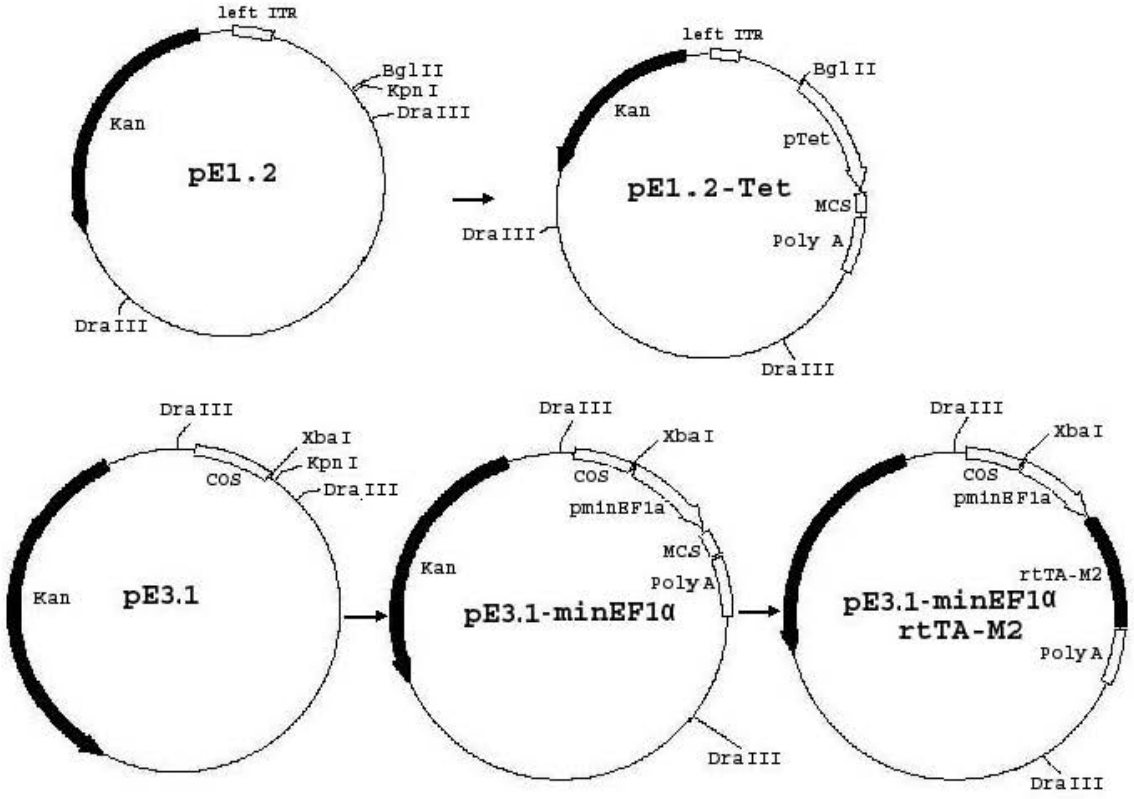
left ITR
Bgl II
Kpn I
DraIII
Kan
pE1.2
DraIII
left ITR
Bgl II
Kan
pTet
pE1.2-Tet
MCS
Poly A
DraIII
DraIII
DraIII
Xba I
Kpn I
COS
DraIII
Kan
pE3.1
DraIII
Xba I
COS
pminEF1a
MCS
Kan
Poly A
pE3.1-minEF1α
DraIII
DraIII
Xba I
COS
pminEF1a
rtTA-M2
pE3.1-minEF1α
rtTA-M2
Poly A
DraIII

Fig.2

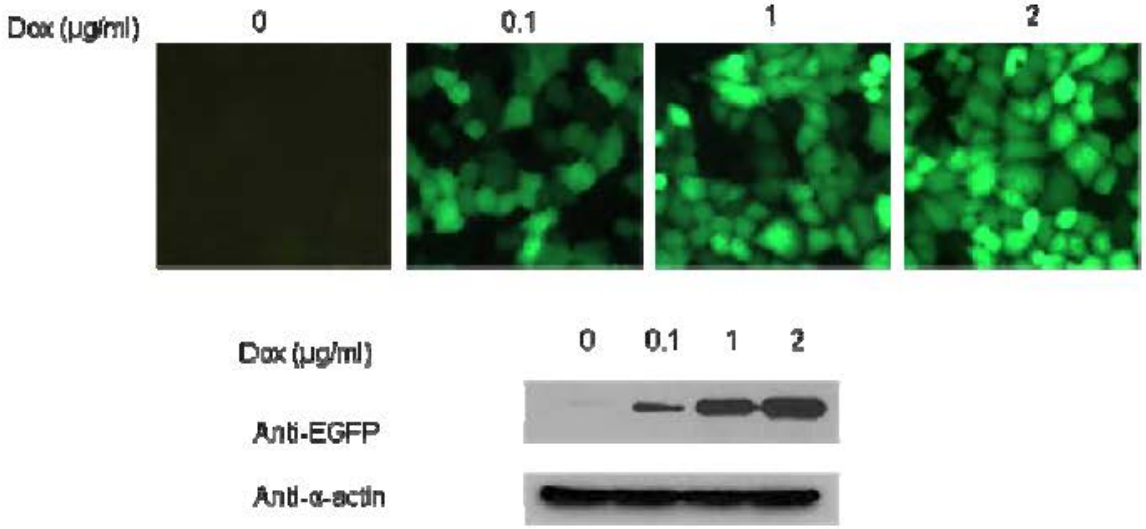
Dox (μg/ml)
0
0.1
1
2
Dox (μg/ml)
0
0.1
1
2
Anti-EGFP
Anti-α-actin

For office use only

THE UNIVERSITY OF TENNESSEE INVENTION DISCLOSURE FORM

For office use only

1. TITLE OF THE INVENTION.
MicroRNA-21 (miR-21)-based gene knockdown system

---

2. DESCRIBE THE INVENTION BRIEFLY. *(If possible, attach a manuscript, a drawing, an abstract, or any other materials that would assist in the understanding of the invention.)*

This invention describes a microRNA-21 (miR-21)-based gene knockdown system. MicroRNAs are a class of non-coding small RNAs that negatively regulate gene expression by degrading the target messenger RNA (mRNA) or inhibiting protein translation. Increasingly, miRNA-based gene interference is being used as an alternative to gene knockout strategies, which are complicated by the need for embryonic stem (ES) cells, complex molecular manipulations and inefficient homologous recombination. In addition, gene knockout technologies are only feasible in experimental animal models in which ES cells are available (i.e., mice). **We have constructed a lentiviral vector that contains the ubiquitously expressed mammalian promoter *Ubiquitin* (*Ubc*, plus exon 1, intron 1 and part of exon 2) driving expression of a bicistronic transgene that includes a recombinant miR-21 sequence and the enhanced green fluorescent protein (EGFP) reporter gene.** In this construct, the miR-21 sequence is inserted into intron 1 of the UBC gene, which may facilitate processing of the bicistronic transgene. The native miR-21 hairpin (targets include the tumor suppressor genes, *Pten*, *Pcdc4* and *Tpm1*) can be modified to target any gene of interest. We have generated and initiated testing of several gene targeting constructs on this backbone (e.g., *EGFP*, *Vasa*).

This miR-21-based gene knockdown system may provide advantages over miR-30- and miR-155-based gene knock down system systems that are commercially available from Open Biosystems and Invitrogen, respectively. First, the commercially available systems employ the cytomegalovirus (CMV) promoter, which drives high expression of recombinant transgenes in many cell lines, but is sometimes silenced in stem cells and during in vivo development. Stable expression of Ubc and other mammalian promoters has been demonstrated in stem cells and through development in transgenic animal models. Second, our initial investigations indicate that the commercial miR30-based system (Open Biosystems) exhibits incomplete processing of the miR-30 hairpin sequence and the EGFP reporter gene, which may negatively effect expression of both the hairpin and reporter gene. In our miR-21 based system, the bicistronic transgene was completely processed and this may have implications for the level of target gene knockdown. Third, our preliminary evaluations suggest that the miR-21 sequence may have enhancer activity that leads to increased expression of both the recombinant miR-21 and the reporter gene. These features need to be confirmed by additional designed experimentation.

---

3. CONTRIBUTORS/POSSIBLE INVENTORS. *(For a definition of the term "inventor," please refer to the document titled, "Who is an Inventor?," available from your Campus Research Office. All individuals who contributed to the conception of the invention should be listed below, whether or not they are affiliated with The University of Tennessee. Please note that a patent can be rendered invalid by including as an inventor an individual who did not contribute to the conception of the invention. The individual who is named in section A.1. below is designated as the primary contact for additional information and for all correspondence.*

A. Contributors whose *primary* affiliation at the time of invention was The University of Tennessee

(1) Name __Junming Yue_____ Dr., Mr., or Ms.? ___Dr._____

Title ____Assistant Professor_____ Dept. Physiology_____

Work address _19 S. Manassas st. Rm266_____ e-mail ____jyue@utmem.edu_____

Work phone __901-448-2091_____Fax ____901-448-3910_Social Security No. 411855234_____

(2) Name ___Gabor Tigyi_____ Dr., Mr., or Ms.?__Dr._____

Title _____Professor and Chair_____ _____Dept.____Physiology_____

Work address 894 Union Ave._____ e-mail _____gtigyi@physio1.utmem.edu_____

Work phone _____ Fax _____ Social Security No. _____

(3) Name _____ Dr., Mr., or Ms.? _____

Title _____ Dept. _____

Work address _____ e-mail _____

Work phone _____ Fax _____ Social Security No. _____

(4) Name _____ Dr., Mr., or Ms.? _____

Title _____ Dept. _____

Work address _____ e-mail _____

Work phone _____ Fax _____ Social Security No. _____

(5) Name _____ Dr., Mr., or Ms.? _____

Title _____ Dept. _____

Work address _____ e-mail _____

Work phone _____ Fax _____ Social Security No. _____

B. Contributors whose primary affiliation at the time of invention was *other than* The University of Tennessee

(1) Name _____Kyle Orwig_____ Dr., Mr., or Ms.? Dr._____

Title _Assistant Professor_____Employer: University of Pittsburgh School of Medicine_

Work address Magee-Womens Research Institute, 204 Craft Ave. Pittsburgh, PA 15213_ e-mail: korwig@pdc.magee.edu

Work phone _412-641-2460_____ Fax _412-641-3899_____ Social Security No. _544-82-1317_____

(2) Name _ Yi Sheng_____ Dr., Mr., or Ms.? _____Dr._____

Title _Assistant Professor_____ Employer __University of Pittsburgh School of Medicine_

Work address _ Magee-Womens Research Institute, 204 Craft Ave. Pittsburgh, PA 15213 e-mail: _ysheng@pdc.magee.edu_

Work phone: _412-641-2462_____ Fax _412-641-3899__ Social Security No. _219-57-3496__

4. LIST ALL SOURCES OF FUNDING OR SPONSORSHIP OF THE WORK WHICH LED TO THE INVENTION.

A. Federal sponsorship

(1) Agency name _____Department of Defense_____ Contract or grant no._____

Principal Investigator _____Gabor Tigyi_____
Dept._____physiology_____

(2) Agency name _NIH/NCRR_____ Contract or grant no. _R01 RR18500_____

Principal Investigator Kyle Orwig_ Dept. Ob/Gyn & Reproductive Sciences, University of Pittsburgh School of Med.

(3) Agency name __ _____ Contract or grant no. _____

Principal Investigator _____ Dept. _____

B. Private sponsorship

(1) Company name _____ Contract or grant no. _____

Principal Investigator _____ Dept. _____

(2) Company name _____ Contract or grant no. _____

Principal Investigator _____ Dept. _____

C. University sponsorship

(1) Department _____ Dept. Head _____

(2) Department _____ Dept. Head _____

(3) Center or Institute ___

(4) Special program *(e.g., Distinguished Scientist Program or Collaborating Scientist Program)*

_____

(5) Other _____

D. Other sponsorship

(1) Department ___Ob/Gyn & Reproductive Sciences (Pittsburgh)_____Dept. Head__W. Allen Hogge_____

(2) Center or Institute__Magee-Womens Research Institute and Foundation_(Pittsburgh___Director_Yoel Sadovsky_____

E. Did you use any material in the development of this invention that was acquired from a third party and was subject to a Material Transfer Agreement? Yes _____ No x_____
If your answer is yes, please attach a copy of each such agreement.

F. During the period of time when this technology was being developed, did any of the contributor(s) receive salary support from the Department of Veterans Affairs ("VA")? Yes _____ No x_____
If your answer is yes, please provide (attach) details.
Were any VA funds or facilities used in the course of work which led to this invention? Yes_____ No__x_____
If your answer is yes, please provide (attach) details.

5. DISCLOSURE. *In order to obtain valid patent protection on an invention in this country, a patent application must be filed with the United States Patent and Trademark Office within one year after the invention is first described in a printed publication anywhere in the world and within one year after the invention is first on sale or in public use in the United States. To preserve patent rights in many foreign countries, a United States patent application must be filed before any public disclosure in any form anywhere in the world and an application must be filed in the foreign country within one year from the U.S. filing date. If these deadlines are not met, the invention is deemed no longer "new" for patent purposes, and therefore not patentable. For additional information, please see, "The Impact of Public Disclosure on Patent Protection," available from your Campus Research Office.*

A. Journals. *Include all manuscripts describing the invention that have been published, those that have been accepted but not yet published, and those that have simply been submitted but not yet accepted or rejected. Also include any manuscripts that you intend to submit within the next six months. In that case, give the best information that you have at the present time. Please note that authors of a manuscript concerning the invention may not necessarily qualify as inventors.*

(1) Name of journal _____

Title of manuscript _____

Author(s) _____

(Anticipated) Dates of submission/acceptance/publication _____

(2) Name of journal _____

Title of manuscript _____

Author(s) _____

(Anticipated) Dates of submission/acceptance/publication _____

B. Conferences. *Include conferences at which any presentation concerning the invention has been made, as well as conferences which have not yet occurred but for which a manuscript or abstract has been submitted. Also include any conferences at which you intend to disclose information concerning the invention within the next six months. In that case, give the best information that you have at the present time.*

(1) Title of conference _____

Date _____ Location _____

Title of abstract or manuscript submitted _____

Is (or was) the abstract or manuscript distributed prior to the conference? _____ If so, when _____

_____

(2) Title of conference _____

Date _____ Location _____

Title of abstract or manuscript submitted _____

Is (or was) the abstract or manuscript distributed prior to the conference? _____ If so, when _____

_____

C. Theses and dissertations. *Include any thesis or dissertation describing the invention that has been submitted to meet the requirements of graduation. Also include any thesis or dissertation that may be submitted within the next twelve months.*

(1) Title of thesis or dissertation _____

Author _____ (Anticipated) Date of graduation _____

(2) Title of thesis or dissertation _____

Author _____ (Anticipated) Date of graduation _____

D. Offer for sale or public use.

(1) Has any embodiment of this invention been offered for sale (i.e., has a "thing" embodying the invention or capable of performing the invention been offered for sale)?_____

If so, when? _____ To whom and under what circumstances?

_____

_____

(2) Has any embodiment of this invention been used publicly?

_____

If so, when? _____ Under what circumstances?

_____

_____

E. Other.

Has any other disclosure of the invention (written or oral) been made to a third party who is not bound by a written obligation of confidentiality? If so, when? _____ To whom and under what circumstances? _____

_____

6. WITNESS. *This individual should be sufficiently knowledgeable in the field to enable him or her to understand the invention; a faculty member or research associate in the same department is usually a good choice if he or she is not listed as a contributor to this invention.*

I have read and understood the foregoing disclosure.

_____	_____	_____
Signature	*Title*	*Date*

7. ALLOCATION OF RIGHTS IN THE INVENTION. *(This section applies only to those contributors who are subject to The University of Tennessee's Policy on Patents, Copyrights, and Other Intellectual Property. The rights of any contributors who are not subject to such policy will be addressed separately as appropriate under the circumstances.)*

A. Rights of The University of Tennessee. *The University of Tennessee does not claim rights in inventions that are not developed in performing the duties of employment by the University or with substantial use of University funds or facilities. That determination is made on an individual basis with regard to each contributor. To assist in that determination, each University contributor should sign either in the "Yes" or the "No" column below. If your answer is "No," please attach a separate sheet of paper explaining the reasons for your position.*

YES	NO
In my opinion, my contribution to this invention <u>was</u> made in performing the duties of employment by the University or through the substantial use of facilities or funds provided by the University.	In my opinion, my contribution to this invention was <u>not</u> made in performing the duties of employment by the University or through the substantial use of facilities or funds provided by the University.
_____ *(signature of contributor)*	_____ *(signature of contributor)*
_____ *(signature of contributor)*	_____ *(signature of contributor)*
_____ *(signature of contributor)*	_____ *(signature of contributor)*
_____ *(signature of contributor)*	_____ *(signature of contributor)*
_____ *(signature of contributor)*	_____ *(signature of contributor)*

B. Recommendations of Contributor(s):

(1) It is my (our) recommendation that ownership of primary rights in this invention should remain with/ be assigned to:

___ the sponsoring agency because of contractual obligations.

___ the contributor(s) with recognition of contractual obligations of the University to sponsor(s), if any.

___ UTRF because of possibility of commercial value.

___ other _____

(2) Division of income *(Complete only when the disclosed invention was developed by more than one individual.)*

Contributors agree and request that any income accruing to them as a result of this invention be allocated in the following percentages *(which should total 100%)*:

_____	_____%	_____(Date)
_____	_____%	_____(Date)
_____	_____%	_____(Date)
_____	_____%	_____(Date)
_____	_____%	_____(Date)

Note: The issue of Division of Income will be revisited in the event that it is determined that some of the named contributors are not inventors or that there are one or more additional inventors not named on this disclosure.

8. COMMENTS BY DEPARTMENT HEAD: _____

_____

_____ _____
Signature of Department Head Date

9. COMMENTS BY DEAN: _____

_____

_____ _____
Signature of Dean Date

10. COMMENTS BY CAMPUS RESEARCH/ADMINISTRATIVE OFFICER:

_____

_____

There are ___/ are not ___ contractual restrictions precluding an assignment of this invention by the University to UTRF.

_____ _____
Signature of Campus Research Officer Date

11. ACTION TAKEN BY THE UNIVERSITY'S PATENT, COPYRIGHT, AND OTHER INTELLECTUAL PROPERTY COMMITTEE:

___ Ownership assigned to or to remain with contributor(s)

___ Ownership assigned to UTRF

___ Ownership assigned to sponsor pursuant to contractual obligations

___ Other _____

_____ _____
Signature of Chairman, PCIP Committee Date

1/14/05

For office use only

THE UNIVERSITY OF TENNESSEE
INVENTION DISCLOSURE FORM

For office use only

1. TITLE OF THE INVENTION.

Lentiviral vector mediated antagomiR-21 in cancer and cardiovascular disease gene therapy

2. DESCRIBE THE INVENTION BRIEFLY. *(If possible, attach a manuscript, a drawing, an abstract, or any other materials that would assist in the understanding of the invention.)*

MiRNA are a new class of non-coding small RNAs that negatively regulate gene expression by either degrading mRNA or blocking protein translation. MiR-21 has been identified as an oncogene and highly expressed in most of cancers, such as breast, bladder, lung, pancreatic, ovary ,cervical, gastric cancer, head and neck squamous cell carcinoma, glioma, myeloma, hepadnavirus-associated hepatocellular carcinoma, cholangiocarcinoma ,chronic lymphocytic leukemia, uterine leiomyomas et al. This miRNA was also a highly upregulated in hypertrophic cardiomyocytes and vascular injured rat models. There are several targeted genes of miR-21 identified, such as phosphatase and tensin homolog (PTEN), programmed cell death (PDCD4), Tropomycin tumor suppressor genes. We designed a lentiviral vector to express the antisense miR-21 gene using human U6 promoter and found that miR-21 gene can be efficiently knocked down in cancer cells and vascular smooth muscle cells. We detected one of targets, PTEN and found that PTEN was significantly increased in vascular smooth muscle cells and B16 melanoma cells. A lentiviral vector we designed for knockdown miR-21 can be used for potential cancer or cardiovascular disease gene therapy by inhibiting cell proliferation during pathological conditions through gene delivery.

3. CONTRIBUTORS/POSSIBLE INVENTORS. *(For a definition of the term "inventor," please refer to the document titled, "Who is an Inventor?," available from your Campus Research Office. All individuals who contributed to the conception of the invention should be listed below, whether or not they are affiliated with The University of Tennessee. Please note that a patent can be rendered invalid by including as an inventor an individual who did not contribute to the conception of the invention. The individual who is named in section A.1. below is designated as the primary contact for additional information and for all correspondence.*

A. Contributors whose *primary* affiliation at the time of invention was The University of Tennessee

(1) Name _____Dr._____Junming Yue_____ Dr., Mr., or Ms.? _____

Title _____Assistant Professor_____ Dept.. Physiology_____

Work address _19S. Manassas St. Rm.266_____ e-mail:jyue@utmem.edu_____

Work phone ____901-448-2091_____ Fax ___901-448-3910 Social Security No. _411-85-5234_____

(2) Name ___Dr. Gabor Tigyi_____ Dr., Mr., or Ms.? _____

Title _____Professor_____Dept. __Physiology_____

Work address: _894 Uinon Av. Rm.426_____ e-mail__gtigyi@physio1.utmem.edu_____

Work phone ___901-448-4973_____ Fax 901-448-7126__Social Security No. _____

(3) Name ____Aixia Ren_____ Dr., Mr., or Ms.? _____

Title ___Senior Research Assistant _____Dept._Physiology_____

Work address _19S. Manassas St_____e-mail ___aren@physio1.utmem.edu___

Work phone ___901-448-2087_____ Fax 901-448-3910_____ Social Security No. _____

(4) Name _____ Dr., Mr., or Ms.? _____

Title _____ Dept. _____

Work address _____ e-mail _____

Work phone _____ Fax _____ Social Security No. _____

B. Contributors whose primary affiliation at the time of invention was *other than* The University of Tennessee

(1) Name _____ Dr., Mr., or Ms.? _____

Title _____ Employer _____

Work address _____ e-mail _____

Work phone _____ Fax _____ Social Security No. _____

(2) Name _____ Dr., Mr., or Ms.? _____

Title _____ Employer _____

Work address _____ e-mail _____

Work phone _____ Fax _____ Social Security No. _____

4. LIST ALL SOURCES OF FUNDING OR SPONSORSHIP OF THE WORK WHICH LED TO THE INVENTION.

A. Federal sponsorship

(1) Agency name _____Department of Defense_____Contract or grant no. _____

Principal Investigator ____Gabor Tigyi_____Dept. ___Physiology_____

(2) Agency name _____ Contract or grant no. _____

Principal Investigator _____ Dept. _____

B. Private sponsorship

(1) Company name _____ Contract or grant no. _____

Principal Investigator _____ Dept. _____

(2) Company name _____ Contract or grant no. _____

Principal Investigator _____ Dept. _____

C. University sponsorship

(1) Department _____ Dept. Head _____

(2) Department _____ Dept. Head _____

(3) Center or Institute _____ Director _____

(4) Special program *(e.g., Distinguished Scientist Program or Collaborating Scientist Program)*

_____

(5) Other _____

D. Other sponsorship

(1) _____

(2) _____

E. Did you use any material in the development of this invention that was acquired from a third party and was subject to a Material Transfer Agreement? Yes _____ No _____
If your answer is yes, please attach a copy of each such agreement.

F. During the period of time when this technology was being developed, did any of the contributor(s) receive salary support from the Department of Veterans Affairs ("VA")? Yes _____ No _____
If your answer is yes, please provide (attach) details.
Were any VA funds or facilities used in the course of work which led to this invention? Yes_____ No_____
If your answer is yes, please provide (attach) details.

5. DISCLOSURE. *In order to obtain valid patent protection on an invention in this country, a patent application must be filed with the United States Patent and Trademark Office within one year after the invention is first described in a printed publication anywhere in the world and within one year after the invention is first on sale or in public use in the United States. To preserve patent rights in many foreign countries, a United States patent application must be filed before any public disclosure in any form anywhere in the world and an application must be filed in the foreign country within one year from the U.S. filing date. If these deadlines are not met, the invention is deemed no longer "new" for patent purposes, and therefore not patentable. For additional information, please see, "The Impact of Public Disclosure on Patent Protection," available from your Campus Research Office.*

A. Journals. *Include all manuscripts describing the invention that have been published, those that have been accepted but not yet published, and those that have simply been submitted but not yet accepted or rejected. Also include any manuscripts that you intend to submit within the next six months. In that case, give the best information that you have at the present time. Please note that authors of a manuscript concerning the invention may not necessarily qualify as inventors.*

(1) Name of journal _____

Title of manuscript _____

Author(s) _____

(Anticipated) Dates of submission/acceptance/publication _____

(2) Name of journal _____

Title of manuscript _____

Author(s) _____

(Anticipated) Dates of submission/acceptance/publication _____

B. Conferences. *Include conferences at which any presentation concerning the invention has been made, as well as conferences which have not yet occurred but for which a manuscript or abstract has been submitted. Also include any conferences at which you intend to disclose information concerning the invention within the next six months. In that case, give the best information that you have at the present time.*

(1) Title of conference _____

Date _____ Location _____

Title of abstract or manuscript submitted _____

Is (or was) the abstract or manuscript distributed prior to the conference? _____ If so, when _____

_____

(2) Title of conference _____

Date _____ Location _____

Title of abstract or manuscript submitted _____

Is (or was) the abstract or manuscript distributed prior to the conference? _____ If so, when _____

_____

C. Theses and dissertations. *Include any thesis or dissertation describing the invention that has been submitted to meet the requirements of graduation. Also include any thesis or dissertation that may be submitted within the next twelve months.*

(1) Title of thesis or dissertation _____

Author _____ (Anticipated) Date of graduation _____

(2) Title of thesis or dissertation _____

Author _____ (Anticipated) Date of graduation _____

D. Offer for sale or public use.

(1) Has any embodiment of this invention been offered for sale (i.e., has a "thing" embodying the invention or capable of performing the invention been offered for sale)?_____

If so, when? _____ To whom and under what circumstances? _____

_____

(2) Has any embodiment of this invention been used publicly?

_____

If so, when? _____ Under what circumstances? _____

_____

E. Other.

Has any other disclosure of the invention (written or oral) been made to a third party who is not bound by a written obligation of confidentiality? If so, when? _____ To whom and under what circumstances? _____

_____

6. WITNESS. *This individual should be sufficiently knowledgeable in the field to enable him or her to understand the invention; a faculty member or research associate in the same department is usually a good choice if he or she is not listed as a contributor to this invention.*

I have read and understood the foregoing disclosure.

Signature	*Title*	*Date*

7. ALLOCATION OF RIGHTS IN THE INVENTION. *(This section applies only to those contributors who are subject to The University of Tennessee's Policy on Patents, Copyrights, and Other Intellectual Property. The rights of any contributors who are not subject to such policy will be addressed separately as appropriate under the circumstances.)*

A. Rights of The University of Tennessee. *The University of Tennessee does not claim rights in inventions that are not developed in performing the duties of employment by the University or with substantial use of University funds or facilities. That determination is made on an individual basis with regard to each contributor. To assist in that determination, each University contributor should sign either in the "Yes" or the "No" column below. If your answer is "No," please attach a separate sheet of paper explaining the reasons for your position.*

YES	NO
In my opinion, my contribution to this invention <u>was</u> made in performing the duties of employment by the University or through the substantial use of facilities or funds provided by the University.	In my opinion, my contribution to this invention was <u>not</u> made in performing the duties of employment by the University or through the substantial use of facilities or funds provided by the University.
_____ *(signature of contributor)*	_____ *(signature of contributor)*
_____ *(signature of contributor)*	_____ *(signature of contributor)*
_____ *(signature of contributor)*	_____ *(signature of contributor)*
_____ *(signature of contributor)*	_____ *(signature of contributor)*
_____ *(signature of contributor)*	_____ *(signature of contributor)*

B. Recommendations of Contributor(s):

(1) It is my (our) recommendation that ownership of primary rights in this invention should remain with/ be assigned to:

___ the sponsoring agency because of contractual obligations.

___ the contributor(s) with recognition of contractual obligations of the University to sponsor(s), if any.

___ UTRF because of poss bility of commercial value.

___ other _____

(2) Division of income *(Complete only when the disclosed invention was developed by more than one individual.)*

Contributors agree and request that any income accruing to them as a result of this invention be allocated in the following percentages *(which should total 100%)*:

_____ _____ % _____(Date)

_____ _____ % _____(Date)

_____ _____ % _____(Date)

_____ _____ % _____(Date)

_____ _____ % _____(Date)

Note: The issue of Division of Income will be revisited in the event that it is determined that some of the named contributors are not inventors or that there are one or more additional inventors not named on this disclosure.

8. COMMENTS BY DEPARTMENT HEAD: _____

_____

_____ _____

Signature of Department Head Date

9. COMMENTS BY DEAN: _____

_____

_____ _____

Signature of Dean Date

10. COMMENTS BY CAMPUS RESEARCH/ADMINISTRATIVE OFFICER:

_____

_____

There are ___/ are not ___ contractual restrictions precluding an assignment of this invention by the University to UTRF.

_____ _____

Signature of Campus Research Officer Date

11. ACTION TAKEN BY THE UNIVERSITY'S PATENT, COPYRIGHT, AND OTHER INTELLECTUAL PROPERTY COMMITTEE:

___ Ownership assigned to or to remain with contributor(s)

___ Ownership assigned to UTRF

___ Ownership assigned to sponsor pursuant to contractual obligations

___ Other _____

_____ _____

Signature of Chairman, PCIP Committee Date

1/14/05